Ministry of Higher Education and Scientific Research

Hassiba Benbouali University of Chlef

Faculty of Technology

Department of Mechanical Engineering

THESIS

Submitted in fulfillment of the requirements for the degree of

DOCTORATE (LMD)

Field: Mechanical Engineering

Specialty: Mechanics & Energetics

By

Bassam Gamal Nasser MUTHANNA

Title:

NUMERICAL AND EXPERIMENTAL STUDY OF ELLIPTICAL CRACKS IN THE CRITICAL POSITIONS OF PIPELINE

Defended on **December 09, 2021,** in front of the committee members:

Mr. Miloud TAHAR ABBES	Professor	UHB-Chlef	President
Mr. Madjid MERIEM BENZIANE	Professor	UHB-Chlef	Supervisor
Mr. Mohammed HADJ MELIANI	Professor	UHB-Chlef	Co-Supervisor
Mr. Hamou ZAHLOUL	Professor	UHB-Chlef	Examiner
Mr. Ahmed BOUZIDANE	Professor	UIK-Tiaret	Examiner
Mr. Ridha MAZOUZI	Professor	UDB-Khemis Miliana	Examiner
Mr. Ibrahim ZIDANE	Professor	UHB-Chlef	Invited

DEDICATIONS

to

My deceased mother, my greatest father, my greatest grandfather, my dear brothers and my dear sisters.

My wonderful big family "uncles, aunts and cousins"

My earliest teachers who inspired me a desire for lifelong learning.

My best friends and colleagues.

ACKNOWLEDGEMENTS

First and foremost, I would like to express my most profound gratitude to my supervisors **Pr. Madjid MERIEM BENZIANE** and **Pr. Mohammed HADJ MELIANI** for their constant supervision, guidance, support, trust, encouragement, advices and for helpful discussions and useful comments. Their leadership, motivation, insights and passion for science and research were the driving force behind the success of this doctorate thesis. Although having a huge amount of responsibilities, they were always approachable kind and generous. Their rich knowledge and experience offered clear guidance throughout my doctorate period.

I would also like to extend my sincere appreciation to the chairman **Pr. Miloud TAHAR ABBES** and committee members **Pr. Hamou ZAHLOUL**, **Pr. Ahmed BOUZIDANE**, and **Dr. Ridha MAZOUZI** for giving me the honor and agreed to review this doctorate thesis. Thank you very much for the time and efforts that you devoted to reviewing, evaluating and commenting on my thesis. Furthermore, I would like to thank **Pr. Ibrahim ZIDANE** as an invited committee member in the defense ceremony. I would also like to give a special thanks to **Pr. Chahinaz FARES** for the great extensive discussion on the corrosion phenomenon and electrochemical analysis. In addition, many thanks to her great team in the department of process engineering for their time, help and great discussion.

A special thanks to my dear friend **Dr. Omar BOULEDROUA**, who has given me a lot of his time and helped me on the numerical analysis.

I also wish to thank all the teachers and the staff of the faculty of technology and department of mechanical engineering for their patience, assistance, support and everything they have made for me.

I would like to express my deep gratitude to my family for their moral and personal support, and for their encouragement in every step of my life.

Finally, my huge thanks and appreciations to everyone who has helped, supported, and guided me through this period of my academic life.

Bassam

Abstract:

Hydrocarbon's transportation is a very significant aspect of the economic where it must be used with much efficacy. Pipelines are used to transport the aggressive fluids with large volumes over great distance. The structural integrity of piping system is very essential in order to guarantee the transportation continue of energy resources from production fields to their locations of exportation. Pipe elbow is a main component in the piping networks which considers as a critical and sensitive tool due to their stress intensification and the effect of bend curvature. They are more exposed to different corrosion failure modes than straight pipes. The aim of this thesis was to investigate the causes of cracks and defects that occur in the critical positions of piping systems. This work was divided in two axes; numerical investigation and inspection analysis. The numerical axis was performed in two sections; (i) effect of semi-elliptical cracks on the degradation of pipe elbow, and (ii) assessment validity of the international mathematical standards on the pipe bends. A rectangular corrosion defect at the intrados section was done and compared to different codes for calculating limit pressure. Moreover, the area with the corrosion cracks and defects with different relative defect depth to wall thickness ratios was FEM modeled at the intrados section of the pipe elbow where the highest hoop stress exists. The second axis was focused on a real case of pipe elbow which occurred to the erosion-corrosion phenomenon. Different inspection methods such as; (i) optical visualization, (ii) scanning electron microscope (SEM), (iii) X-ray diffraction (XRD) and (iv) X-ray fluorescence (XRF) test, were used to discover the main factors which were responsible for this failure. The obtained results proved that the critical position can be located in different zones according to the boundary and additional service conditions. The numerical results proved that the critical position was found at 72° of intrados side based on the value of Von-Mises stress and SIFs. In fact, the critical position could change with the presence of butterfly valve before the elbow. In addition, the increase percentage of Silicon (Si) on the corroded structure explained that the sand particles were responsible to the erosion-corrosion phenomenon.

ملخص:

يعتبر نقل المواد الهيدروكربونية أمراً ضروريًا من الناحية الاقتصادية حيث يجب استخدامه بفعالية كبيرة. تُستخدم خطوط الأنابيب لنقل السوائل العدوانية بكميات كبيرة ولمسافات طويلة. تعد السلامة الهيكلية لنظام الأنابيب غاية في الأهمية من أجل ضمان استمرار نقل موارد الطاقة من حقول الإنتاج إلى مواقع تصديرها. يعتبر كوع الأنبوب مكونًا رئيسيًا في شبكات الأنابيب والذي يعتبر أداة حرجة وحساسة بسبب تركز الاجهادات وتأثير الانحناء على الهيكل الصلب. تعتبر الأكواع أكثر عرضة لأنماط الفشل والتآكل مقارنة بالأنابيب المستقيمة. الهدف من هذه الاطروحة هو التحقيق في أسباب التشققات والعيوب التي تحدث في المواضع الحرجة لأنظمة الأنابيب. تم تقسيم هذا العمل إلى محورين. المحور الأول ركز على التحليل العددي والمحور الثاني استخدم أدوات التحقيق وطرق الفحص المخبرية. تم تنفيذ المحور العددي في قسمين ؛ (1) تأثير الشقوق شبه الإهليلجية على تدهور كوع الأنبوب ، و (2) تقييم صلاحية المعايير الرياضية الدولية على انحناءات الأنابيب. تم إنشاء عيب تآكل مستطيل في الجزء الداخلي للكوع ومقارنته بأكواد هندسية مختلفة لحساب الضغط الحدي. علاوة إلى ذلك، فإن المنطقة التي بها شقوق التآكل والعيوب ذات عمق عيب نسبي مختلف إلى نسب سمك الجدار تم نمذجة محاكاة رقمية في الجزء الداخلي من كوع الأنبوب حيث يوجد أعلى إجهاد. ركز المحور الثاني على دراسة حالة لكوع أنبوب متأثر بظاهرة erosion-corrosion. تم استخدام طرق الفحص المختلفة مثل؛ (1) التصور البصري، (2) مسح المجهر الإلكتروني (SEM) ، (3) حيود الأشعة السينية (XRD) و (4) اختبار ومضان الأشعة السينية (XRF) ، لاكتشاف العوامل الرئيسية التي كانت مسؤولة عن هذا الفشل. أثبتت النتائج التي تم الحصول عليها أنه يمكن تحديد الموقع الحرج في مناطق مختلفة وفقًا للحدود وشروط الخدمة الإضافية. أثبتت النتائج العددية أنه تم العثور على الموضع الحرج عند 72 درجة من جانب intrados بناءً على قيمة إجهاد Von-Mises و SIFs. في الواقع ، يمكن أن يتغير الوضع الحرج بوجود صمام الفراشة قبل الكوع. بالإضافة إلى ذلك ، فإن زيادة نسبة السيليكون (Si) على الهيكل المتآكل يؤكد أن جزيئات الرمل كانت مسؤولة عن ظاهرة erosion-corrosion.

Table of contents

CHAPTER IV: EROSION-CORROSION IN THE CRITICAL POSITIONS OF PIPE ELBOWS: CASE STUDY

CONCLUSIONS AND RECOMMENDATIONS

LIST OF PUBLICATIONS AND COMMUNICATIONS

List of Figures

CHAPTER I: PIPELINE INCIDENTS, INSPECTION TECHNIQUES AND PROTECTION METHODS

CHAPTER II: INTEGRITY ASSESSMENT OF CORRODED PIPELINES

CHAPTER III: ASSESSMENT OF CRITICAL POSITIONS IN PIPE ELBOWS

CHAPTER IV: EROSION-CORROSION IN THE CRITICAL POSITIONS OF PIPE ELBOWS: CASE STUDY

List of Tables

CHAPTER I: PIPELINE INCIDENTS, INSPECTION TECHNIQUES AND PROTECTION METHODS

CHAPTER II: INTEGRITY ASSESSMENT OF CORRODED PIPELINES

CHAPTER III: ASSESSMENT OF CRITICAL POSITIONS IN PIPE ELBOWS

CHAPTER IV: EROSION-CORROSION IN THE CRITICAL POSITIONS OF PIPE ELBOWS: CASE STUDY

List of Symbols

C	Half-length of surface crack (mm)
D	Depth of defect (mm)
D or D_{ext}	Outer diameter of pipe (mm)
D_m	Mean diameter of pipe (mm)
E	The coefficient base of the natural logarithm
E	Young's modulus (MPa)
F	The geometry and crack size correction factor
K	Material constant
K	Coefficient of the power-law stress-strain relationship in the plastic domain
K_I, K_{II}, K_{III}	Stress intensity factors for mode one, two and three (MPa√m)
K_{IC} , K_{IIC} , K_{IIIC}	Fracture toughness for mode one, two and three (MPa√m)
K_{eq}	Equivalent stress intensity factor (MPa√m)
K_r	Non-dimensional crack driving force
L	Longitudinal corrosion defect length (m)
L_r	Non-dimensional applied stress
M	Geometry correction factor (Folias factor) (bulging factor)
N	The strain hardening exponent
P_i , P_s	Internal pressure (MPa)
P_f	Failure pressure (MPa)
Q	The shape factor for an elliptical crack
R	Internal radius of straight pipes and pipe elbows (mm)
t	Pipe wall thickness (mm)
α	Parametric angle of elliptical crack (°)
ε	True strain
ρ	Bending radius (mm)
σ	True stress (MPa)
σ_1 , σ_2 , σ_3	Principal stresses (MPa)

σ_C	Critical normal stress (MPa)
σ_{flow}	Flow stress (MPa)
σ_y	Yield strength (MPa)
σ_{ult}	Ultimate strength (MPa)
σ_{VM}	Von-Mises (MPa)
σ_θ	Hoop stress (MPa)
σ_l	Longitudinal stress (MPa)
σ_r	Radial stress (MPa)
τ_{ASSY}	Average Shear Stress Yield (MPa)
τ_C	Critical shear stress (MPa)
$\tau_{\max}$	Tresca stress (MPa)

List of Acronyms and Abbreviations

APDL	Ansys Parametric Design Language
API	American Petroleum Institute
ASME	American Society of Mechanical Engineers
CFD	Computational Fluid Dynamics
DIN	Deutsches Institut für Normung (German Institute for Standardization)
FAD	Failure Assessment Diagram
MFMC	Material Failure Master Curve
NFAD	Notch Failure Assessment Diagram
FE	Finite Element
FEA	Finite Element Analysis
FEM	Finite Element Method
FV	Finite Volume
FSI	Fluid-Structure Interaction
GDP	Gross Domestic Product
HIC	Hydrogen Induced Cracking
ISO	International Organization for Standardization
LEFM	Linear Elastic Fracture Mechanics
MEA	Monoethanolamine
NACE	National Association of Corrosion Engineers
pH	potential of hydrogen / power of hydrogen
PWC	Preferential Weld Corrosion
SEM	Scanning Electron Microscope
SIF	Stress Intensity Factors
SOHIC	Stress Oriented Hydrogen Induced Cracking
SSC	Sulfide Stress Cracking
SWC	Step-Wise Cracking
TOLC	Top of the Line Corrosion
UDC	Under Deposit Corrosion
UV	Ultra Violet
XRD	X-Ray Diffraction
XRF	X-Ray Fluorescence

INTRODUCTION

1. INTRODUCTION

Nowadays, the energy becomes a necessary parameter for many industry fields. The use of modern technologies is also required for whole world in different processes including the oil and natural gas treatment and their transport. The transport of corrosive liquids (simple or complexes) can be achieved using different ways such as; pipeline, pipeline offshore, cargo tanks for chemical tankers, storage tank, road tankers, rail tank wagons and many other solutions [1-3]. With the increasing high demand for hydrocarbons of oil and natural gas around the world, pipeline applications with higher strength are required. The processes of oil and natural gas treatment and their transport depend on the piping systems especially the elbow which is one of among important parts. Indeed, the piping system is still the best tool and safest way to transport the corrosive liquids such as carbon dioxide (CO_2), hydrogen, methanol, hydrogen sulfide (H_2S), hydrochloric acid (HCl), sulfuric acid (H_2SO_4) and ammonia (NH_3) [4-8].

Various hazardous phenomena, such as cracking, fatigue, and corrosion of pipelines allow increasing the risk of leaks or even bursting, are now critical cases to be considered. Many problems when analyzing a pipe with an under internal pressure, the detecting effect of the pressure and the poorly defined geometry permit a presence of a local defect [9-12]. The effect of corrosion phenomenon on the global energy, environment and humanity is considered as a major problem which take the attention and efforts of researches around the world. The global economy faces a lot of dangerous due to this issue in the transportation networks and storage units. Depending on the statistic reports of the National Association of Corrosion Engineering (NACE), the corrosion problem costs about 2.5 trillion of dollars per year for the global economy which is almost 3.3 % of global GDP (Gross Domestic Product) [13,14]. In addition, the cost of these challenges is greater than all natural disasters losses such as; hurricanes, storms, floods, fires and earthquakes [15].

2. PROBLEMATIC

The Fluid-Structure Interaction (FSI) in the pipeline components may lead to the chemical reactions in the elbow. Pipe elbows are considered critical pressurized components in the piping systems and pipelines due to their stress intensification and the effect of bend curvature. They are prone and hence more exposed to different corrosion failure modes than straight pipes. Late

detection of such elbow damages can lead to different dangerous and emergency situations which cause environmental disasters, pollution, substantial consumer losses and a serious threat to human life. Adverse but common chemical side reactions such as hydrogen evolution [16-19], microbial reactions [20], oxidation [21,22], and sulfidation of materials could provoke pipelines deterioration, particularly elbows, due to severe corrosion attack [5, 23-24]. Also, hard solid particles may cause strong erosion attack on the internal surface of the pipe elbow upon the transport of solid-liquid or gas-solid mixtures, an internal erosion-corrosion attack, and the erosion of external surfaces due to impact of sand particles [25-28]. Furthermore, corrosion in the energy plants such as desalination station or oilfield is increased due to the presence of CO_2 in the fluid flow. In addition, the small particles of sand (high concentration of Silicon) in the fluid flow may cause the erosion phenomenon in the piping system as the case study which will present in the chapter IV.

3. OBJECTIVES OF THIS STUDY

A comprehensive safety and reliability assessment of pipe elbows, including continuous maintenance and usage of different inspection methods, can provide significant increases in the service life of pipelines. The main aim of this thesis is to study the critical positions of pipe elbows. Furthermore, this thesis is investigated to discover the main causes of pipeline degradation especially in the elbow part. In addition, international standards of limit pressure will be evaluated and developed using numerical analysis. In order to perform the objectives of this thesis, both experimental and numerical techniques are used to assess the influence of various aspects on the performance of pipeline under service. In numerical analysis, Finite Element (FE) and Finite Volume (FV) methods are combined to generate a tool capable of predicting the service life of piping system components using Failure Assessment Diagram (FAD). In the experimental investigation, real corroded elbows will be inspected to detect the main causes of corrosion-erosion phenomenon.

4. THESIS OUTLINE

This thesis is divided into four chapters. The first chapter shows the pipeline incidents which occurred around the world. In addition, the inspection techniques and protection methods which used in the engineering industrial are presented.

The second chapter presents the integrity assessment of corroded pipelines indicated to the

mathematical equations of fracture mechanics, power law, international standards. Furthermore, the international standards which are used for calculating the failure and limit pressure on the straight pipes is discussed. In particular, the pipe elbows are critical elements in the piping network due to their curvature where the known standards are not applicable on them. Few researchers evaluate and modified the engineering codes in order to measure the limit pressure on pipe bends and prevent the burst.

In the third chapter, two main sections which explain the crack phenomenon and corrosion defect in API X52 pipe elbows were simulated. First section focuses on the critical position of elbow bends using by finite volume method (FVM) and finite element analysis (FEA). In order to analyze this section which is divided into four main parts: the first part concentrated on analyzing and comparing the results which appear the effect of bending radius of elbow on the maximum values of Von-Mises stress for each radius taking into account the characteristics of mechanical including the yield stress of the elbow material. The second part concentrated on the creation of a semi-elliptical crack for different locations along the elbow to define the critical position by using the stress intensity factors. In the third part, the semi-elliptical crack angle orientation was studied at the critical position to indicate the critical angle which allows evaluating the effect of crack during the transporting of energy. The last part is focused on the check of the elbow safety where the failure assessment diagram (FAD) is one of most technique to analyze the damage of piping systems to show the critical crack depth ratios at a critical position and a critical angle. The second section reserved to evaluate the integrity assessment of elbows damaged of API 5L X52 steel which was carried out in the framework of numerical study by using the finite element method (FEM) and finite element analysis (FEA). To evaluate the damage, the FEM is used to simulate this phenomenon taking into consideration the limit pressure in the elbow containing a rectangular shaped corrosion defect at the intrados side. This study was accurately performed and compared to literature studies which have been carried out by different codes for calculating limit pressure.

The last chapter IV, an investigation on the probably failure of two pipe elbows which transport an aggressive fluid will be presented. The microstructure and the composition of the surface films on the surface of the corroded specimen were investigated using scanning electron microscope (SEM), X-ray diffraction (XRD) and X-ray fluorescence (XRF) test.
Finally, this thesis is concluded by principal conclusions and recommendations.

References

[1] Meriem-Benziane, M., Bou-Saïd, B., Muthanna, B.G.N. and Boudissa, I., 2021. Numerical study of elbow corrosion in the presence of sodium chloride, calcium chloride, naphthenic acids, and sulfur in crude oil. *Journal of Petroleum Science and Engineering*, 198, pp.108124, https://doi.org/10.1016/j.petrol.2020.108124;

[2] Zhu, H., Zhao, H., Pan, Q. and Li, X., 2014. Coupling analysis of fluid-structure interaction and flow erosion of gas-solid flow in elbow pipe. *Advances in Mechanical Engineering*, 6, pp.815945, https://doi.org/10.1155/2014/815945;

[3] Meriem-Benziane, M., Abdul-Wahab, S.A., Benaicha, M. and Belhadri, M., 2012. Investigating the rheological properties of light crude oil and the characteristics of its emulsions in order to improve pipeline flow. *Fuel*, 95, pp.97-107, https://doi.org/10.1016/j.fuel.2011.10.007;

[4] Bagdasarian, A., Feather, J., Hull, B., Stephenson, R. and Strong, R., 1996, August. Crude unit corrosion and corrosion control. *In Corrosion-National Association of Corrosion Engineers Annual Conference, NACE*, https://eduwavepool.unizwa.edu.om/lmsdatapool/00015220/LearningObjects/Distillation%20Unit%20Corrosion.pdf.

[5] Meriem-Benziane, M., Bou-Saïd, B. and Boudouani, N., 2017. The effect of crude oil in the pipeline corrosion by the naphthenic acid and the sulfur: A numerical approach. *Journal of Petroleum Science and Engineering*, 158, pp.672-679, https://doi.org/10.1016/j.petrol.2020.108124;

[6] Simanzhenkov, V. and Idem, R., 2003. Crude oil chemistry. Crc Press;

[7] Larché, N. and Dézerville, P., 2011. Review of material selection and corrosion in seawater reverse osmosis desalination plants. *Desalination and Water Treatment*, 31(1-3), pp.121-133, https://doi.org/10.5004/dwt.2011.2362;

[8] Ilman, M.N., 2014. Analysis of internal corrosion in subsea oil pipeline. *case studies in Engineering Failure Analysis*, 2(1), pp.1-8, https://doi.org/10.1016/j.csefa.2013.12.003;

[9] Shuai, Y., Wang, X.H., Li, J., Wang, J.Q., Wang, T.T., Han, J.Y. and Cheng, Y.F., 2021. Assessment by finite element modelling of the mechano-electrochemical interaction at corrosion defect on elbows of oil/gas pipelines. *Ocean Engineering*, 234, pp.109228, https://doi.org/10.1016/j.oceaneng.2021.109228;

[10] Terán, G., Capula-Colindres, S., Velázquez, J.C., Angeles-Herrera, D. and Torres-Santillán, E., 2019. On the Influence of the Corrosion Defect Size in the Welding Bead, Heat-Affected Zone, and Base Metal in Pipeline Failure Pressure Estimation: A Finite Element Analysis Study. *Journal of Pressure Vessel Technology*, 141(3), pp. 031001, https://doi.org/10.1115/1.4042908;

[11] Lu, Y.J. and Wang, C.H., 2020. Effects of geometry of a local thin area defect on remaining strength and fitness of pressure equipment. *Journal of Loss Prevention in the Process Industries*, 65, p.104125, https://doi.org/10.1016/j.jlp.2020.104125;

[12] Kutz, M., 2018. Handbook of environmental degradation of materials. William Andrew.

[13] Fayomi, O.S.I., Akande, I.G. and Odigie, S., 2019, December. Economic impact of corrosion in oil sectors and prevention: An overview. *In Journal of Physics: Conference Series* (Vol. 1378, No. 2, pp. 022037). IOP Publishing, https://iopscience.iop.org/article/10.1088/1742-6596/1378/2/022037/pdf;

[14] Koch, G., Varney, J., Thompson, N., Moghissi, O., Gould, M. and Payer, J., 2016. International measures of prevention, application, and economics of corrosion technologies study. *NACE International*, p.216;

[15] Michel, P.H., Brongers, C.C., Gerhardus, H.K. and Neil, G., 2019. Corrosion costs and preventive strategies in the United States. Publication No. FHWA-RD-01-156. *Technologie and NACE*. https//www.Nace.or/uploadedfiles/publications/ccsupp.pdf ;

[16] Djukic, M.B., Zeravcic, V.S., Bakic, G.M., Sedmak. A. and Rajicic B., 2015. Hydrogen damage of steels: A case study and hydrogen embrittlement model. *Engineering Failure Analysis*, 58, pp.485-498, https://doi.org/10.1016/j.engfailanal.2015.05.017;

[17] Popov, B.N., Lee, J.W. and Djukic, M.B., 2018. Hydrogen permeation and hydrogen-induced cracking. In Myer Kutz, editor. Handbook of Environmental Degradation of Materials, Third Edition. *William Andrew Publishing*, pp.133-162, https://doi.org/10.1016/B978-0-323-52472-8.00007-1;

[18] Wasim, M. and Djukic, M.B., 2020. Hydrogen embrittlement of low carbon structural steel at macro-, micro- and nano-levels. *International Journal of Hydrogen Energy*, 45(3), pp.2145-2156, https://doi.org/10.1016/j.ijhydene.2019.11.070;

[19] Djukic, M.B., Bakic, G.M., Zeravcic, V.S., Sedmak, A. and Rajicic, B., 2019. The synergistic action and interplay of hydrogen embrittlement mechanisms in steels and iron: Localized plasticity and decohesion. *Engineering Fracture Mechanics*, 216, pp.106528, https://doi.org/10.1016/j.engfracmech.2019.106528;

[20] Wasim, M. and Djukic, M.B., 2020. Long-term external microbiologically influenced corrosion of buried cast iron pipes in the presence of sulfate-reducing bacteria (SRB). *Engineering Failure Analysis*, 115, pp.104657, https://doi.org/10.1016/j.engfailanal.2020.104657;

[21] Bakic, G.M., Djukic, M.B., Rajicic, B., Zeravcic, V.S., Maslarevic, A. and Milosevic, N., 2016. Oxidation behavior during prolonged service of boiler tubes made of 2.25Cr1Mo and 12Cr1Mo0.3V heat resistance steels. *Procedia Structural Integrity*, 2, pp.3647-3653, https://doi.org/10.1016/j.prostr.2016.06.453;

[22] Bakić, G.M., ŠijačkiŽeravčić, V.M., Djukić, M.B., Maksimović, S.M., Plešinac, D.S. and Rajičić, B.M., 2011. Thermal history and stress state of a fresh steam-pipeline influencing its remaining service life. *Thermal Science*, 15(3), pp.691-704, https://doi.org/10.2298/TSCI110509050B;

[23] Soudani, M., Bouledroua, O., Hadj Meliani, M., El-miloudi, K., Muthanna, B.G.N., Khelil, A., Elhoud, A., Matvienko, Y.G. and Pluvinage, G., 2018. Corrosion inspection and recommendation on the internal wall degradation caused rupture of 6" gas line pipe. *Journal of Bio-and Tribo-Corrosion*, 4(2), p.28, https://doi.org/10.1007/s40735-018-0145-0;

[24] Amara, M., Bouledroua, O., Hadj Meliani, M., Muthanna, B.G.N., Abbes, M.T. and Pluvinage, G., 2018. Assessment of pipe for CO2 transportation using a constraint modified CTOD failure assessment diagram. *Structural Integrity and Life*, 18(2), pp.149-153, http://divk.inovacionicentar.rs/ivk/ivk18/149-IVK2-2018-MA-OB-MHM-BGNM-MTA-GP.pdf;

[25] Yu, W., Fede, P., Climent, E. and Sanders, S., 2019. Multi-fluid approach for the numerical prediction of wall erosion in an elbow. *Powder Technology*, 354, pp.561-583, https://doi.org/10.1016/j.powtec.2019.06.007;

[26] Peng, W., Cao, X., Hou, J., Xu, K., Fan, Y. and Xing, S., 2020. Experiment and numerical simulation of sand particle erosion under slug flow condition in a horizontal pipe bend. *Journal of Natural Gas Science and Engineering*, 76, p.103175, https://doi.org/10.1016/j.jngse.2020.103175;

[27] Amara, M., Muthanna, B.G.N., Abbes, M.T. and Hadj Meliani, M., 2018. Effect of sand particles on the Erosion-corrosion for a different locations of carbon steel pipe elbow. *Procedia Structural Integrity*, 13, pp.2137-2142, https://doi.org/10.1016/j.prostr.2018.12.151;

CHAPTER I:

PIPELINE INCIDENTS, INSPECTION TECHNIQUES AND PROTECTION METHODS

I.1 INTRODUCTION

The hydrocarbon transportation including the emulsions (crude oil-gas-water or crude oil-gas) is one of the challenging operations which face many petroleum companies around the world due to the nature of piping systems, operating conditions, the origin of the oil, and the nature of the geological layers of wells (aggressive components). To exploit the hydrocarbons, the piping systems are still suitable tools for transmission and distribution with different geometries (pipelines, and elbows) taking into account the grade of materials such as (X42, X52, X60, X65, X70, X80, .., X120).

In the last decades, piping systems are considered as the principal engine of the global economy especially after increasing the demand for energy due to the increase of population and the decrease of the energy sources. Despite the use of high technology in order to control the piping systems, many catastrophic incidents have increased in the worldwide. Piping system aging, long term usage, neglecting and irregular maintenance, crude oil nature (with/without corrosive components) and the environmental severe conditions are serious parameters which face the energy transport companies, where these reasons are directly influence on the universal economy such as the price of the barrel. To continue the development of energy in all fields of life, the objective consists of avoiding catastrophic accidents and preserving human health. There are great challenges to avoid the catastrophic explosions, preserve human health and the maintain the environmental climate which is the main goal of each company.

The aim of this chapter is to concentrate on the piping system incidents that involved two periods including straight pipes and pipe elbows. There are many factors to investigate any incident which has direct/indirect relationship with the hydrocarbons transport, where these accidents can classify through the degree of dangerous on the human life and environment on the one hand, and their effects on the infrastructure of energy on long-term, on the other hand. The dangerous degree of incident is classified on the basis of: degree and nature of accident (explosion or corrosion), kind of material, form of pipeline (straight line or elbow), critical location (joint, welding position, elbow, repaired surface) and service period taking into account the operating conditions such as pressure, temperature and piping geometry (pipeline or elbow) [1,2].

Depending on the analyses of the previous incidents in the piping system, the inspection method is one of the effective plans to know the reasons of problems, where it must take all aspects

physic-chemical into considerations which allow obtaining the appropriate and permanent solutions. This chapter is divided into five parts to show the most steps related to the analyses of piping systems accidents, where it includes the reasons and solutions to avoid dangerous accidents. The important points which can take into consideration to understand this phenomenon:

- Accident sources;
- Study of piping systems (elbows and pipelines) out service;
- Investigations and inspections of the piping systems defected;
- Effect of crude oil nature and natural gas on the corrosion phenomenon;
- Repairing methods and piping system safety from the corrosion phenomenon.

I.2 PIPELINE ACCIDENT STATISTICS

Hydrocarbons such as emulsions (crude oil-gas or crude oil-gas-water) pass through many operations including extraction, transportation and refining process in order to arrive to the local or international markets and energy centers [3,4]. In fact, the piping system considers a principal tool to transport the crude oils with/without aggressive compounds taking into account the safety and low cost of maintenance. In order to assess and increase the life time of pipelines under service, it is essential to understand their role and avoid the incidents which based to the human errors or environmental attack. In this section, the statistical incidents around the world based on the literature publications and international standards were presented. Thus, it allows to evaluate the efficiency of piping systems taking into consideration the nature of fluid and the pipeline materials.

The safety of piping network is the challenge of each company, where the corrosion phenomenon becomes the first issue in the worldwide due to the impact on the universal economy, environment and human health. The economic reports indicated that the corrosion issue is an obsession for energy experts and scientific organisations such as the National Association of Corrosion Engineering (NACE). According to NACE reports about the piping systems, it appears that losses have exceeded 2.5 trillion dollars per year for the worldwide economy due to the corrosion phenomenon including all kinds of piping systems (offshore, above ground, and underground) in addition to the refineries stations. These losses represent about 3.3 % of global GDP (Gross Domestic Product) [5-7]. In addition, this value in some

development countries is considered greater than all-natural disasters cost such as; hurricanes, storms, floods, fires and earthquakes [7]. The corrosion phenomenon affects directly on the collapse of the global economy where most companies attempt to activate many procedures such as inspection, repairing and maintenance, control, protection, and development methods in order to decrease the effect of corrosion issue in the energy fields. Thus, it can avoid the production stoppage, the environmental pollution, the increase the maintenance costs, etc [5, 8].

Due to this dangerous issue, most laboratories and companies around the world try to obtain durable and suitable solutions to decrease the severe damages. It is a great challenge faced researchers and engineers for many decades. They are attempting to discover suitable solutions for defeating or decreasing this unpleasant lesion. Generally, there are different reasons for this problem which have a direct relationship with the nature of piping systems materials, hydrocarbons components (with/without sulfur), interaction phenomenon (fluid-fluid and fluid-solid), operating conditions (temperature and pressure) and extern environment (dryness and dampness). These reasons may help to give an idea for stopping and reducing this industrial pandemic.

Depending on the dangerous incidents which happened during the recent decades according to the Pipeline and Hazardous Materials Safety Administration (PHMSA) [9], the damage can be evaluated in order to give the real view of the situation about this dangerous phenomenon. According to PHMSA, there were 18 fatalities and 69 injuries annually in the United States between 1995 and 2014. While in 2019, the number was decreased to 10 fatalities and 35 injuries due to the necessary interest in the pipeline network [9]. In order to show the damage of piping network, a statistical sample that occurred in the United States between (2010-2019) was shown in Table I.1.

Table I.1: The last decade incidents of piping systems in the US [9].

Report	Incidents	Fatalities	Injuries	Evacuees	Damages ($)	Fires	Explosions
Aggressive Fluids	3,978	10	26	2,482	2,812,391,218	130	15
Gas Transmission & Gathering	1,226	25	108	12,984	1,315,162,976	133	57
Gas Distribution	1,094	105	522	20,526	1,229,189,997	659	257
Totals	**6,298**	**140**	**656**	**35,992**	**5,356,744,191**	**922**	**329**

The main factors that are responsible for failure incidents as stated in PHMSA's reports are; corrosion types, external environment, exploration and extraction, operating conditions (temperature, pressure, piping systems geometries), failure of piping systems, failure at welding positions, appearing of defects/ small cracks in the inner and extern wall of steel, nature of transported liquids, human errors and other reasons (geology of wells, the effect of additives and refinery processes) [10]. Figure I.1 illustrates the main causes of pipeline incidents in last decade in US for three lines of piping system; the pipeline of aggressive fluids (figure I.1.a), transmission and gathering lines (figure I.1.b) and, distribution piping systems (figure I.1.c).

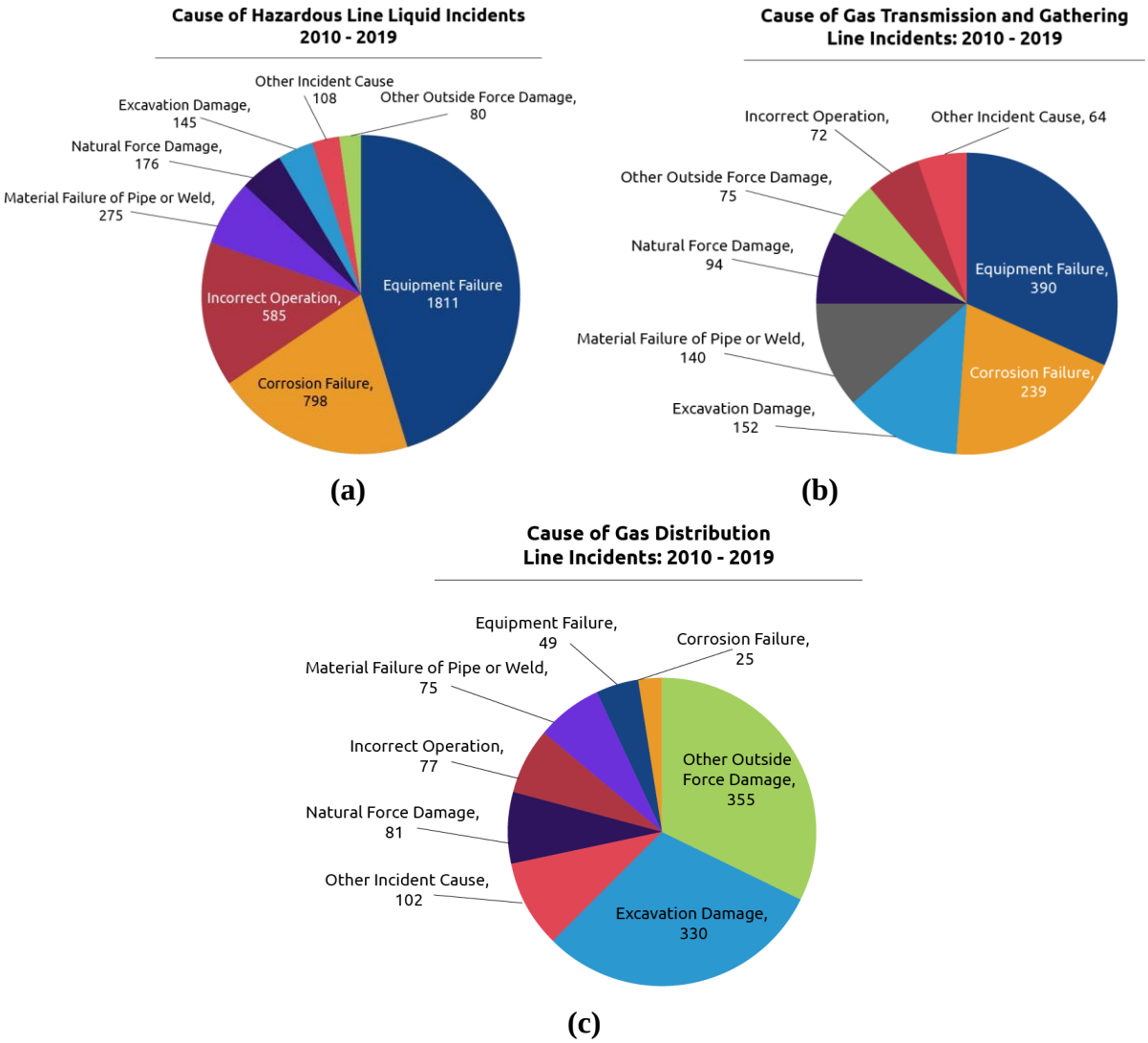

Figure I.1: Cause of Pipeline Incidents in the US last decade, (a) aggressive fluids, (b) gas transmission and gathering and, (c) gas distribution. Data from PHMSA [9].

I.3 CASE STUDIES FOR STRAIGHT PIPES AND PIPE ELBOWS INCIDENTS

Pipeline incidents become a threat to the human safety, environmental life and, global economy. This section elaborates and presents some of incident cases around the world in order to avoid them in future. Furthermore, the pipelines could be very dangerous if they explode in the vital Cities where the citizens live as shown in the figure I.2. This incident was happened in Kaohsiung city - south Taiwan - in 2014 which caused 25 fatalities and more than 259 injuries due to this horrible accident [11,12].

Figure I.2: Catastrophic incident of pipeline explosion in south Taiwan [11,12].

In 2012, pipeline of Colombian gas transmission was failed due the degradation of wall thickness by external corrosion (see figure I.3). The pressure increase and operator error were the main causes of this accident. Furthermore, it was not checked during last 24 years of incident event [13]. According to the investigations, the pipeline also had not the shutoff valves which could prevent the catastrophic damage. This accident left a lot of damages such as;

- damage on the infrastructure;
- destroyed three homes and sabotaged lots of houses near the incident site by hundreds of feet;
- More than 76 million cubic feet of natural gas were lost.

Figure I.3: Incident in Columbian gas transmission natural gas pipeline [13]

Elbows (pipe bends) are considered important compounds which allow to link the piping systems together in order to facilitate the change of flow direction of fluid transport. Due to the sensibility of pipe elbows in transporting hydrocarbons, the manufacturing engineering and type of materials used to become a significant condition to prevent damage and decrease the costs of maintenance and protect the environment. Elbow pipe is the weakest part in the piping system which is exposed to the maximum pressures and complex chemical reactions where the most perturbations of liquids are focused in the more bent positions. Furthermore, the friction between fluid flow and the curvature of pipe bends creates high stresses in the critical positions. Extensive reports and researches [14-19] have investigated on the incidents of pipe bends in the petroleum industries. This issue is repeated in different sections and stations such as; oil–gas separator vessel, crude oil and natural gas subsea pipeline, refineries, CO_2 production, geothermal production, natural gas gathering and different sections. Among the chemical reactions which may lead the corrosion in pipelines are chlorination and sulfidation reactions. They transform the molecular of chemical elements into undesirable layers in the internal surface of steel wall due to the presence the aggressive components [17, 20-22]. The chlorination and sulfidation reactions which may happen in the hydrocarbon's transportation are presented as follow:

$$CaCl_2 + H_2O \rightarrow 2HCl + CaO \quad \textbf{(I.1)}$$

$$NaCl + H_2O \rightarrow HCl + NaOH \quad \textbf{(I.2)}$$

$$MgCl_2 + H_2O \rightarrow 2HCl + MgO \quad \textbf{(I.3)}$$

$$Fe + 2HCl \rightarrow FeCl_2 + H_2 \quad \textbf{(I.4)}$$

$$FeCl_2 + H_2S \rightarrow 2HCl + FeS \quad \textbf{(I.5)}$$

Ilman et al. [18] have investigated on an accident occurred on offshore pipe elbow. The pipeline steel was failed after 27 years under service. The main reason for this incident is an internal corrosion located on the bottom side of an elbow made of API 5L X52 steel as shown in figure I.4. The study has proved that the presence of water and oxidation have led to the corrosion occurrence in the teardrop shaped pits and grooves.

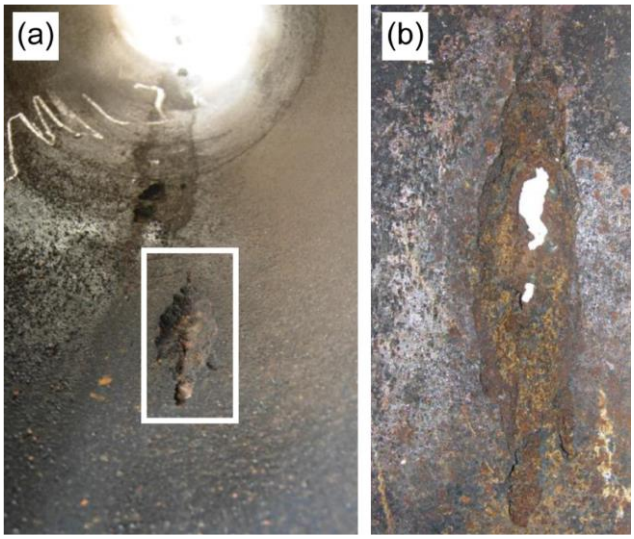

Figure I.4: The location internal corrosion on subsea pipe elbow [18].

Another incident that happened for pipe elbow in the geothermal production was studied by Kusmono et al. [19]. The failure has occurred at the bottom of piping systems' elbow as shown in figure I.5. The presence of steam, water, and solid particles are considered as a result of erosion corrosion processes on the elbow pipe [19].

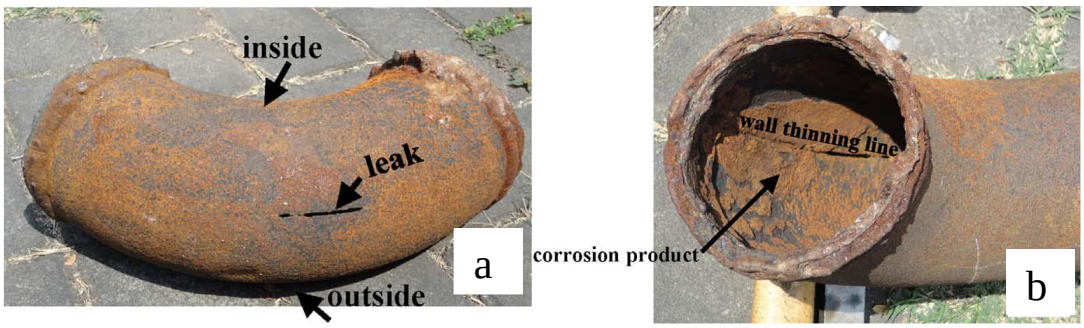

Figure I.5: A view of failure location and wall loss on pipe elbow, (a) external crack and, (b) internal wall loss [19].

Recently in the Chinese oilfield, an accident was occurred due to the inner corrosion of 45° elbow pipe carrying a natural gas which caused the explosion (figure I.6 a). A group of researchers have investigated on the causes of the bursting incident with the aid of visual observation, inspection analysis and CFD calculation. According to the industrial designer, the lifetime expected of pipeline under service is 30 years, but unfortunately, it was failed at the seventh year of its operating work [23]. Moreover, the degradation of wall thickness is clear as shown in the figures I.6 (b and c). The final investigation has proved that the inappropriate structure design, CO_2 corrosion and stress accelerated corrosion are the principal results of the accident [23].

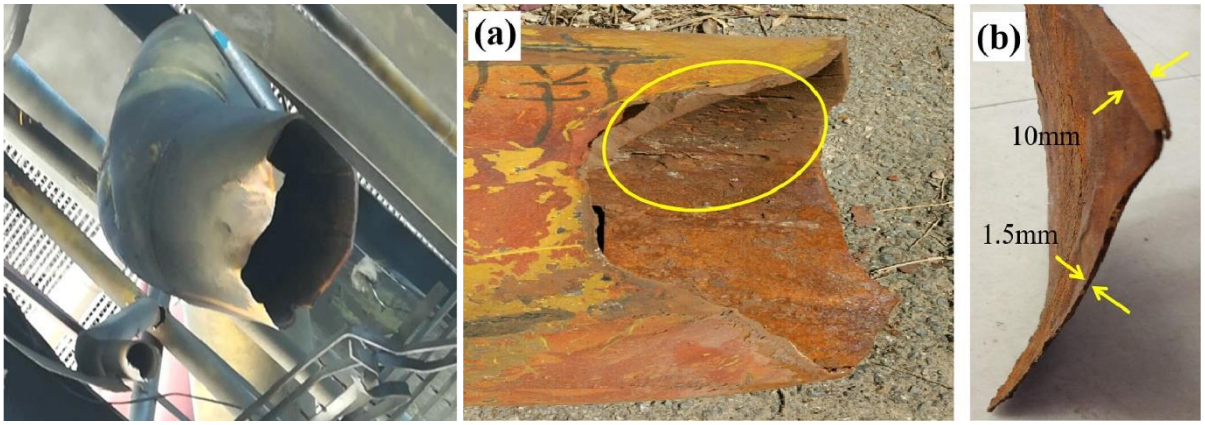

Figure I.6: 45° pipe elbow failure in a natural gas gathering pipeline [23].

I.4 MONITORING, DETECTING AND INSPECTION METHODS

The inspection tools allow to us analyze the main causes that are responsible for pipeline incidents. In order to find out the causes of the problem from all sides, the following processes must be taken into consideration for accurate and complete investigation;

- On-site inspection, including non-destructive testing (NDT);
- Laboratory analysis, including chemical analysis and metallography;
- Mechanical testing, including loads and vibration measurement;
- Data analysis, including analytical calculation, statistical analysis and numerical methods.

Table I.2 summarizes the different inspection methods which used in the hydrocarbon industries and scientific laboratories.

Table I.2: Integrity methods for assessment and investigation pipeline incidents

Integrity type	Instrument or method	Methodology	Reference
On-site inspection	➢ Visual observation ➢ Penetrant test ➢ Magnetic test ➢ Radiography test ➢ Ultrasonic Tool ➢ Smart pigs ➢ Engineering critical assessment ➢ Mapping ➢ Hydrostatic testing ➢ Long range guided wave	This type of inspection depends on the scanner capture which discovers the internal cracks, capture the defects, clean the internal surface with aid of pressure.	[24-30]
Chemical and electrochemical analysis	➢ X-ray Diffraction (XRD) ➢ X-ray fluorescence (XRF) ➢ Fourier-transform infrared spectrophotometry (FTIR) ➢ Tafel ➢ Electrical Impedance Spectroscopy (EIS)	➢ Discover the crystalline structures and atomic spacing of the materials, ➢ Determine the qualitative and quantitative elemental composition of solids and fluids, ➢ Identify the chemical elements present in the specimen, indicate the percentage of the element in the material.	[31-35]
Mechanical tests	➢ Optical microscope ➢ Scanning Electron Microscope (SEM) ➢ Tensile test ➢ Flexural test ➢ Fatigue ➢ Charpy test	➢ Study small cracks and show the degradation of material; ➢ Investigate the mechanical properties including the yield stress, ultimate strength, hoop stress, stress intensity factors (SIFs) and other parameters; ➢ Improve the fracture resistance.	[36-38]

Statistical analysis	➢ Monte-Carlo Model ➢ The Time-Independent Generalised Extreme Value Distribution (TI-GEVD) model ➢ The Time-Dependent Generalised Extreme Value Distribution (TD-GEVD) model ➢ The Gamma Process ➢ Brownian motion with drift (BMWD) model ➢ Markov Model	Collect, organize and interpret patterns and differences in the data; ➢ Identify relationships between variables; ➢ Determine the appropriate significance test that should be used.	[39-44]
Numerical methods	➢ Finite element ➢ Finite difference ➢ Finite volume	➢ Solve numerical problems; ➢ Study of algorithms that use numerical approximation; ➢ Simulate the real tests with less time, low cost and easy way.	[45-47]
Analytical calculation	➢ ASME B31G ➢ Mod ASME B31 G ➢ DNV RP-F101 ➢ Shell-92 ➢ RSTRENG ➢ PCORRC	➢ Based on the corrosion prediction; ➢ Determine the failure pressure; ➢ Calculate the appropriate pipe wall thickness according to the internal pressure design; ➢ Predict the critical depth ratio of corroded position in pipeline	[48-53]

I.5 CORROSION IN ENERGY TRANSPORTATION

The corrosion is a natural operation that occurs in a piping system (collector and transmission lines) during the production of hydrocarbons (oil and natural gas) [54]. Its reaction may turn the steel into different form of chemical compounds such as; oxide, hydroxide, or sulfide. This change in the material structure may cause to the progressive destruction or degradation. In the petroleum industries, the corrosion problem is always in presence especially in the power stations, refinery process and energy plants. The corrosion phenomenon occurs due to the interaction of fluid-structure (oil-steel wall) taking into account the nature of fluid (Newtonian / Non-Newtonian) and material of piping system (ordinary /composite) with geometry (straight line / bend line).

An example of corrosion reaction that may happened in pipeline steel in the presence of hydrocarbon and water is shown in figure I.7. Due to the oxidation results of corrosion process, solid structure losses the energy which cause the degradation and may stop its operation service [55].

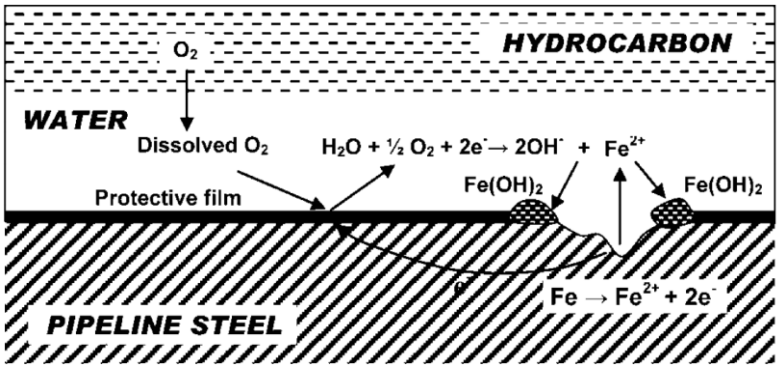

Figure I.7: An example of steel corrosion process [18]

The interaction between metal surface and fluid flow can cause to the oxidation which degrades the wall thickness as shown in figure I.7. This process may express as the following reactions:

At cathode: $O_{2(g)} + 4H^{+}_{(aq)} + 4e^{-} \rightarrow 2H_2O_{(l)}$ **(I.6)**

at anode: $Fe_{(s)} \rightarrow Fe^{2+}_{(aq)} + 2e^{-}$ **(I.7)**

overall: $2Fe_{(s)} + O_{2(g)} + 4H^{+}_{(aq)} \rightarrow 2Fe^{2+}_{(aq)} + 2H_2O_{(l)}$ **(I.8)**

Depending on the many reports of inspections, analysis, and investigations during the hydrocarbon transport, it is clear that the most reasons have direct/indirect relationships with occurring the corrosion phenomenon such as operating conditions, high temperature, high pressure, the external and internal environment (drying / wetting), crude oil origin, pipeline material and the defects in extern/intern wall. In addition, the presence of undesirable compounds in the hydrocarbons fields during transport and refining can form aggressive components such as sulfur, sodium chloride, calcium chloride, acids, and naphthenic acids. In particular, the main factors that can lead to corrosion problem in the hydrocarbons transportation and energy industries are:

- Natural, urban, marine and industrial atmospheres including air and humidity; fresh, distilled, salt and marine water.
- Service conditions such as; high temperature, high pressure, high velocity;
- Aggressive components such as; bacteria, ammonia (NH_3) carbon dioxide (CO_2), hydrogen sulphide (H_2S), sulfur (S) and sulphate (SO_4^{2-}) ;
- Steam and gases, like chlorine;
- Organic acids;
- Emulsions (Oil-Water, Oil-Water-Gas);
- Alkalies;
- Soils.

I.5.1 Types of corrosion

Due to the importance of pipelines which have a significant role of ability to provide global energy, they might expose to the corrosion phenomenon especially at the critical zones (elbows, welded joins, and walls with defects). However, the types of corrosion do not only relate to the nature of crude oil, but they have a serious relation with the type of pipeline materials (ordinary/composite) taking into consideration the geometry and operating conditions. The dangerous effect of corrosion appears in the mechanics of exploration, extraction, and transport of energy through piping systems and the great storage stations, in addition to the refining petroleum stage. The corrosion is presented in different types as shown in figure I.8 which make the dangerous differs from type to other one.

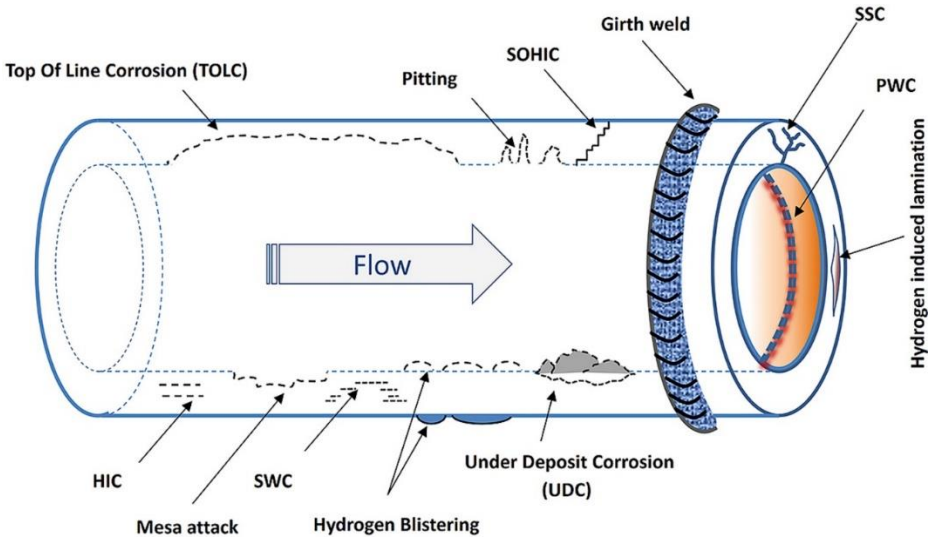

Figure I.8: Various types of corrosion forms in a pipeline [56].

I.5.2 Corrosion by CO_2 and O_2

CO_2 and O_2 could be responsible factors for corrosion causing due to their activity in the natural gas transportation and the produced a dangerous compound during of carbonic acid (H_2CO_3) during the reaction with pipeline steel. According to [57-61], O_2 in the natural gas transportation may cause a black powder issue which lead to catastrophic problems such as; equipment erosion, valve failure, instrumentation malfunction, and increased pressure drop. Furthermore, a sweet corrosion (CO_2) happens in the absence of hydrogen sulfide (H_2S) or other compounds of sulfide. The most known reaction of sweet corrosion is the mixture of carbon dioxide (CO_2) with water (H_2O) which results the carbonic acid (H_2CO_3) as the following reactions:

$$CO_{2(sol)} \rightarrow CO_{2(ad)} \quad \textbf{(I.9)}$$

$$CO_{2(ad)} + H_2O \rightarrow H_2CO_{3(ad)} \quad \textbf{(I.10)}$$

$$O_2 + 2H_2O + 4e^- \rightarrow OH^- \quad \textbf{(I.11)}$$

$$H_2CO_{3(ad)} + H_2O \rightarrow H_3O^+ + HCO_3^- \quad \textbf{(I.12)}$$

$$HCO_3^- + H_2O \rightarrow H_3O^+ + CO_3^{2-} \quad \textbf{(I.13)}$$

$$H_3O^+ + e^- \rightarrow H_{(ad)} + H_2O \quad \textbf{(I.14)}$$

$$H_{(ad)} + H_{(ad)} = H_2 \quad \textbf{(I.15)}$$

$$Fe^{2+} + 2OH^- \rightarrow Fe(OH)_2 \quad \textbf{(I.16)}$$

where the subscript (sol) and (ad) refer to the solution state and adsorption state, respectively.

Figure I.9 shows a case of a sweet corrosion which lead to a failure pipe and stop the operating service. The pitting corrosion is clear shown in the visual and macroscopic observations in the figures I.9 (b and c).

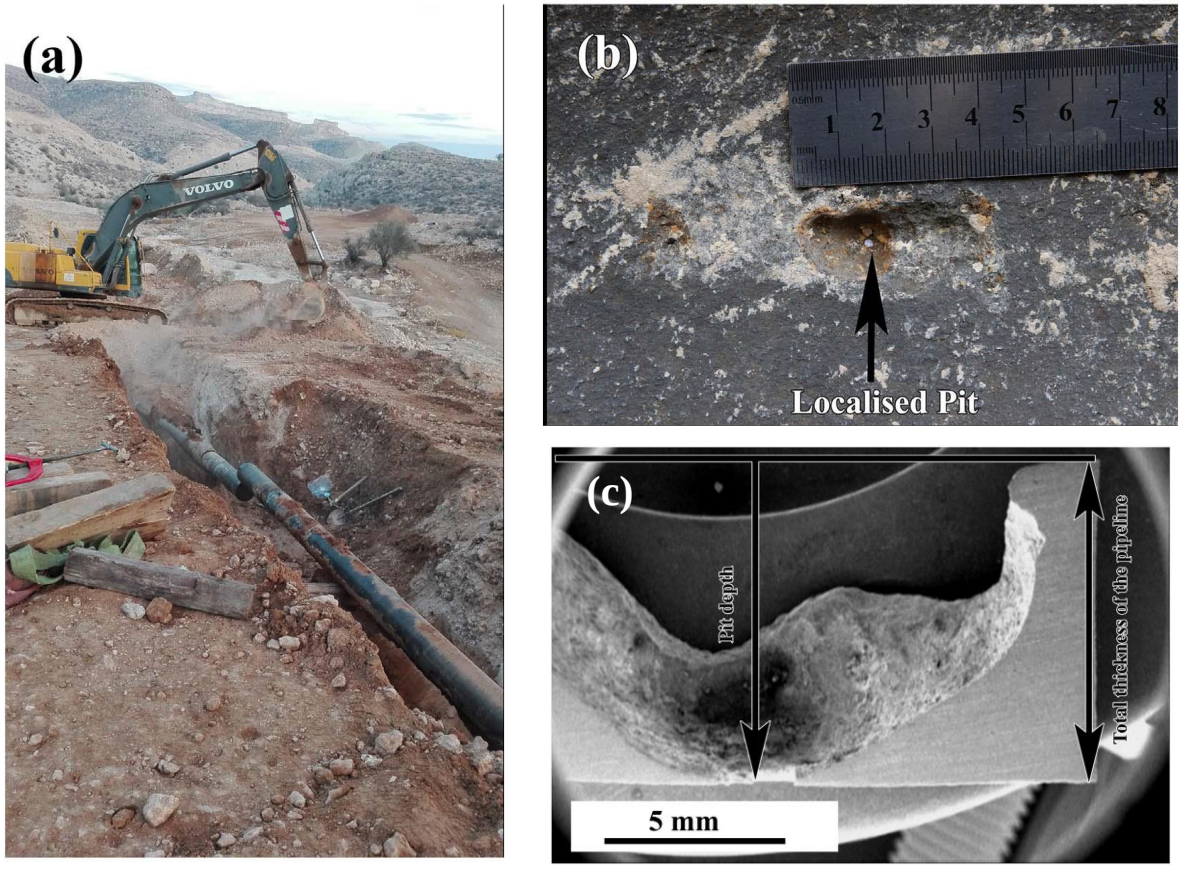

Figure I.9: Failure pipe steel due to CO_2 environment corrosive, (a) Corroded pipe location, (b) visual observation of localized pit corrosion, and (c) metal loss of wall thickness [62].

According to the Javidi and Javidi [62], pipeline steel which covered by iron carbonate is protected to the attack of CO_2 corrosion. Otherwise, the increase of galvanic cell between corrosive media and covered area may create a corrosion due to the difference between anode and cathode.

Zhao et al. have investigated the sweet corrosion on X100 steel based on the temperature effect according to the electrochemical analysis under the static and dynamic conditions. The obtained results present that the temperature has a significant impact on steel corrosive. Furthermore, according to their tests, the corrosion reaction behavior under dynamic condition greatly increases than the static one [63].

I.5.3 Acid corrosion (H_2S)

Hydrogen has a serious effect on corroded metals which could cause the burst on network canalizations. Its embrittlement is a dangerous and complex process that enters within the pipe body and distributes in different locations. Furthermore, these locations may constitute of; grain boundaries, inclusions, voids, dislocation entanglements, micropores, blisters, cracks and dislocation networks. On the other hand, it has also an influence to the mechanical properties of material [64-66].

Hydrogen and sulfur are major elements of hydrocarbon compositions which assist corrosion development and accelerate the failure in the piping systems [67]. As shown in the following reaction (I.17), sulfur (S) and hydrogen sulphide (H_2S) have an influence for initial cracks and create defects on the internal surface of pipeline wall.

$$Fe + H_2S \rightarrow FeS + H_2 \qquad \textbf{(I.17)}$$

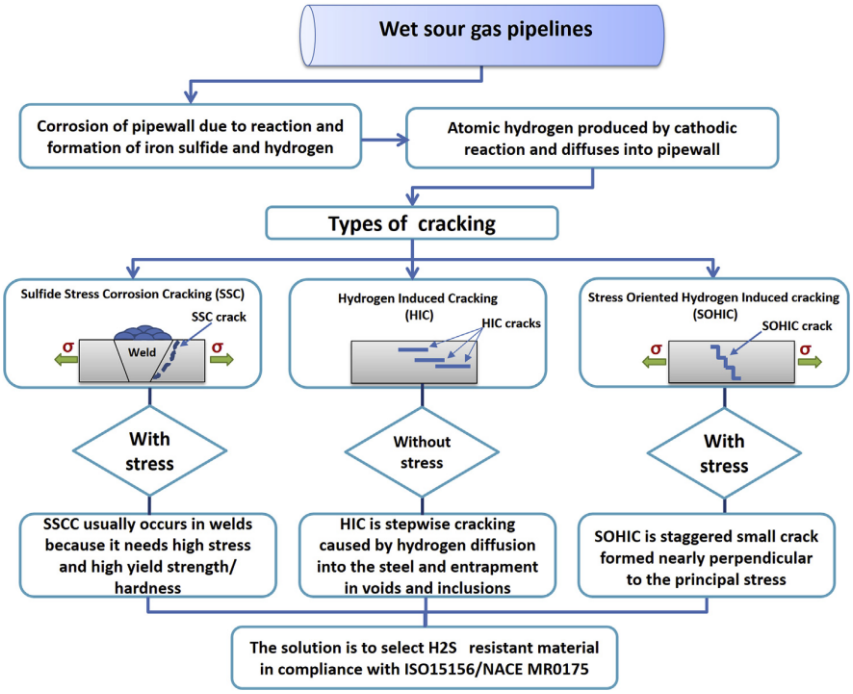

Figure I.10: Most types of cracks caused by H_2S during the transportation of hydrocarbons in pipelines [56].

I.6 CORROSION PROTECTION METHODS

For decades, most companies have attempted to find suitable solutions. Unfortunately, they could not obtain durable solutions heretofore. However, most endeavor in this field classify depending on the maintenance, repairing, and welding. The most used methods in the hydrocarbons field anti-corrosion depend on the control of the boundary conditions, pressure, temperature, the origin of hydrocarbons (with/without presence of undesirable components), nature of piping materials [68]. The commonly used techniques for the protection of hydrocarbons field are as follow [69]:

- Corrosion protection by different layers of coatings;
- Corrosion protection by natural and industrial inhibitors;
- Using the Composite materials at the critical zones;
- Using the welding operation for the ordinary materials

Thus, these techniques lead to an increase in the lifetime of piping system materials. In Order to clarify the common solutions anti-corrosion, the figure I.11 shows the most protection techniques of the corroded piping system taking into account the physical and chemical aspects.

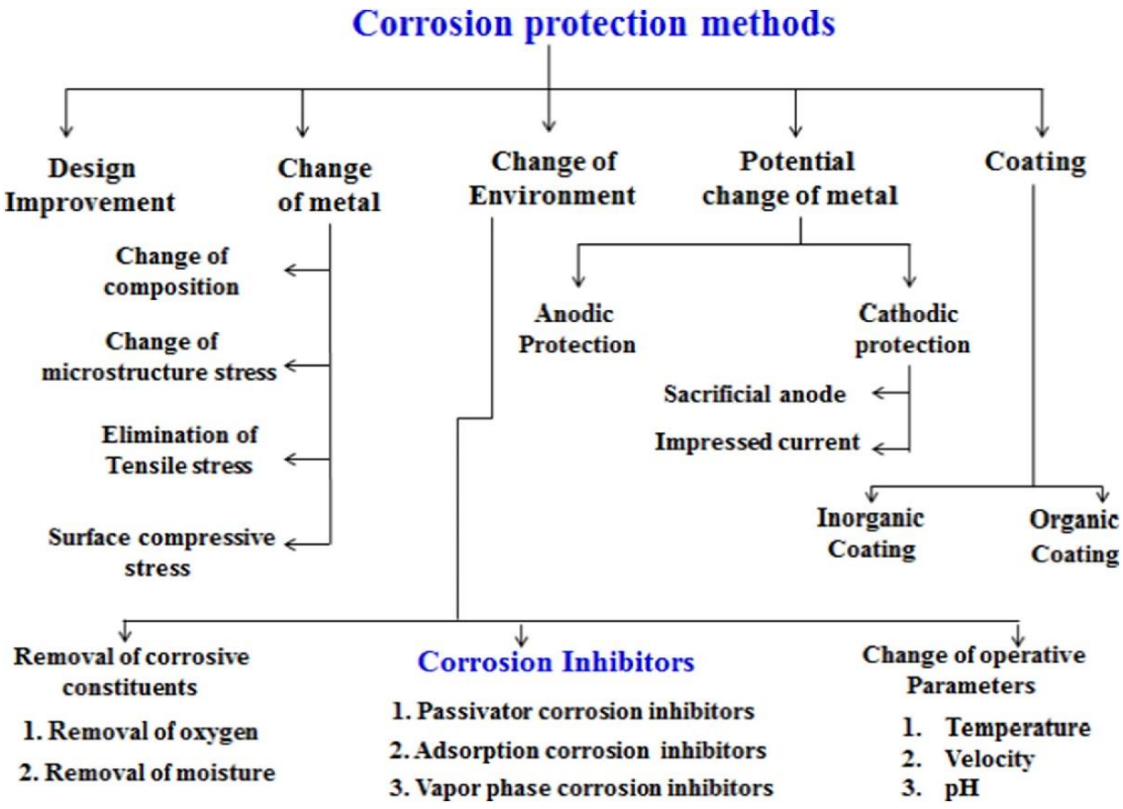

Figure I.11: Protection methods of corroded piping system [69].

I.6.1 Corrosion control by inhibition

In hydrocarbon industries, the inhibitors are among the best solutions for anti-corrosion which have become as important technique to protect piping systems. Furthermore, they create an additional layer in the internal surface of pipeline to prevent corrosive substances such as naphthenic acids, Sulfur, and bacteria which resulted from complex chemical reactions or undesirable components of crude oils to reach into the inner metal surface. The corrosion rate of the pipeline wall depends on the efficiency of the inhibitors taking into account the operating service conditions such as the pressure and the temperature [70-72]. The corrosion inhibitors are activated chemical products that can prevent the corrosion phenomenon where they are added in small concentrations to the transported liquids (crude oil with/without undesirable components) for the aggressive medium (sulfur and naphthenic acids) to avoid, control or decrease the corrosion issue [73].

In fact, there are many kinds of inhibitors such as synthetic inhibitors and eco-friendly inhibitors (green inhibitors). They use depended on the nature of pipeline material and type of fluid flow. Furthermore, the international criteria (human health and environment) must be respected taking into account the operating conditions such as transportation or refining operations.

I.6.2 Composite materials

Another suitable method for repairing corroded pipelines is the composite material which combines from two or more elements with different physical properties and chemical compositions. The composites are used in many fields such as the piping systems, aircraft and medicine even in the satellites. The composite materials are based on the light material with strong mechanical characteristics such as aluminum.

In the last decades, most laboratories in the worldwide attempted to develop some mechanical characteristics of composite materials in order to avoid all kinds of corrosion and damage especially in the critical zones. On the other hand, this technique is based on the fibers composite (materials composite) to repair some corrosion problems or damage of the piping systems especially at elbows and welded joints. Many advantages of composite materials in the hydrocarbon field enable the piping systems to resist the corrosion phenomenon and improve the mechanical characteristics as following [74-77]:

- excellent resistance for corrosion, acids and chemical reactions;
- high strength and stiffness;
- Absorption of crack energy;
- high temperature resistance;
- lightweight;
- low installation and maintenance cost;
- does not mechanically breakdown under ultra violet (UV).

According to the literature, many researchers have proved the qualification of composite materials for restoring the corroded critical pipes into equipment service with a high-quality performance. They have investigated on repair corroded piping systems using experimental investigation and/or numerical analysis in order to prevent the failure and maintain the lifetime of existing line production.

The preparation of composite wrap is based to the international standards, including ASME PCC-2 [78] and ISO/TS 24817 [79] which is suggested in accordance with the company manufacture instruction. Table I.3 presents the different defects that can be repaired by composite materials according to ASME PCC-2 [78] and ISO/TS 24817 [79].

Table I.3: Composite repairs for defective pipes according to ASME PCC-2 and ISO/TS 24817 [80].

Type of defects	ASME PCC-2	ISO/TS 24817
General wall thinning	Y	Y
Local wall thinning	Y	Y
Pitting	Y	Y
Gouges	R	R
Blisters	Y	Y
Laminations	Y	Y
Circumferential cracks	R	Y
Longitudinal cracks	R	R
Through wall penetration	Y	Y

*Y implies generally appropriate

References

[1] Vetter, C.P., Kuebel, L.A., Natarajan, D. and Mentzer, R.A., 2019. Review of failure trends in the US natural gas pipeline industry: An in-depth analysis of transmission and distribution system incidents. *Journal of Loss Prevention in the Process Industries*, 60, pp.317-333, https://doi.org/10.1016/j.jlp.2019.04.014;

[2] Vairo, T., Pontiggia, M. and Fabiano, B., 2021. Critical aspects of natural gas pipelines risk assessments. A case-study application on buried layout. *Process Safety and Environmental Protection*, 149, pp.258-268, https://doi.org/10.1016/j.psep.2020.10.050;

[3] Devold, H., 2013. Oil and gas production handbook: An introduction to oil and gas production, transport, refining and petrochemical industry. *Lulu. com*;

[4] Wauquier, J.P., 1995. Petroleum Refining: Crude oil, petroleum products, process flowsheets (Vol. 1). *Editions Technip*;

[5] Fayomi, O.S.I., Akande, I.G. and Odigie, S., 2019, December. Economic Impact of Corrosion in Oil Sectors and Prevention: An Overview. In *Journal of Physics: Conference Series*, 1378 (2), pp. 022037). IOP Publishing;

[6] Koch, G., Varney, J., Thompson, N., Moghissi, O., Gould, M. and Payer, J., 2016. International measures of prevention, application, and economics of corrosion technologies study. *NACE International*, p.216;

[7] Michel, P.H., Brongers, C.C., Gerhardus, H.K. and Neil, G., 2019. Corrosion costs and preventive strategies in the United States. Publication No. FHWA-RD-01-156. *Technologie and NACE*. https//www. Nace. or/uploadedfiles/publications/ccsupp. pdf Accessed 09 Jan;

[8] Hou, B., Li, X., Ma, X., Du, C., Zhang, D., Zheng, M., Xu, W., Lu, D. and Ma, F., 2017. The cost of corrosion in China. *npj Materials Degradation*, 1(1), pp.1-10, https://doi.org/10.1038/s41529-017-0005-2;

[9] Guidebook, E.R., 2020. Pipeline and Hazardous Materials Safety Administration. *US Department of Transportation*, http://www.phmsa.dot.gov/pipeline/library/data-stats ;

[10] Lam, C. and Zhou, W., 2016. Statistical analyses of incidents on onshore gas transmission pipelines based on PHMSA database. *International Journal of Pressure Vessels and Piping*, 145, pp.29-40, https://doi.org/10.1016/j.ijpvp.2016.06.003;

[11] BBC, 2014, Taiwan gas blasts in Kaohsiung kill at least 25. http://www.bbc.com/news/world-asia-28594693;

[12] Ossai, C.I., Boswell, B. and Davies, I.J., 2015. Pipeline failures in corrosive environments–A conceptual analysis of trends and effects. *Engineering Failure Analysis*, 53, pp.36-58, https://doi.org/10.1016/j.engfailanal.2015.03.004;

[13] Knudson, P., 2012. Accident report, the Columbia gas transmission corporation natural gas pipeline rupture and fire was caused by corrosion and lack of recent inspections. *National Transportation Safety Board (NTSB)*, https://sites.google.com/site/metroforensics3/the-columbia-gas-transmission-corporation-natural-gas-pipeline-rupture-and-fire-was-caused-by-corrosion-and-lack-of-recent-inspections-ntsb-determines;

[14] Shalaby, H.M., Riad, W.T., Alhazza, A.A. and Behbehani, M.H., 2006. Failure analysis of ruptured pipe connected to natural gas pre-heater. *Engineering Failure Analysis*, 13(5), pp.797-804, https://doi.org/10.1016/j.engfailanal.2005.02.005;

[15] Takahashi, K., Ando, K., Matsuo, K. and Urabe, Y., 2014. Estimation of low-cycle fatigue life of elbow pipes considering the multi-axial stress effect. *Journal of Pressure Vessel Technology*, 136(4), p.041405, https://doi.org/10.1115/PVP2012-78678;

[16] Mazhar, H., Ewing, D., Cotton, J.S. and Ching, C.Y., 2013. Experimental investigation of mass transfer in 90 pipe bends using a dissolvable wall technique. *International Journal of Heat and Mass Transfer*, 65, pp.280-288, https://doi.org/10.1016/j.ijheatmasstransfer.2013.06.001;

[17] Tawancy, H.M., Al-Hadhrami, L.M. and Al-Yousef, F.K., 2013. Analysis of corroded elbow section of carbon steel piping system of an oil–gas separator vessel. *Case Studies in Engineering Failure Analysis*, 1(1), pp.6-14, https://doi.org/10.1016/j.csefa.2012.11.001;

[18] Ilman, M.N., 2014. Analysis of internal corrosion in subsea oil pipeline. *case studies in Engineering Failure Analysis*, 2(1), pp.1-8, https://doi.org/10.1016/j.csefa.2013.12.003;

[19] Kusmono and Khasani, 2017. Analysis of a Failed Pipe Elbow in Geothermal Production Facility. *case studies in Engineering Failure Analysis*, 9, pp.71-77, https://doi.org/10.1016/j.csefa.2017.08.001;

[20] Bhowmik, P.K., Hossain, M.E. and Shamim, J.A., 2012. Corrosion and its control in crude oil refining process. *In 6th International Mechanical Engineering & 14th Conference Annual Paper Meet (6IMEC&14APM)*, Dhaka, Bangladesh;

[21] El-Gammal, M., Mazhar, H., Cotton, J.S., Shefski, C., Pietralik, J. and Ching, C.Y., 2010. The hydrodynamic effects of single-phase flow on flow accelerated corrosion in a 90-degree elbow. *Nuclear Engineering and Design*, 240(6), pp.1589-1598, https://doi.org/10.1016/j.nucengdes.2009.12.005;

[22] Saji, V.S. and Umoren, S.A. eds., 2020. Corrosion inhibitors in the oil and gas industry. *John Wiley & Sons*.

[23] Wang, J., Huang, X., Qi, W., Zhang, C., Zhao, Y., Dai, Y., Zhang, T. and Wang, F., 2020. Corrosion failure analysis of the 45-degree elbow in a natural gas gathering pipeline by experimental and numerical simulation. *Engineering Failure Analysis*, 118, p.104889, https://doi.org/10.1016/j.engfailanal.2020.104889;

[24] Dotson, R., Curiel, F., Sacramento, L., Locks, Z. and Duska, J., 2020. Improved methods for sizing metal loss in dents for ECA. *Pipeline Science and Technology*, 4(2), pp.126-136, http://doi.org/10.28999/2514-541X-2020-4-2-126-136;

[25] Wang, L., Yan, C. and Xu, J., 2021. Pipeline Inspection and Quality Assessment. *In Technology Standard of Pipe Rehabilitation*, pp. 21-28, Springer, Singapore, https://doi.org/10.1007/978-981-33-4984-1_6;

[26] Tsai, Y.H., Wang, J., Chien, W.T., Wei, C.Y., Wang, X. and Hsieh, S.H., 2019. A BIM-based approach for predicting corrosion under insulation. *Automation in Construction*, 107, p.102923, https://doi.org/10.1016/j.autcon.2019.102923;

[27] Pei, K.C., Shyu, H.F., Lee, P.H. and Toung, J.C., 2015, October. Development and application of guided wave technology for buried piping inspection in nuclear power plant. *In 2015 IEEE International Ultrasonics Symposium (IUS)*, pp. 1-4. IEEE, https://doi.org/10.1109/ULTSYM.2015.0080;

[28] Vanaei, H.R., Eslami, A. and Egbewande, A., 2017. A review on pipeline corrosion, in-line inspection (ILI), and corrosion growth rate models. *International Journal of Pressure Vessels and Piping*, 149, pp.43-54, https://doi.org/10.1016/j.ijpvp.2016.11.007;

[29] Zelmati, D., Bouledroua, O., Hafsi, Z. and Djukic, M.B., 2020. Probabilistic analysis of corroded pipeline under localized corrosion defects based on the intelligent inspection tool. *Engineering Failure Analysis*, 115, p.104683, https://doi.org/10.1016/j.engfailanal.2020.104683;

[30] Bouledroua, O., Zelmati, D. and Hassani, M., 2019. Inspections, statistical and reliability assessment study of corroded pipeline. *Engineering failure analysis*, 100, pp.1-10, https://doi.org/10.1016/j.engfailanal.2019.02.012;

[31] Soudani, M., Bouledroua, O., Hadj Meliani, M., El-Miloudi, K., Muthanna, B.G.N., Khelil, A., Elhoud, A., Matvienko, Y.G. and Pluvinage, G., 2018. Corrosion inspection and recommendation on the internal wall degradation caused rupture of 6" gas line pipe. *Journal of Bio-and Tribo-Corrosion*, 4(2), pp.1-6, https://doi.org/10.1007/s40735-018-0145-0;

[32] Suleiman, R.K., Kumar, A.M., Adesina, A.Y., Al-Badour, F.A., Hadj Meliani, M. and Saleh, T.A., 2020. Hybrid organosilicon-metal oxide composites and their corrosion protection performance for mild steel in 3.5% NaCl solution. *Corrosion Science*, 169, p.108637, https://doi.org/10.1016/j.corsci.2020.108637;

[33] Muthanna, B.G.N., Amara, M., Hadj Meliani, M., Mettai, B., Božić, Ž., Suleiman, R. and Sorour, A.A., 2019. Inspection of internal erosion-corrosion of elbow pipe in the desalination station. *Engineering Failure Analysis*, 102, pp.293-302, https://doi.org/10.1016/j.engfailanal.2019.04.062;

[34] Mishra, P., Yavas, D., Bastawros, A.F. and Hebert, K.R., 2020. Electrochemical impedance spectroscopy analysis of corrosion product layer formation on pipeline steel. *Electrochimica Acta*, 346, p.136232, https://doi.org/10.1016/j.electacta.2020.136232;

[35] Khamaysa, O.M.A., Selatnia, I., Zeghache, H., Lgaz, H., Sid, A., Chung, I.M., Benahmed, M., Gherraf, N. and Mosset, P., 2020. Enhanced corrosion inhibition of carbon steel in HCl solution by a newly synthesized hydrazone derivative: Mechanism exploration from electrochemical, XPS, and computational studies. *Journal of Molecular Liquids*, 315, p.113805, https://doi.org/10.1016/j.molliq.2020.113805;

[36] Al-Owaisi, S., Becker, A.A., Sun, W., Al-Shabibi, A., Al-Maharbi, M., Pervez, T. and Al-Salmi, H., 2018. An experimental investigation of the effect of defect shape and orientation on the burst pressure of pressurised pipes. *Engineering Failure Analysis*, 93, pp.200-213, https://doi.org/10.1016/j.engfailanal.2018.06.011;

[37] Soudani, M., Hadj Meliani, M., El-Miloudi, K., Azari, Z., Sorour, A.A., Merah, N. and Pluvinage, G., 2018. Reduction of hydrogen embrittlement of API 5l X65 steel pipe using a green inhibitor. *International Journal of Hydrogen Energy*, 43(24), pp.11150-11159, https://doi.org/10.1016/j.ijhydene.2018.04.236;

[38] Contreras, A., Hernández, S.L., Orozco-Cruz, R. and Galvan-Martínez, R., 2012. Mechanical and environmental effects on stress corrosion cracking of low carbon pipeline steel in a soil solution. *Materials & Design*, 35, pp.281-289, https://doi.org/10.1016/j.matdes.2011.09.011;

[39] Nasser, A.M.M., Montasir, O.A., Zawawi, N.W.A. and Alsubal, S., 2020, April. A review on oil and gas pipelines corrosion growth rate modelling incorporating artificial intelligence approach. *In IOP Conference Series: Earth and Environmental Science*, 476 (1), p. 012024, https://doi.org/10.1088/1755-1315/476/1/012024;

[40] Shuai, Y., Shuai, J. and Xu, K., 2017. Probabilistic analysis of corroded pipelines based on a new failure pressure model. *Engineering failure analysis*, 81, pp.216-233, https://doi.org/10.1016/j.engfailanal.2017.06.050;

[41] Wang, Y., Zhang, P. and Qin, G., 2021. Reliability assessment of pitting corrosion of pipeline under spatiotemporal earthquake including spatial-dependent corrosion growth. *Process Safety and Environmental Protection*, 148, pp.166-178, https://doi.org/10.1016/j.psep.2020.10.005;

[42] Caleyo, F., Velázquez, J.C., Valor, A. and Hallen, J.M., 2009. Probability distribution of pitting corrosion depth and rate in underground pipelines: A Monte Carlo study. *Corrosion Science*, 51(9), pp.1925-1934, https://doi.org/10.1016/j.corsci.2009.05.019;

[43] Velázquez, J.C., Van Der Weide, J.A.M., Hernández, E. and Hernández, H.H., 2014. Statistical modelling of pitting corrosion: extrapolation of the maximum pit depth-growth. *International Journal of Electrochemical Science*, 9(8), pp.4129-4143, http://www.electrochemsci.org/papers/vol9/90804129.pdf;

[44] Caleyo, F., Velázquez, J.C., Valor, A. and Hallen, J.M., 2009. Markov chain modelling of pitting corrosion in underground pipelines. *Corrosion Science*, 51(9), pp.2197-2207, https://doi.org/10.1016/j.corsci.2009.06.014;

[45] Jiménez-Come, M.J., Turias, I.J. and Ruiz-Aguilar, J.J., 2016. A two-stage model based on artificial neural networks to determine pitting corrosion status of 316L stainless steel. *Corrosion Reviews*, 34(1-2), pp.113-125, https://doi.org/10.1515/corrrev-2015-0048;

[46] Valeh-e-Sheyda, P., Rashidi, H. and Azimi, N., 2018. Structural improvement of a control valve to prevent corrosion in acid gas treating plant pipeline: an experimental and computational analysis. *International Journal of Pressure Vessels and Piping*, 165, pp.114-125, https://doi.org/10.1016/j.ijpvp.2018.06.008;

[47] Hu, H. and Cheng, Y.F., 2016. Modeling by computational fluid dynamics simulation of pipeline corrosion in CO2-containing oil-water two phase flow. *Journal of Petroleum Science and Engineering*, 146, pp.134-141, https://doi.org/10.1016/j.petrol.2016.04.030;

[48] ASME, Manual for Determining the Remaining Strength of Corroded Pipelines- a Supplement to ASME B31 Code for Pressure Piping, *The American Society of Mechanical Engineers*, New York, 1991;

[49] Kiefner, J. and Vieth, P., 1989. A Modified Criterion for Evaluating the Remaining Strength of Corroded Pipe, Final Report on Project PR 3-805, *Battelle Memorial Institute*, Columbus, OH;

[50] DNV Recommended Practice, RP-F101. Corroded pipelines. *Det Norske Veritas*, 2004;

[51] Ritchie, D. and Last, S., 1995, April. Burst criteria of corroded pipelines-defect acceptance criteria. *In Proceedings of the EPRG/PRC 10th biennial joint technical meeting on line pipe research*, UK, Paper 32, pp. 1-11;

[52] Kiefner, J.F. and Vieth, P.H., 1990. PC program speeds new criterion for evaluating corroded pipe. *Oil and Gas Journal*, (USA), 88(34);

[53] Stephens, D.R. and Leis, B.N., 2000, October. Development of an alternative criterion for residual strength of corrosion defects in moderate-to high-toughness pipe. *In international pipeline conference*, (Vol. 40252, p. V002T06A012). *American Society of Mechanical Engineers (ASME)*, https://doi.org/10.1115/IPC2000-192;

[54] Bhardwaj, A., 2017. Petroleum fluids properties and production schemes: Effect on corrosion. *Trends in Oil and Gas Corrosion Research and Technologies*, pp.31-52, https://doi.org/10.1016/B978-0-08-101105-8.00002-4;

[55] Palanisamy, G., 2019. Corrosion inhibitors. *Corrosion inhibitors*, p.24.;

[56] Askari, M., Aliofkhazraei, M. and Afroukhteh, S., 2019. A comprehensive review on internal corrosion and cracking of oil and gas pipelines. *Journal of Natural Gas Science and Engineering*, 71, p.102971, https://doi.org/10.1016/j.jngse.2019.102971;

[57] Sridhar, N., Dunn, D.S., Anderko, A.M., Lencka, M.M. and Schutt, H.U., 2001. Effects of water and gas compositions on the internal corrosion of gas pipelines—modeling and experimental studies. *Corrosion*, 57(3), pp.221-235;

[58] Lyle Jr, F.F., 1997. Carbon dioxide/hydrogen sulfide corrosion under wet low-flow gas pipeline conditions in the presence of bicarbonate, chloride, and oxygen. *Final report (No. AGA-99001937). Southwest Research Inst. (United States)*;

[59] Colahan, M., Young, D., Singer, M. and Nogueira, R.P., 2018. Black powder formation by dewing and hygroscopic corrosion processes. *Journal of Natural Gas Science and Engineering*, 56, pp.358-367, https://doi.org/10.1016/j.jngse.2018.06.021;

[60] Trabulsi, M.M., 2007. Black powder in sales'-gas transmission pipelines. *Journal of Pipeline Engineering*, 6(4), p.245;

[61] Khan, T.S. and Al-Shehhi, M.S., 2015. Review of black powder in gas pipelines–An industrial perspective. *Journal of Natural Gas Science and Engineering*, 25, pp.66-76, https://doi.org/10.1016/j.jngse.2015.04.025;

[62] Javidi, M. and Bekhrad, S., 2018. Failure analysis of a wet gas pipeline due to localised CO_2 corrosion. *Engineering Failure Analysis*, 89, pp.46-56, https://doi.org/10.1016/j.engfailanal.2018.03.006;

[63] Zhao, J., Xiong, D., Gu, Y., Zeng, Q. and Tian, B., 2019. A comparative study on the corrosion behaviors of X100 steel in simulated oilfield brines under the static and dynamic conditions. *Journal of Petroleum Science and Engineering*, 173, pp.1109-1120, https://doi.org/10.1016/j.petrol.2018.10.072;

[64] Djukic, M.B., Zeravcic, V.S., Bakic, G.M., Sedmak, A. and Rajicic, B., 2015. Hydrogen damage of steels: A case study and hydrogen embrittlement model. *Engineering Failure Analysis*, 58, pp.485-498, https://doi.org/10.1016/j.engfailanal.2015.05.017;

[65] Boukortt, H., Amara, M., Hadj Meliani, M., Bouledroua, O., Muthanna, B.G.N., Suleiman, R.K., Sorour, A.A. and Pluvinage, G., 2018. Hydrogen embrittlement effect on the structural integrity of API 5L X52 steel pipeline. *International Journal of Hydrogen Energy*, 43(42), pp.19615-19624, https://doi.org/10.1016/j.ijhydene.2018.08.149;

[66] Elazzizi, A., Hadj Meliani, M., Khelil, A., Pluvinage, G. and Matvienko, Y.G., 2015. The master failure curve of pipe steels and crack paths in connection with hydrogen embrittlement. *International Journal of Hydrogen Energy*, 40(5), pp.2295-2302, https://doi.org/10.1016/j.ijhydene.2014.12.040;

[67] Meriem-Benziane, M., Bou-Saïd, B. and Boudouani, N., 2017. The effect of crude oil in the pipeline corrosion by the naphthenic acid and the sulfur: A numerical approach. *Journal of Petroleum Science and Engineering*, 158, pp.672-679, https://doi.org/10.1016/j.petrol.2017.08.073;

[68] Lyon, S.B., Bingham, R. and Mills, D.J., 2017. Advances in corrosion protection by organic coatings: What we know and what we would like to know. *Progress in Organic Coatings*, 102, pp.2-7, https://doi.org/10.1016/j.porgcoat.2016.04.030;

[69] Verma, C., Ebenso, E.E. and Quraishi, M.A., 2017. Ionic liquids as green and sustainable corrosion inhibitors for metals and alloys: an overview. *Journal of Molecular Liquids*, 233, pp.403-414, https://doi.org/10.1016/j.molliq.2017.02.111;

[70] Bharatiya, U., Gal, P., Agrawal, A., Shah, M. and Sircar, A., 2019. Effect of corrosion on crude oil and natural gas pipeline with emphasis on prevention by ecofriendly corrosion inhibitors: a comprehensive review. *Journal of Bio-and Tribo-Corrosion*, 5(2), pp.1-12, https://doi.org/10.1007/s40735-019-0225-9;

[71] Umoren, S.A., Obot, I.B., Madhankumar, A. and Gasem, Z.M., 2015. Performance evaluation of pectin as ecofriendly corrosion inhibitor for X60 pipeline steel in acid medium: Experimental and theoretical approaches. *Carbohydrate polymers*, 124, pp.280-291, https://doi.org/10.1016/j.carbpol.2015.02.036;

[72] Tian, H., Li, W., Hou, B. and Wang, D., 2017. Insights into corrosion inhibition behavior of multi-active compounds for X65 pipeline steel in acidic oilfield formation water. *Corrosion Science*, 117, pp.43-58, https://doi.org/10.1016/j.corsci.2017.01.010;

[73] Orazem, M. ed., 2014. Underground pipeline corrosion (No. 63). *Elsevier*;

[74] da Costa Mattos, H.S., Reis, J.M.L., Paim, L.M., Da Silva, M.L., Junior, R.L. and Perrut, V.A., 2016. Failure analysis of corroded pipelines reinforced with composite repair systems. *Engineering Failure Analysis*, 59, pp.223-236, https://doi.org/10.1016/j.engfailanal.2015.10.007;

[75] Budhe, S., Banea, M.D. and de Barros, S., 2020. Composite repair system for corroded metallic pipelines: an overview of recent developments and modelling. *Journal of Marine Science and Technology*, 25(4), pp.1308-1323, https://doi.org/10.1007/s00773-019-00696-3;

[76] Junior, M.W., Reis, J.M.L. and da Costa Mattos, H.S., 2017. Polymer-based composite repair system for severely corroded circumferential welds in steel pipes. *Engineering Failure Analysis*, 81, pp.135-144, https://doi.org/10.1016/j.engfailanal.2017.08.001;

[77] Meriem-Benziane, M., Abdul-Wahab, S.A., Zahloul, H., Babaziane, B., Hadj-Meliani, M. and Pluvinage, G., 2015. Finite element analysis of the integrity of an API X65 pipeline with a longitudinal crack repaired with single-and double-bonded composites. *Composites Part B: Engineering*, 77, pp.431-439, https://doi.org/10.1016/j.compositesb.2015.03.008;

[78] PCC, A., 2011. 2 (2011) Repair of pressure equipment and piping. *The American Society of Mechanical Engineers*, New York;

[79] ISO, 2006. Petroleum, Petrochemical and Natural Gas Industries. Composite Repairs for Pipe Work—Qualification and Design, Installation, Testing and Inspection. *ISO/TS 24817*;

[80] Lim KS, Azraai SN, Noor NM, Yahaya N. An overview of corroded pipe repair techniques using composite materials. *International Journal of Materials and Metallurgical Engineering*, 2016;10(1):19-25, https://doi.org/10.5281/zenodo.1110684;

CHAPTER II:

INTEGRITY ASSESSMENT OF CORRODED PIPELINES

II.1 INTRODUCTION

The fracture mechanics is one of the main domains to evaluate the behavior of piping systems. Furthermore, it can be used to analyze the structural safety especially the pipes and elbows including welded joins. In addition, the nature of piping systems, fluid behavior and operating conditions should be taken into account as parts of pipeline integrity. In this chapter, the assessment of pipelines with and without defects was presented. The pipeline integrity including the engineering codes and developed mathematical formula were described due to their great importance for maintaining the pipelines and elbows under service a long time possible. Generally, there are many methods used in the industrial companies such as ASME B31G, RSTRENG, Shell-92, DNV RP-F101, PCORRC and CHOI model in order to evaluate the corrosion phenomenon. Finally, the failure assessment diagram (FAD) was mentioned as an important technique to evaluate the effect of crack on the safety of piping systems which can indicate the critical points.

II.2 RELIABILITY ASSESSMENT OF INTACT PIPELINES

The piping systems are exposed to dangerous phenomena including fatigue, corrosion, erosion, damage, and other problems due to the severe operating conditions such as the pressure, temperature and external environment on the one hand and on other hand the material used, the dimensions and the forms of transport systems (elbows or straight-line). In fact, it presents the model of stress–strain which is considered as power low for nonlinear types of steel as follow:

$$\begin{cases} \sigma = E\varepsilon & \sigma < \sigma_y \\ \sigma = K\varepsilon^n & \sigma \geq \sigma_y \end{cases} \quad \textbf{(II.1)}$$

where σ and ε represent the true stress and true strain in the uniaxial direction, respectively. E and σ_y represent Young's modulus and yield strength, respectively. K is a coefficient of the power-law stress-strain relationship in the plastic domain case and n is the strain hardening exponent.

To define the mechanical properties of piping system materials, engineering stress-strain and true stress-strain are still the important parameters which can be obtained by the experimental tests and numerical predictions [1]. To study the mechanical characteristics of piping systems for different kinds of material, the finite element method is used to simulate the behaviour,

where this method is used in our study (chapter III). For example, the mechanical properties of API 5L X52 pipeline steel were selected according to the nonlinear true stress-strain behaviour as shown in figure II.1 [2].

The engineering stress-strain curve was converted to a true stress-strain curve using logarithmic equations. This conversation covers a large region of the engineering stress-strain curves – from the beginning of the test until the moment when the ultimate strength of the specimen is reached [2]. In the brittle domain, $\sigma(\varepsilon)$ is given to $\sigma'(\varepsilon')$. In the ductile domain, $\sigma(\varepsilon)$ is changed to $\sigma'(\varepsilon')$ as follows up through the test conditions:

$$\varepsilon = \ln(1+\varepsilon') \quad \textbf{(II.2)}$$

$$\sigma = \sigma'(1+\varepsilon') \quad \textbf{(II.3)}$$

The appreciation value of *n* can be written as following [3]:

$$n = 0.239\left(\frac{1}{\sigma_y / \sigma'_{ult}} - 1\right)^{0.596} \quad \textbf{(II.4)}$$

The value of *n, K* can be appreciated through the following equation [4]:

$$K = \left(e/n\right)^n \sigma'_{ult} \quad \textbf{(II.5)}$$

where *e* is the coefficient base of the natural logarithm which is equal to 2.7183 [5].

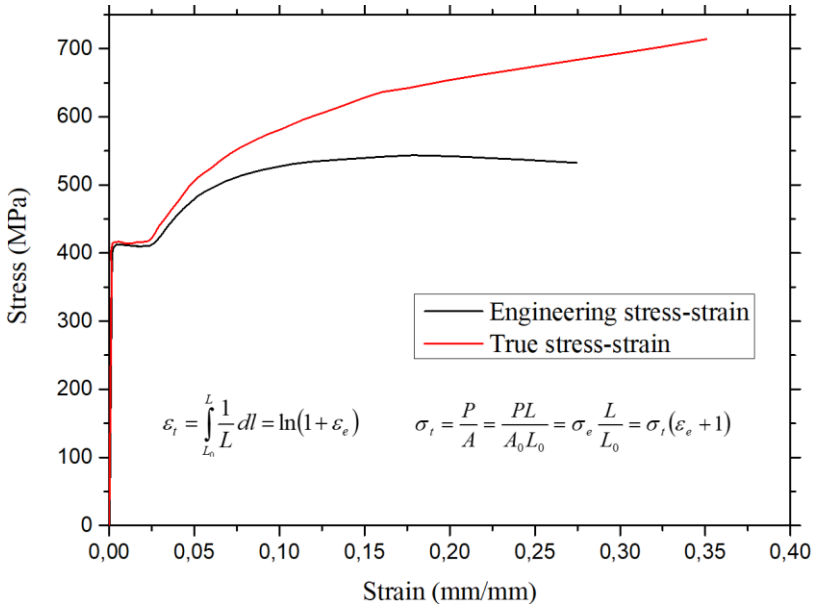

Figure II.1. Engineering and true stress-strain curves of API 5L X52 pipeline steel [2].

Table II.1: Mechanical properties of API X-grade pipelines [6-9]

API 5L pipeline	Yield Strength (σ_y) min – max (MPa)	Ultimate Strength (σ_{ult}) min – max (MPa)	Elongation to Failure A%
X42	290 - 495	415 - 655	23
X46	320 - 525	435 - 655	22
X52	360 - 530	460 - 760	21
X56	390 - 545	490 - 760	19
X60	415 - 565	520 - 760	19
X65	450 - 600	535 - 760	18
X70	485 - 635	570 - 760	18
X80	555 - 705	625 - 825	17
X100	690 - 840	760 - 990	7
X120	830 – 1050	915 - 1145	7

Due to the operating conditions such as the pressure and temperature taking into account the mechanical characteristics of the material, patterns of flow, and nature of fluid flow, the piping systems are subjected to three types of stresses; hoop stress (σ_θ), longitudinal stress (σ_l) and radial stress (σ_r) as shown in figure II.2 which are expressed by equations (II.6, II.7 and II.8) [1].

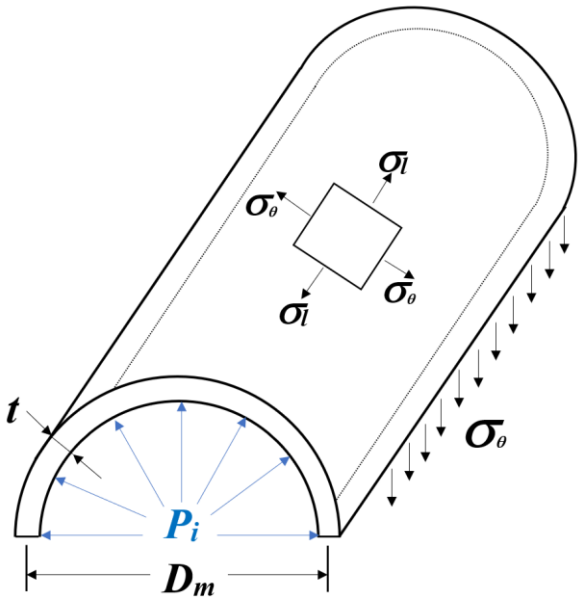

Figure II.2: Hoop and longitudinal stresses in pipeline which subjected to internal pressure.

$$\sigma_\theta = \frac{P_i D_m}{2t} \quad \textbf{(II.6)}$$

$$\sigma_l = \frac{P_i D_m}{4t} \quad \textbf{(II.7)}$$

$$\sigma_r \approx 0 \quad \textbf{(II.8)}$$

The elbow is one of the important parts of the piping system which used to connect and to change the direction of fluid flow. In addition, it is considered a critical component in the piping system due to its geometry, its dimensions and the degree of bend radius. On the using aspect, its curvature makes the value of hoop stress is greater than the on straight pipe (see figure II.3). On the other hand, the longitudinal and radial stresses keep the same value for straight pipes and elbows. Thus, the degree of bend does not affect on the longitudinal stress [10].

The behavior analysis of elbow during flow shows that the intrados area is subjected to the highest hoop stress, while the extrados zone has the lowest hoop stress as illustrated in equation II.9 [10]. In addition, the increasing of bend radius leads to increase the hoop stress at the extrados area, but it decreases at the intrados area [11].

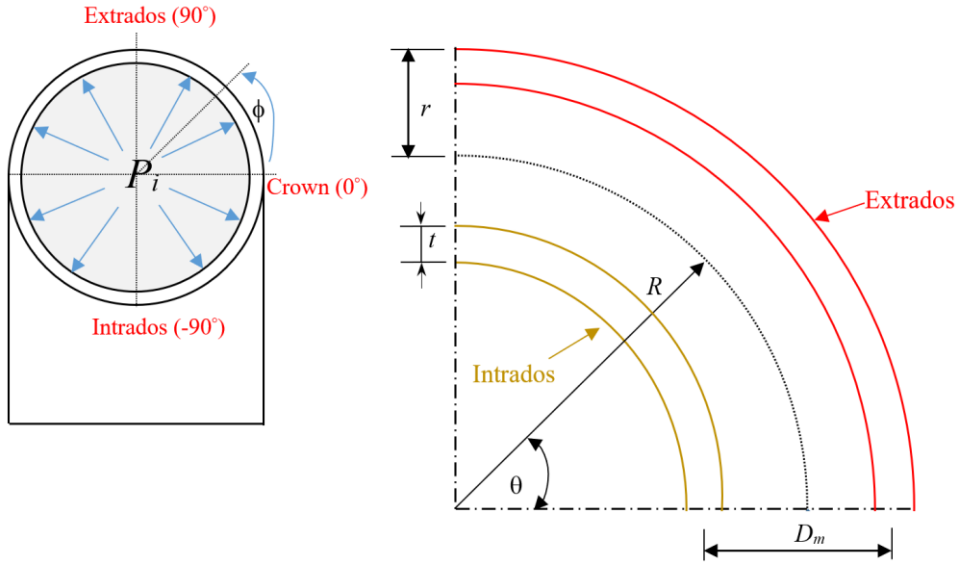

Figure II.3: Geometrical model of a 90° pipe elbow subjected to internal pressure.

To study the behaviour of piping systems including the elbows, the hoop stress is still an important factor where the constant value *C* has directly relationship with the circumferential stress of straight pipe as shown in the equation II.9. However, the constant C changes according

to the selected location along the bend of elbow and its sides (intrados, crown or extrados), where it is calculated through the equations II.9 and II.10 [1, 12-14].

$$\sigma_\theta = \frac{1}{C} \times \frac{P_i D_m}{2t} \qquad \textbf{(II.9)}$$

$$C = \begin{cases} \dfrac{(R/r)-1}{(R/r)-(1/2)} & \rightarrow Intrados \\ 1 & \rightarrow Crown \\ \dfrac{(R/r)+1}{(R/r)+(1/2)} & \rightarrow Extrados \end{cases} \qquad \textbf{(II.10)}$$

However, the circumferential stress calculation (hoop stress) at the crown section is still the same with straight pipe formulation (equation II.6).

The piping systems without defect or corrosion phenomena taking into account the operating conditions can calculate the burst pressure through the following equation [15]:

$$P_f = \left(\frac{k}{2}\right)^{n+1} \frac{4t}{D} \sigma_{ult} \qquad \textbf{(II.11a)}$$

k considers a material constant which based on the yield failure criterion in accordance to one of the three approaches; Tresca, Von-Mises or ASSY (Average Shear Stress Yield) criteria [15].

$$k = \begin{cases} 1 & \rightarrow \quad Tresca \\ 2/\sqrt{3} & \rightarrow \quad Von-Mises \\ (1/2)+(1/\sqrt{3}) & \rightarrow \quad ASSY \end{cases} \qquad \textbf{(II.11b)}$$

$$\tau_{\max} = \max\left(\frac{|\sigma_1-\sigma_2|}{2}, \frac{|\sigma_2-\sigma_3|}{2}, \frac{|\sigma_1-\sigma_3|}{2}\right) = \frac{\sigma_0}{2} \qquad \textbf{(II.12)}$$

$$\sigma_{VM} = \sqrt{\frac{1}{6}\left[(\sigma_1-\sigma_2)^2+(\sigma_2-\sigma_3)^2+(\sigma_3-\sigma_1)^2\right]} = \frac{\sigma_0}{\sqrt{3}} \qquad \textbf{(II.13)}$$

$$\tau_{ASSY} = \frac{1}{2}\left(\tau_{\max} + \sqrt{\frac{3}{2}}\tau_{oct}\right) = \frac{2+\sqrt{3}}{4\sqrt{3}}\sigma_0 \qquad \textbf{(II.14)}$$

II.3 CRACK APPROXIMATION

The crack is one of the principal indicators to detect the state of piping systems through the manner of propagation of crack along the critical zones [16]. The concentration of pressure in the critical zones such as defects, small cracks, and welding joint is considered the main reasons which lead to corrosion, wear, and damage taking into account the temperatures and geometry of piping systems.

The figure II.4 shows that the estimated stress leads to ideal crack which can exhibit the linear elasticity without using the LEFM concept [17]. Thus, this method involves a flaw due to the relating with real conditions which find on the plastic zone when the ideal crack is able to be warranted to present the same behavior as the real crack. Consequently, the LEFM concept includes a large warranted to show the same behavior as the real crack [17].

II.4 STRESS INTENSITY FACTORS (SIFs)

The stress intensity factor considers as a main parameter for assessing the fracture mechanics and pipeline integrity. In particular, it is used to determinate the stress at critical positions such as the weak location, crack area, welding position and elbows.

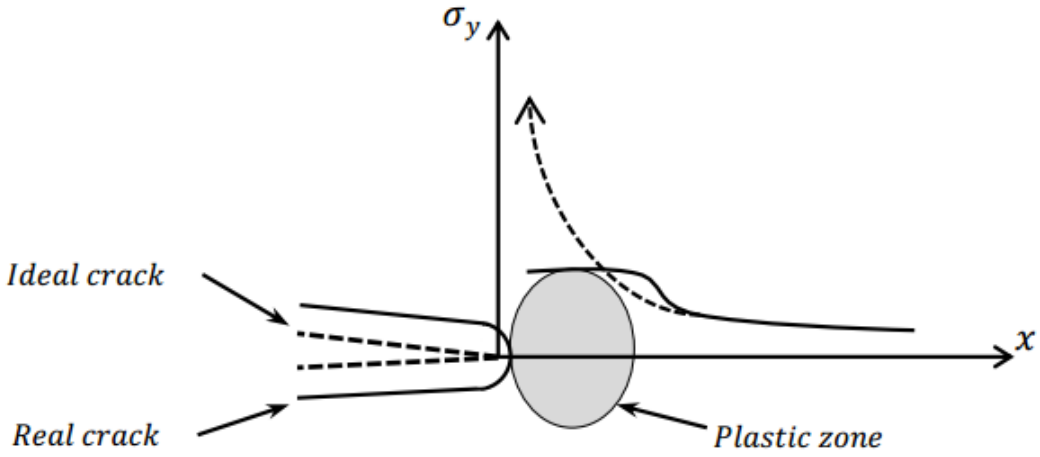

Figure II.4 Stress behavior for an ideal and real crack [17].

In fact, the stress intensity factors are still important factors to measure the durability taking into consideration the nature of cracks, their form, their thickness and their position (elbows, welded joins). The stress intensity factor is considered as a factor to measure maximum values of stresses which are depended to the mechanical characteristics.

Irwin [18] is one of the first scientists who has studied the behavior of energy around cracks using SIFs. He has presented that there are three kinds of SIF depending on the distribution of forces on the surfaces and the propagation of the energy along the crack. The three modes (figure II.5) are as follow: (i) mode I (an opening; tensile), (ii) mode II (in-plane shear), and (iii) mode II (tearing-antiplane shear). In fact, K_I (mode I) has more influence than the other modes K_{II} (mode II) and K_{III} (mode III) in the longitudinal crack case [18-21].

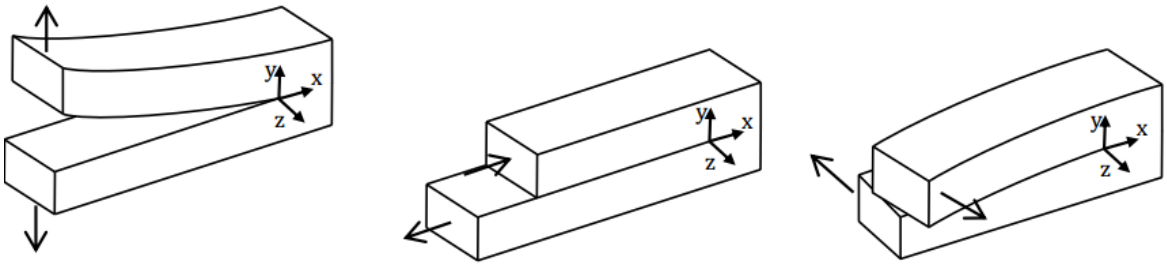

(a) (b) (c)

Figure II.5 Three standard loading modes of a crack, (a) opening mode, (b) in-plane shear mode, and (c) tearing-antiplane shear mode [17].

To analyze the cracks, SIFs are based on the stresses /shears in three directions X, Y and Z. Figure II.6 shows the coordinate system describing the stresses near the crack front.

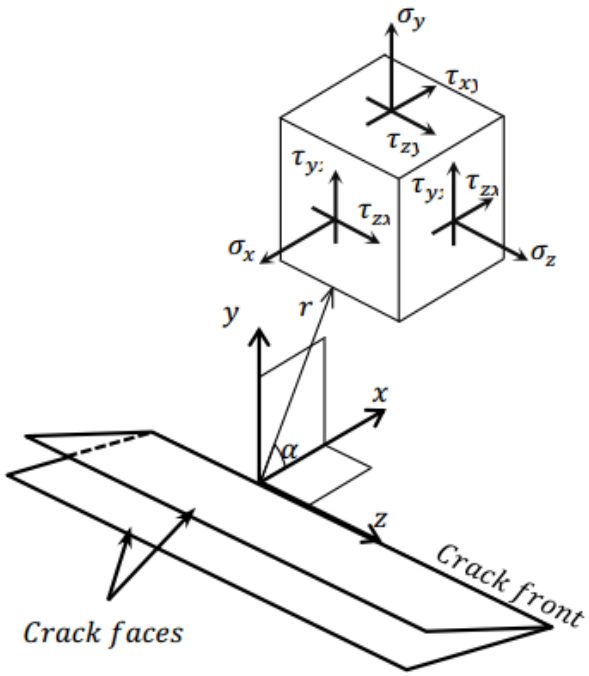

Figure II.6 Coordinate system and typical stress components near the crack extremities [17].

SIFs for mode I (an opening; tensile), mode II (in-plane shear), and mode III (tearing-antiplane

shear) are given as following equations respectively:

$$\lim_{r\to 0}\sigma_{ij}^{(I)} = \frac{K_I}{\sqrt{2\pi r}} f_{ij}^{(I)}(\phi) \quad \textbf{(II.15a)}$$

$$\lim_{r\to 0}\sigma_{ij}^{(II)} = \frac{K_{II}}{\sqrt{2\pi r}} f_{ij}^{(II)}(\phi) \quad \textbf{(II.15b)}$$

$$\lim_{r\to 0}\sigma_{ij}^{(III)} = \frac{K_{III}}{\sqrt{2\pi r}} f_{ij}^{(III)}(\phi) \quad \textbf{(II.15c)}$$

where σ_{ij} is the stress/shear in the particular direction. A mixed-mode phenomenon depends on the form of geometry and crack direction, where the calculate of total stress is given by the sum of different stresses [22]:

$$\sigma_{ij}^{(total)} = \sigma_{ij}^{(I)} + \sigma_{ij}^{(II)} + \sigma_{ij}^{(III)} \quad \textbf{(II.16)}$$

However, the curvature is the main feature of elbow, where the mixed mode of loading (K_I, K_{II}, and K_{III}) can be shown. Moreover, it increases the difficulty to analyze the crack behavior due to the presence of three patterns (modes) at the same position. Depending on the presence of three modes, the equivalent stress intensity factor (K_{eq}) is written by the following equation:

$$K_{eq}^2 = K_I^2 + K_{II}^2 + (1+\nu)K_{III}^2 \quad \textbf{(II.17)}$$

II.4.1 SIF for semi-elliptical cracks

Piping systems including elbows are still as important tools to transport hydrocarbons energy worldwide. The external environment and operating conditions including temperature, humidity, drought, high velocity, and welding positions can accelerate the corrosion phenomenon especially with the presence of defects in the pipelines. The corrosion usually appears in irregular forms which make the difficulty for studying them. To overcome these difficulties and approach to the real conditions, many studies have proposed regular forms such as a semi-elliptic (parabolic), a semi spheric or a semi-rectangular to analyze their behavior through analytical, experimental and/or numerical methods according to standard conditions [23-32].

The analyses proved that the concentration of stress in the semi-elliptic is focused at the middle zone of cracks and defects while in the case of the rectangular shape is located in the rounded zones along the defect area [33]. Figure II.5 illustrates the semi-elliptical corrosion shape in the external surface of pipeline.

Stress intensity factor of mode I at any point along the semi-elliptical surface crack can be calculate using the following equation:

$$K_I = \sigma_\theta . F \sqrt{\pi d / Q} \left(\frac{d}{t}, \frac{d}{c}, \frac{R}{t}, \phi \right) \quad \textbf{(II.18)}$$

The K factor for an external surface crack in pipeline under the high pressure is written as following [34]

$$K_I = \frac{P_i D_{ext}}{2t} \times F \sqrt{\pi d / Q} \left(\frac{d}{t}, \frac{d}{c}, \frac{R}{t}, \phi \right) \quad \textbf{(II.19)}$$

Where the parameters P_i, r, t, F, d, and c are the internal pressure, internal radius, wall thickness of pipeline, the geometry and crack size correction factor, crack depth, the crack half-length on the surface, respectively. ϕ is the parametric angle where the stress can be concentrated along the crack front (Figure II.7).

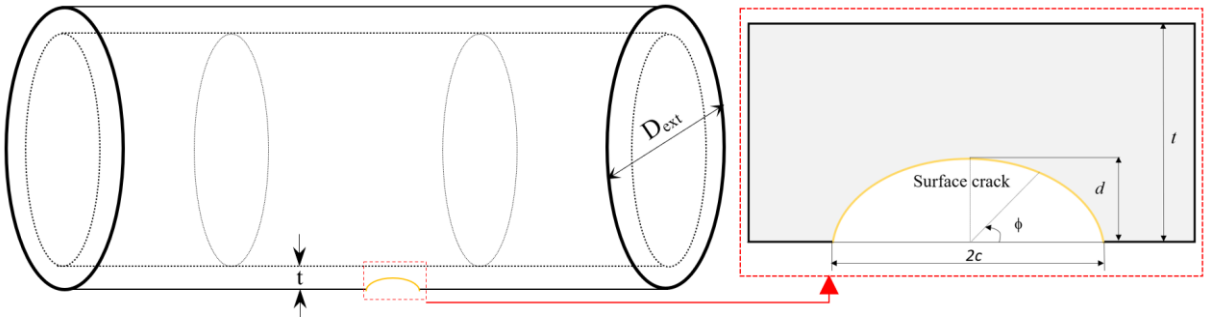

Figure II.7: Semi-elliptical crack in a piping system

The maximum value of K_I is located at the deepest point of the crack front ϕ = 90° [22]. Q is the form of an ellipse which is formed by different cases through values of d/c [34]. An empirical equation for Q is given by follow equations:

$$Q = 1 + 1.464\left(\frac{d}{c}\right)^{1.65} \quad for \frac{d}{c} \le 1 \qquad \textbf{(II.20a)}$$

$$Q = 1 + 1.464\left(\frac{c}{d}\right)^{1.65} \quad for \frac{d}{c} > 1 \qquad \textbf{(II.20b)}$$

$$F = 0.97\left[M_1 + M_2\left(d/t\right)^2 + M_3\left(d/t\right)^4\right] f_c \qquad \textbf{(II.20c)}$$

$$M_1 = 1.13 + 0.09\left(d/c\right) \qquad \textbf{(II.20d)}$$

$$M_2 = -0.54 + \frac{0.89}{\left[0.2 + \left(d/c\right)\right]} \qquad \textbf{(II.20e)}$$

$$M_3 = 0.5 - \frac{1}{\left[0.65 + \left(d/c\right)\right]} + 14\left(1 - \left(d/c\right)\right)^{24} \qquad \textbf{(II.20f)}$$

$$f_c = 1.152 - 0.05\sqrt{\left(d/t\right)} \qquad \textbf{(II.20g)}$$

II.4.2 Fracture toughness

The piping system is one of principal keys on the world energy, where the hydrocarbon industries sought to improve the mechanical characteristics. However, the scientific laboratories face a challenge to provide the durable solutions about the cracks and corrosions. The improvement of materials is depended to the mechanical properties which are based on different factors such as; thickness, surface roughness and length, percentage of chemical elements taking into account the importance of carbonization, defect geometry (defected length, depth and width), or loading mode, and environment (sea, desert, city, temperature, etc).

The critical value of SIF is called a fracture toughness (K_{IC}) and considered as an important material property for the failure assessment of pipelines [35,36]. Fracture toughness expresses the material's resistance to the brittle fracture and is often used in design applications [37]. The fracture mechanics is considered as important during the evaluation of the structural integrity of

piping systems. Based on the theory of linear elastic fracture mechanics (LEFM), failure occurs when the value of stress intensity factor (K_I) is greater than the critical value of plane strain fracture toughness for mode I crack displacement (K_{IC}), which can be expressed as following:

$$K_I \geq K_{IC} \quad \textbf{(II.21)}$$

A failure criterion for mixed mode (case of pipe elbow) of loading was used [38-40]:

$$\left(\frac{K_{I\varphi}}{K_{IC}}\right)^2 + \left(\frac{K_{II\varphi}}{K_{IIC}}\right)^2 + \left(\frac{K_{III\varphi}}{K_{IIIC}}\right)^2 = C \quad \textbf{(II.22)}$$

Failure condition is given by C=1, $K_{I\varphi}$, $K_{II\varphi}$ and $K_{III\varphi}$ are applied in elbow at critical zone for mode I, II and III K_{IC}, K_{IIC} and K_{IIIC} are the fracture toughness of three modes. In steel, fracture toughness of mode I is equal to the fracture toughness of mode II [38]:

$$K_{IC} = K_{IIC} \quad \textbf{(II.23a)}$$

And where the equation of calculation K_{IIIC} is given by as follow:

$$K_{IIIC} = \frac{\tau_C}{\sigma_C} K_{IIC} \quad \textbf{(II.23b)}$$

where τ_C and σ_C are critical shear and normal stresses.

II.5 CORROSION ASSESSMENT ON PIPELINE STEELS

The corrosion phenomenon has become one of the difficult challenges in the hydrocarbon industries. In order to keep the continuity of energy transport, many studies have been presenting the durable solutions and new ideas about industrial and natural inhibitors.

In this section, the pipeline integrity continues to attach the great importance to improving components function in order to maintain them under service a long time possible. Generally, there are many methods to evaluate the corrosion problem which is based on the inspection (material of piping, operating conditions, nature of hydrocarbons) and analyses (layer compounds of corrosion). In addition, the pipeline integrity has been developed by international standards or researchers' models in order to maintain the continuity of operating service using experimental tests, numerical analysis and/or analytical models [41-44].

II.5.1 Failure pressure models based on yield stress

In the 60s, many studies proposed the mathematical formulas for allowing the prediction and the evaluation of the burst capacity of corroded pipes [24, 45-47]. In addition, depending many factors such as flow stress (σ_{flow}), wall thickness (t), outer diameter (D_{ext}) and defected area function ($f(d/t)$) are used to calculate the failure pressure of piping systems.

(a) Battelle NG-18 model

In order to study the failure criterion, the first formula is named Battelle NG-18 which had been proposed by Maxey et al. [24]. This formula is applied using the rectangular shape of corrosion phenomenon to analyze the piping systems. The NG-18 equation for failure criterion is written as following:

$$P_f = \sigma_{flow} \frac{2t}{D_{ext}} . f\left(d/t\right) \quad \textbf{(II.24)}$$

$$\sigma_{flow} = \sigma_y + 69 \quad \textbf{(II.25)}$$

$$f\left(d/t\right) = \left(\frac{1-(A/A_0)}{1-(A/A_0)/M} \right) \quad \textbf{(II.26)}$$

where P_f is the failure pressure. A and A_0 are area of the river-bottom profile and the reference area respectively. M dsecribes the geometry correction factor (Folias factor) as follow:

$$M = \left(1 + 0.6275 \times \frac{L^2}{D_{ext} t} - 0.003375 \times \left(\frac{L^2}{D_{ext} t} \right)^2 \right)^{0.5} \quad \textbf{(II.27)}$$

However, based on this criterion, engineering models were developed depending to the flow stress (σ_{flow}), correction factor (M) and corroded profile [25]. Analytically, the flow stress depends upon the yield strength, σ_y, (B31G, mod B31G and RSTRENG) or ultimate strength, σ_{ult}, (DNV RP-101, PCORRC and Shell-92).

(b) Original ASME B31G

Based on Battelle NG-18 standard, American Society of Mechanical Engineers (ASME) has started to develop the industrial codes in order to predict the burst capacity for pressurized defected pipes. It is considered as the important code to predict the burst capacity for pressurized pipes due to the high pressure and temperature with small defects and cracks. Furthermore, many studies have been providing engineering models to examine this phenomenon using the semi-elliptical as a simulated shape which is proportional to the mathematical models taking into account the operating conditions [26]. According to the ASME, the first model is called an original ASME B31G [26] which is used for a parabolic defect shape and the maximum circumferential stress (σ_θ) cannot exceed the yield strength of the material $\sigma_\theta \le \sigma_y$. Moreover, the flow stress depends to the yield strength ($\sigma_{flow} = 1.1\sigma_y$). According to B31G, failure function may express as following equation, where the defect depth must not exceed 80% of wall thickness.

$$f\left(\frac{d}{t}\right) = \frac{1-(2/3)(d/t)}{1-(2/3)(d/t)/M} \qquad \textbf{(II.28)}$$

$$\text{where } M = \begin{cases} \left(1+0.8\times\dfrac{L^2}{D_{ext}t}\right)^{0.5} & \rightarrow \left(0.8\times\dfrac{L^2}{D_{ext}t}\right)^{0.5} \le 4 \\ \infty & \rightarrow \left(0.8\times\dfrac{L^2}{D_{ext}t}\right)^{0.5} > 4 \end{cases} \qquad \textbf{(II.29)}$$

Where *d*, *t*, and *L* are the crack depth, wall thickness, and longitudinal corrosion defect length, respectively.

(c) Modified ASME B31G model

Kiefner et al. [27] have modified the original ASME B31G standard which is used for an arbitrary defect shape. In addition, the defect depth should not exceed 85% of wall thickness. The flow stress depends to the yield strength which is approximately equal to $\sigma_y + 69MPa$.

$$f\left(\frac{d}{t}\right) = \frac{1-0.85(d/t)}{1-\left(0.85(d/t)/M\right)} \qquad \textbf{(II.30)}$$

Where the correction factor (bulging factor) equation is expressed as follow:

$$M = \begin{cases} \left(1 + 0.6275 \times \frac{L^2}{D_{ext} t} - 0.003375 \times \left(\frac{L^2}{D_{ext} t}\right)^2\right)^{0.5} & \rightarrow \left(\frac{L^2}{D_{ext} t}\right) \leq 50 \\ 3.3 + 0.032 \times \frac{L^2}{D_{ext} t} & \rightarrow \left(\frac{L^2}{D_{ext} t}\right) > 50 \end{cases} \quad \textbf{(II.31)}$$

(d) RSTRENG model

Due to the importance the energy transport and its safety, researchers had to think for an adequate model. RSTRENG model [28] is used for effective area and effective length (river bottom profile) as presented in the equation of failure function (equation II.32) while the flow stress is still as ASME B31G modification model ($\sigma_{flow} = \sigma_y + 69$) taking into consideration the condition of defect depth ratio ($d / t \leq 0.8$).

$$f\left(d/t\right) = \left(\frac{1 - (A_{eff} / A_0)}{1 - (A_{eff} / A_0) / M}\right) \quad \textbf{(II.32)}$$

Where the geometry correction factor (M) can be calculated using the following equation:

$$M = \begin{cases} \left(1 + 0.6275 \times \frac{L_{eff}^2}{D_{ext} t} - 0.003375 \times \left(\frac{L_{eff}^2}{D_{ext} t}\right)^2\right)^{0.5} & \rightarrow \left(\frac{L_{eff}^2}{D_{ext} t}\right) \leq 50 \\ 3.3 + 0.032 \times \frac{L_{eff}^2}{D_{ext} t} & \rightarrow \left(\frac{L_{eff}^2}{D_{ext} t}\right) > 50 \end{cases} \quad \textbf{(II.33)}$$

II.5.2 Failure pressure models based on ultimate strength

Developing the prediction technology is one of among ways to keep the safety of energy transported. Depending on the inspections and analyses and investigations [25,12-14,19-21, 38], the most results indicate to the standard B31G, modified B31G and RSTRENG formulas are not suitable to predict the modern pipelines with high toughness. Thus, improving the quality of piping components is based to develop new models for predicting in real times the burst and the prevent catastrophic incidents taking into account the boundary conditions especially the pressure and temperature and nature of the material. The developed models are based on ultimate strength.

(a) Shell-92 model

Depending on the inspections and analyses and investigations [25,12-14,19-21, 38], the most results indicate to the standard B31G, modified B31G and RSTRENG formulas are very conservative predictions for modern pipelines (high toughness). Consequently, the development of pipeline steels is required new models in order to predict the real time of burst and to prevent the catastrophic incidents. However, Ritchie and Last [29] have suggested a new mathematical model for failure pressure calculation known as Shell-92 which presented in equation II.34. The flow stress (σ_{flow}) in Shell-92 model is identified by ultimate strength which equal to $0.9\sigma_{ult}$.

$$P_f = \sigma_{flow} \frac{2t}{D_{ext} - t} . f\left(d/t\right) \quad \textbf{(II.34)}$$

The failure function *f(d/t)* is given by equation II.35 taking into account the condition of defect depth which must not exceed 85 % of pipeline thickness.

$$f\left(d/t\right) = \frac{1-(d/t)}{1-(d/t)/M} \quad \textbf{(II.35)}$$

$$\text{where, } M = \sqrt{1+0.8\left(\frac{L}{D}\right)^2\left(\frac{D}{t}\right)} \quad \textbf{(II.36)}$$

(b) DNV RP-F101

Veritas [30] has presented a theory to evaluate the burst capacity on corroded pressurized piping systems which is called DNV RP-F101 basing on the previous model shell-92 (equation II.34). This model is dedicated to high toughness in defective piping systems with rectangular shape defects and river bottom profile [25]. He has believed that the use of flow stress as ultimate strength ($\sigma_{flow} = \sigma_{ult}$) and correction factor, M (equation II.37) may give a relatively conservative prediction on burst capacity of corroded pipeline. However, this method is not applicable for defect depths which are greater than 85% of a pipe wall thickness.

$$M = \left(1+0.31\frac{L^2}{D_{ext}t}\right)^{0.5} \quad \textbf{(II.37)}$$

(c) PCORRC

The integrity assessment of piping systems with long defects for moderate and high toughness becomes the great challenge facing most petroleum companies, where the new burst capacity criterion that is named PCORRC model, has been presented by Stephens and Leis [31] taking into account the operating conditions. Based on FE, they have investigated their analysis on elliptical defect shapes using a plastic collapse failure. Furthermore, the demonstrated model proved that the flow stress is controlled by ultimate strength ($\sigma_{flow} = \sigma_{ult}$). In addition, the defect depth and length are considered the critical parameters for corroded pipes assessment which are defined by failure function (equation II.38) and bulging factor (equation II.39).

$$f\left(d/t\right) = 1 - (d/t) * M \qquad \textbf{(II.38)}$$

$$M = 1 - \exp\left(-0.157 \frac{L}{\sqrt{D(t-d)/2}}\right) \qquad \textbf{(II.39)}$$

(d) CHOI model

According to the failure pressure of piping systems, Choi et al [32] have proposed a new formula based on limit load analysis which are performed on API X65 pipeline steels using a numerical analysis. Moreover, the failure pressure calculation is established according to the flow pressure and failure function which are dependent on a condition of $L/\sqrt{rt}$ as stated by Choi et al [32]. However, the flow stress is related to the ultimate strength ($\sigma_{flow} = 0.9\sigma_{ult}$) if $L/\sqrt{rt} < 6$ and the failure function can be determined by a quadratic equation as follow:

$$f\left(d/t\right) = C_2\left(\frac{L}{\sqrt{rt}}\right)^2 + C_1\left(\frac{L}{\sqrt{rt}}\right) + C_0 \qquad \textbf{(II.40)}$$

where,

$$\begin{cases} C_2 = 0.1163\left(d/t\right)^2 - 0.1053\left(d/t\right) + 0.0292 \\ C_1 = -0.6913\left(d/t\right)^2 + 0.4548\left(d/t\right) - 0.1447 \\ C_0 = 0.06\left(d/t\right)^2 - 0.1035\left(d/t\right) + 1 \end{cases} \qquad \textbf{(II.41)}$$

On the contrary, if the $L/\sqrt{rt} \geq 6$, the flow stress is equal to the ultimate strength ($\sigma_{flow} = \sigma_{ult}$) and the failure function (equation II.40) will change into the first degree which can be rewritten as follow:

$$f\left(d/t\right) = C_1\left(\frac{L}{\sqrt{rt}}\right) + C_0 \qquad \textbf{(II.42)}$$

where the constant parameters, C_0 and C_1 are expressed as follow:

$$\begin{cases} C_1 = 0.0071\left(d/t\right) - 0.0126 \\ C_0 = 0.9847\left(d/t\right) + 1.1101 \end{cases} \qquad \textbf{(II.43)}$$

(e) Zhu and Leis model

In 2012, new analytical method was developed for assessing corroded piping system and predicting the failure pressure by Zhu and Leis [48]. The analytical method was based on three approaches; Tresca, von Mises, and ASSY which provide the enough analyses about the defects on piping systems taking into account the strain hardening parameter [48]. Their analyses were carried out on specimens which had long real defects removed from critical zones of corroded pipes (crack or welded joins) under service in order to understand the behavior of defects taking into consideration the operating conditions. In consequence, the final function of failure pressure can be expressed by following equation:

$$P_f = \left(\frac{k}{2}\right)^{n+1} \frac{4t}{D}\sigma_{ult}\left(1 - \frac{d}{t}\right) \qquad \textbf{(II.44)}$$

where the parameter "*k*" was defined in equation II.11.b.

II.6 Failure Assessment Diagram (FAD)

To study the efficiency of piping systems, the FAD is still the important tool to measure the quality and durability of material depending on many parameters such as depth, thickness, length, surface roughness, taking into account the operating conditions such as the temperature and pressure. Depending on the value of fracture toughness (K_{IC}) parameter that is important material property of resulted of critical value of SIF, indicates the failure assessment of pipelines [35,36]. In addition, the FAD curve (see figure II.8) is still an important technique to define

accurately the orientation of pipeline lifetime, where this technique is divided into three zones (i) security zone, (ii) safety zone, and (iii) failure zone.

FAD presents defect loading conditions in a graph where the non-dimensional crack driving force K_r is plotted versus non-dimensional applied stress L_r. K_r is defined as the ratio of maximal stress intensity factor, $K_{I,\,max}$, to the fracture toughness of material, K_{IC}.

$$K_r = f(L_r) = \sqrt{\left(1+\frac{L_r^2}{2}\right)}\left[0.3+0.7\times\exp(-\mu\times L_r^6\right] \quad \rightarrow \quad 0 \le L_r \le 1 \qquad \textbf{(II.6)}$$

$$K_r = K_{I,\,max}/K_{IC} \qquad \textbf{(II.6)}$$

L_r is the ratio of hoop stress σ_θ to flow stress σ_{flow} which is given by the following equation:

$$L_r = \sigma_\theta/\sigma_{flow} \qquad \textbf{(II.6)}$$

where σ_g and σ_{flow} are given by following equations

$$\sigma_{flow} = (\sigma_y + \sigma_{ult})/2 \qquad \textbf{(II.6)}$$

Due to the complex geometry of pipe bends, the mixed mode loading allows to appear the K_{II} and K_{III} through the crack driving force K_r which is represented by the ratio of maximum equivalent stress intensity factor, $K_{eq,\,max}$, taking into account the fracture toughness of material in mode K_{IC}.

$$K_r = K_{eq}/K_{IC} \qquad \textbf{(II.6)}$$

The FAD is based on the interpolation curve $K_r = f(L_r)$ and it is typically presented in polar coordinates $(r,\ \theta)$ [49]. A schematic representation of a typical FAD with two characteristic polar angle values (θ_1 and θ_2) that defined three typical domains:

- Brittle fracture, if $\theta > \theta_1$
- elasto-plastic fracture, if $\theta_1 > \theta > \theta_2$
- plastic collapse, if $\theta < \theta_2$

In FAD, failure is given by the following condition; if the assessment point of coordinate [L_r, K_r] is under the failure curve given by the following equation $K_{r,c} = f(L_{r,c})$ where the subscript c

indicates critical condition, the structure is safe. If the assessment point is above the curve, failure occurs [49].

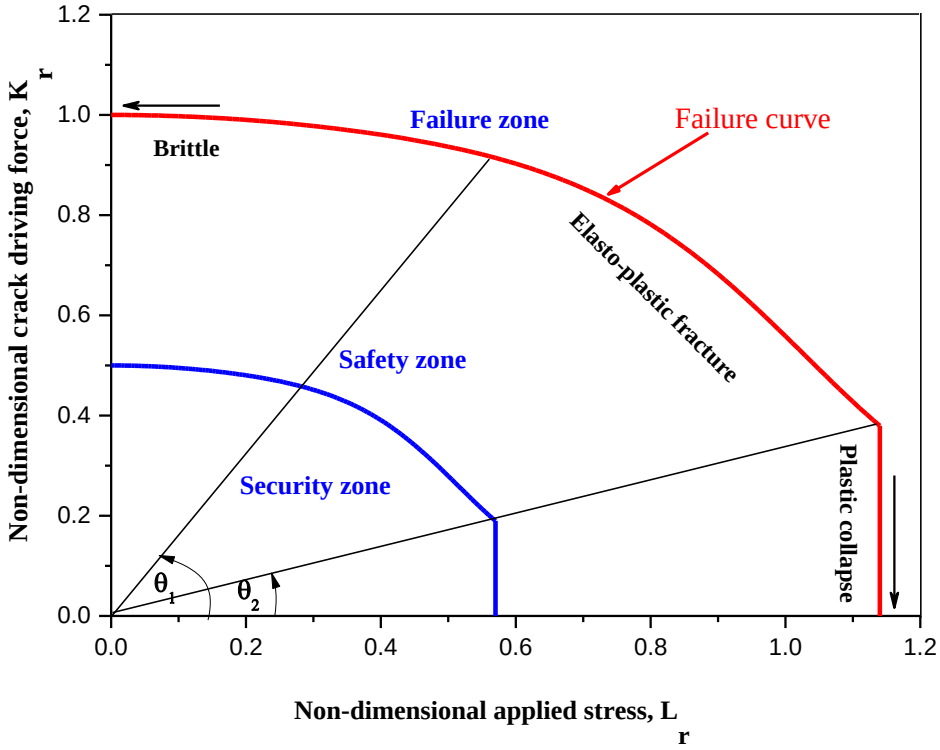

Figure II.8: Schematic view of the Failure Assessment Diagram (FAD) and three typical domains.

References

[1] Wang, Q. and Zhou, W., 2019. A new burst pressure model for thin-walled pipe elbows containing metal-loss corrosion defects. *Engineering Structures*, 200, pp.109720, https://doi.org/10.1016/j.engstruct.2019.109720;

[2] Petrík, A. and Ároch, R., 2019. Usage of true stress-strain curve for FE simulation and the influencing parameters. *In IOP Conference Series: Materials Science and Engineering*, 566 (1), pp. 012025, IOP Publishing, https://doi.org/10.1088/1757-899X/566/1/012025;

[3] Zhu, X.K. and Leis, B.N., 2005. Influence of yield-to-tensile strength ratio on failure assessment of corroded pipelines. *Journal of Pressure Vessel Technology*, 127(4), pp. 436-442, https://doi.org/10.1115/1.2042481;

[4] Dowling, N.E., 2012. Mechanical behavior of materials: engineering methods for deformation, fracture, and fatigue. *Pearson*;

[5] Zhu, X.K. and Leis, B.N., 2005. Analytic prediction of plastic collapse failure pressure of line pipes. *In ASME 2005 Pressure Vessels and Piping Conference*, pp. 109-118, American Society of Mechanical Engineers Digital Collection, https://doi.org/10.1115/PVP2005-71204;

[6] Pluvinage, G., 2021. Mechanical properties of a wide range of pipe steels under influence of pure hydrogen or hydrogen blended with natural gas. *International Journal of Pressure Vessels and Piping*, 190, pp.104293, https://doi.org/10.1016/j.ijpvp.2020.104293;

[7] Race, J., Oterkus, S. and Chang, E., 2020. A new methodology for the prediction of burst pressure for API 5L X grade flawless pipelines. *Ocean Engineering*, 212, pp.107602, https://doi.org/10.1016/j.oceaneng.2020.107602;

[8] Kolawole, F.O., Kolawole, S.K., Agunsoye, J.O., Adebisi, J.A., Bello, S.A. and Hassan, S.B., 2018. Mitigation of corrosion problems in API 5L steel pipeline-a review. *Journal of Materials and Environmental Sciences*, 9(8), pp.2397-2410, https://www.jmaterenvironsci.com/Document/vol9/vol9_N8/264-JMES-2611-Kolawole.pdf;

[9] American Petroleum Institute, 2013. Specification for line pipe. API specification 5L, 45th edn. *American Petroleum Institute*, Washington, DC, https://www.amerpipe.com/steel-pipe-products/api-5l-pipe-specifications/;

[10] Zhang, S.H., Gao, C.R., Zhao, D.W. and Wang, G.D., 2013. Limit analysis of defect-free pipe elbow under internal pressure with mean yield criterion. *Journal of Iron and Steel Research, International*, 20(4), pp.11-15, https://doi.org/10.1016/S1006-706X(13)60075-8;

[11] Li, Z., Yinpei, W., Jin, C. and Cengdian, L., 2001. Evaluation of local thinned pressurized elbows. *International Journal of Pressure Vessels and Piping*, 78(10), pp.697-703, https://doi.org/10.1016/S0308-0161(01)00125-9;

[12] Bao, S., Liu, Y., Mao, J., Ge, R. and Li, X., 2019. Numerical and experimental investigation on limit load of elbow with local thinning area. *International Journal of Pressure Vessels and Piping*, 172, pp.414-422, https://doi.org/10.1016/j.ijpvp.2019.04.014;

[13] Kang, S.J., Choi, J.H., Lee, H., Cho, D.H., Choi, J.B. and Kim, M.K., 2019. Limit load solutions for elbows with circumferential through-wall crack under the pressure-induced bending restraint effect. *International Journal of Pressure Vessels and Piping*, 177, p.103983, https://doi.org/10.1016/j.ijpvp.2019.103983;

[14] Kim, Y.J. and Oh, C.S., 2006. Closed-form plastic collapse loads of pipe bends under combined pressure and in-plane bending. *Engineering Fracture Mechanics*, 73(11), pp.1437-1454, https://doi.org/10.1016/j.engfracmech.2006.02.001;

[15] Amaya-Gómez, R., Sanchez-Silva, M., Bastidas-Arteaga, E., Schoefs, F. and Munoz, F., 2019. Reliability assessments of corroded pipelines based on internal pressure–A review. *Engineering Failure Analysis*, 98, pp.190-214, https://doi.org/10.1016/j.engfailanal.2019.01.064;

[16] Kastner, W., Röhrich, E., Schmitt, W. and Steinbuch, R., 1981. Critical crack sizes in ductile piping. *International Journal of Pressure Vessels and Piping*, 9(3), pp.197-219, https://doi.org/10.1016/0308-0161(81)90002-8;

[17] Levén, M. and Daniel, R., 2012. Stationary 3D crack analysis with Abaqus XFEM for integrity assessment of subsea equipment (Master's thesis), *Chalmers University of Technology*, https://publications.lib.chalmers.se/records/fulltext/164269.pdf;

[18] Irwin, G.R., 1957. Analysis of stresses and strains near the end of a crack traversing a plate, Transactions, ASME, *Journal of applied mechanics*, 24, pp. 361-364, https://doi.org/10.1115/1.4011547;

[19] Ritchie, R.O. and Liu, D., 2021. Introduction to Fracture Mechanics. *Elsevier*, https://doi.org/10.1016/C2020-0-03038-0;

[20] Erdogan, F., 1983. Stress intensity factors. *Journal of Applied Mechanics*, 50(4b): pp.992–1002, https://doi.org/10.1115/1.3167212;

[21] Newman Jr, J.C. and Raju, I.S., 1981. An empirical stress-intensity factor equation for the surface crack. *Engineering fracture mechanics*, 15(1-2), pp.185-192, https://doi.org/10.1016/0013-7944(81)90116-8;

[22] Anderson, T.L., 2017. Fracture Mechanics: Fundamentals and Applications, *Fourth Edition, CRC Press*, https://doi.org/10.1201/9781315370293;

[23] Mazurkiewicz, L., Tomaszewski, M., Malachowski, J., Sybilski, K., Chebakov, M., Witek, M., Yukhymets, P. and Dmitrienko, R., 2017. Experimental and numerical study of steel pipe with part-wall defect reinforced with fibre glass sleeve. *International journal of pressure vessels and piping*, 149, pp.108-119, https://doi.org/10.1016/j.ijpvp.2016.12.008;

[24] Maxey, W.A., Kiefner, J.F., Eiber, R.J. and Duffy, A.R., 1972. Ductile fracture initiation, propagation, and arrest in cylindrical vessels. *In Fracture Toughness: Part II. ASTM International*, pp.70-81, https://doi.org/10.1520/STP38819S;

[25] Cosham, A., Hopkins, P. and Macdonald, K.A., 2007. Best practice for the assessment of defects in pipelines–Corrosion. *Engineering Failure Analysis*, 14(7), pp.1245-1265, https://doi.org/10.1016/j.engfailanal.2006.11.035;

[26] ASME B31G, A.S.M.E., 1991. Manual for determining the remaining strength of corroded pipelines. *ASME B31G-1991*;

[27] Kiefner, J.F. and Vieth, P.H., 1989. A modified criterion for evaluating the remaining strength of corroded pipe (No. PR-3-805). *Battelle Columbus Div., OH (USA)*;

[28] Kiefner, J.F. and Vieth, P.H., 1990. Evaluating pipe--conclusion. Pc program speeds new criterion for evaluating corroded pipe. *Oil and Gas Journal*, 88(34), http://worldcat.org/issn/00301388;

[29] Ritchie, D. and Last, S., 1995, April. Burst criteria of corroded pipelines-defect acceptance criteria. *In Proceedings of the EPRG/PRC 10th biennial joint technical meeting on line pipe research* (pp. 1-11);

[30] Veritas, D.N., 2004. Recommended practice DNV-RP-F101 corroded pipelines. *Hovik, Norway*, 11, pp.135-138;

[31] Stephens, D.R. and Leis, B.N., 2000, October. Development of an alternative criterion for residual strength of corrosion defects in moderate-to high-toughness pipe. *In international pipeline conference (Vol. 40252, p. V002T06A012). American Society of Mechanical Engineers*, https://doi.org/10.1115/IPC2000-192;

[32] Choi, J.B., Goo, B.K., Kim, J.C., Kim, Y.J. and Kim, W.S., 2003. Development of limit load solutions for corroded gas pipelines. *International journal of pressure vessels and piping*, 80(2), pp.121-128, https://doi.org/10.1016/S0308-0161(03)00005-X.

[33] Mokhtari, M. and Melchers, R.E., 2018. A new approach to assess the remaining strength of corroded steel pipes. *Engineering Failure Analysis*, 93, pp.144-156, https://doi.org/10.1016/j.engfailanal.2018.07.011;

[34] Raju, I.S. and Newman Jr, J.C., 1982. Stress-intensity factors for internal and external surface cracks in cylindrical vessels. *Journal of Pressure Vessel Technology*, 104(4) pp.293-298, https://doi.org/10.1115/1.3264220;

[35] Kim, J.W., Yoon, M.S. and Park, C.Y., 2013. The effect of load-controlled bending load on the failure pressure of wall-thinned pipe elbows. *Nuclear Engineering and Design*, 265, pp.174-183, https://doi.org/10.1016/j.nucengdes.2013.07.027

[36] Pluvinage, G., Capelle, J. and Hadj Meliani, M., 2019. Pipe networks transporting hydrogen pure or blended with natural gas, design and maintenance. *Engineering Failure Analysis*, 106, pp.104-164, https://doi.org/10.1016/j.engfailanal.2019.104164

[37] Adib-Ramezani, H., Jeong, J. and Pluvinage, G., 2006. Structural integrity evaluation of X52 gas pipes subjected to external corrosion defects using the SINTAP procedure. *International Journal of Pressure Vessels and Piping*, 83(6), pp.420-432, https://doi.org/10.1016/j.ijpvp.2006.02.023.

[38] Gross, D. and Seelig, T., 2017. Fracture mechanics: with an introduction to micromechanics. *Springer*, https://doi.org/10.1007/978-3-319-71090-7;

[39] Cabrero, J.M., Iraola, B. and Yurrita, M., 2018. Failure of timber constructions. *In Handbook of Materials Failure Analysis*, pp. 123-152, Butterworth-Heinemann, https://doi.org/10.1016/B978-0-08-101928-3.00007-0;

[40] Quadratischer, E.G.L.U., De Rupture, U.C.D.C., Et, L., De Lamelles, Q.P.D.P. and Le Plan, O.S.D., 2001. Linear versus quadratic failure criteria for inplane loaded wood based panels. *Otto-Graf-Journal*, 12, p.187, https://citeseerx.ist.psu.edu/viewdoc/download?doi=10.1.1.560.5582&rep=rep1&type=pdf;

[41] Kim, J.W., Na, Y.S. and Lee, S.H., 2009. Experimental evaluation of the bending load effect on the failure pressure of wall-thinned elbows. *Journal of pressure vessel technology*, 131(3), pp. 031210, https://doi.org/10.1115/1.3122032;

[42] Lee, G.H., Seo, J.K. and Paik, J.K., 2017. Condition assessment of damaged elbow in subsea pipelines. *Ships and Offshore Structures*, 12(1), pp.135-151, https://doi.org/10.1080/17445302.2015.1116245;

[43] Zelmati, D., Ghelloudj, O. and Amirat, A., 2017. Correlation between defect depth and defect length through a reliability index when evaluating of the remaining life of steel pipeline under corrosion and crack defects. *Engineering Failure Analysis*, 79, pp.171-185, https://doi.org/10.1016/j.engfailanal.2017.04.025;

[44] Bouledroua, O., Hafsi, Z., Djukic, M.B. and Elaoud, S., 2020. The synergistic effects of hydrogen embrittlement and transient gas flow conditions on integrity assessment of a precracked steel pipeline. *International Journal of Hydrogen Energy*, https://doi.org/10.1016/j.ijhydene.2020.04.262;

[45] Folias, E.S., 1965. An axial crack in a pressurized cylindrical shell. *International Journal of Fracture Mechanics*, 1(2), pp.104-113, https://doi.org/10.1007/BF00186748;

[46] Folias, E.S., 1967. A circumferential crack in a pressurized cylindrical shell. *International Journal of Fracture Mechanics*, 3(1), pp.1-11, https://doi.org/10.1007/BF00188640;

[47] Erdogan, F. and Kibler, J.J., 1969. Cylindrical and spherical shells with cracks. *International Journal of Fracture Mechanics*, 5(3), pp.229-237, https://doi.org/10.1007/BF00184614;

[48] Zhu, X.K. and Leis, B.N., 2012, September. Assessment criteria and burst pressure prediction for pipelines with long blunt defects. *In International Pipeline Conference*, *American Society of Mechanical Engineers*, Vol. 45134, pp. 863-871, https://doi.org/10.1115/IPC2012-90625;

[49] Hadj Meliani, M., Matvienko, Y.G., Pluvinage, G., 2011. Corrosion defect assessment on pipes using limit analysis and notch fracture mechanics. *Engineering Failure Analysis*, 18(1), pp.271-283, https://doi.org/10.1016/j.engfailanal.2010.09.006;

CHAPTER III:

ASSESSMENT OF CRITICAL POSITIONS IN PIPE ELBOWS

III.1 INTRODUCTION

Piping systems including the pipelines, joints and elbows used in the refineries, exploration and production, are considered as important instruments for transporting the hydrocarbons with safety method. Moreover, they are major parts to provide the energy all over the world taking into account the operating conditions such as pressure and temperature. Despite the importance of the piping components, the repeated failures and defects in the critical parts of elbows especially joins and welded parts become the main challenge that face the engineers in the hydrocarbon industries. This phenomenon most probably causes due to the corrosion which is a dangerous and enormously costly issue.

In this chapter, we focus on two main sections which explain the crack and defect phenomena in pipe elbows. First section investigates the critical position in the API 5L X52 pipe elbow according to the Fluid-Structure Interaction (FSI) using numerical analysis of CFD and FEA. In order to perform this section, it is divided into four main parts: the first part concentrated on analyzing and comparing the results which appear the effect of bending radius of elbow on the maximum values of Von-Misses stress for each radius taking into account the characteristics of mechanical including the yield stress of the elbow material. The second part focused on the creation of a semi-elliptical crack for different locations along the elbow to define the critical position according to the stress intensity factors. In the third part, the semi-elliptical crack angle orientation was studied at the critical position to indicate the critical angle which allows evaluating the effect of crack during the transporting of energy. The last part is focused on the check of the elbow safety where the failure assessment diagram (FAD) is one of most techniques which used to analyze the damage of piping systems in order to show the critical crack depth ratios at a critical position and a critical angle.

The second section evaluates the integrity assessment of damaged API 5L X52 steel elbows which was carried out within the framework of numerical study using the finite element method (FEM) and finite element analysis (FEA). To evaluate the damage, the FEM is used to simulate this phenomenon taking into consideration the limit pressure in the elbow containing a rectangular shaped corrosion defect at the intrados side. This study was accurately performed and compared to different codes for calculating limit pressure. To analyze the state of elbows at the intrados side with highest hoop stress, the FEM is used to predict the corrosion area.

Different relative defect depths to wall thickness ratios are created at the critical area and used as a principal parameter in the corrosion assessment.

III.2 NUMERICAL ANALYSIS OF SEMI-ELLIPTICAL CRACKS

Piping systems are exposed to catastrophe issues including corrosion and erosion which are the most common defects due to the operating conditions such as pressure and temperature and other external factors. The figure III.1 shows a real case of corrosion phenomenon in the intrados section of pipe elbow resulted by the complex chemical reactions due to the interaction gas-solid. We have performed a numerical study to understand the corrosion phenomenon on the one hand and on the other hand to avoid the corrosion problems and its reasons as much as possible. Depending on the boundary conditions to corroded elbows, the numerical study was carried out by ANSYS software [1] under the effect of the interaction between elbow and natural gas. The elbow of 90° made of API X52 steel was investigated by FVM and FEM techniques taking into account its dimensions as shown in figure III.1.

The geometry of the elbow is shown in figure III.1b where the dimensions are as presented as follow: internal radius R_i=285.75 mm, wall thickness t = 12.7 mm and the length L = 1000 mm. ρ is the elbow bending radius.

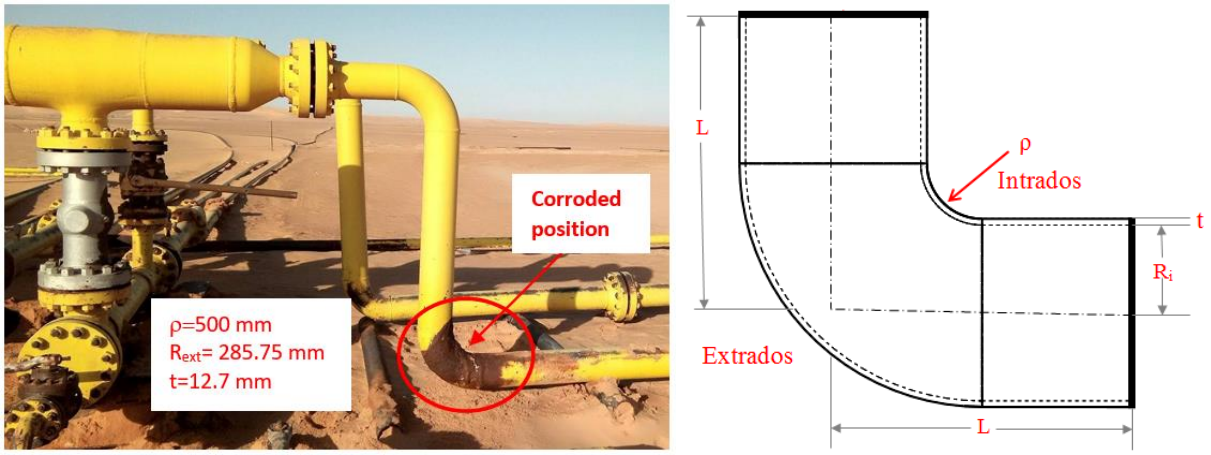

(a) (b)

Figure III.1: API X52 pipeline steel (a) an example of real corroded steel (b) Geometrical model of the pipe elbow.

Due to the difficulties of carrying out an experimental study under very complicated conditions, we have used a numerical software in order to understand the interaction between elbow and

natural gas. In fact, we have used the FVM of computational fluid dynamics (CFD) to study the behavior of gas flow and pressure distributions along pipe elbow. These pressures across the elbow were obtained by the importation of the other section called APDL (Ansys Parametric Design Language) using FEM. The figure III.2 illustrates the methodology of numerical steps. First of all, elbow radius was applied progressively in order to show the stress. At stabilization, the study of stress distributions along elbow curvature under gas pressure of 7 MPa was conducted in order to get the critical position defined as the position of maximum stress.

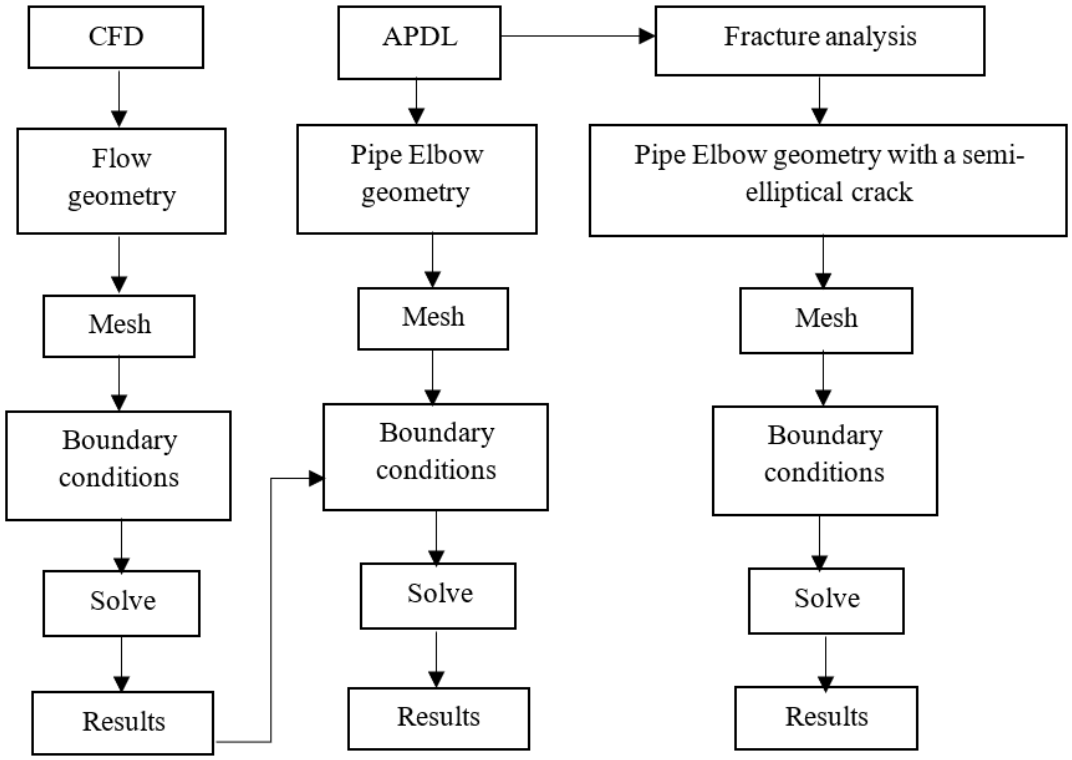

Figure III.2: Schematic description for numerical methodology.

At this critical position, a semi-elliptical crack was introduced and its orientation θ effect was studied in order to get the critical crack angle. This will create different semi-elliptical crack depths (*d/t*) in the range of 0.1 to 0.8; where "*d*" is the crack depth and "*t*" is the pipe elbow thickness. Failure assessment diagram (FAD) curve was used to evaluate the critical crack depth ratios at a critical position and a critical angle.

III.2.1 Effect of elbow radius

The numerical study including the finite element method is still as a suitable technique to investigate the behavior of crack and critical positions along the elbows. The numerical study was performed using the important steps to define the critical positions and applying the boundary conditions including the suitable mesh to obtain the accurate results.

Figure III.3 illustrates the elbow geometry, meshing and boundaries conditions of our case study, where the pressure was distributed along of the internal surface of elbow to appear the defects zones and leakage points.

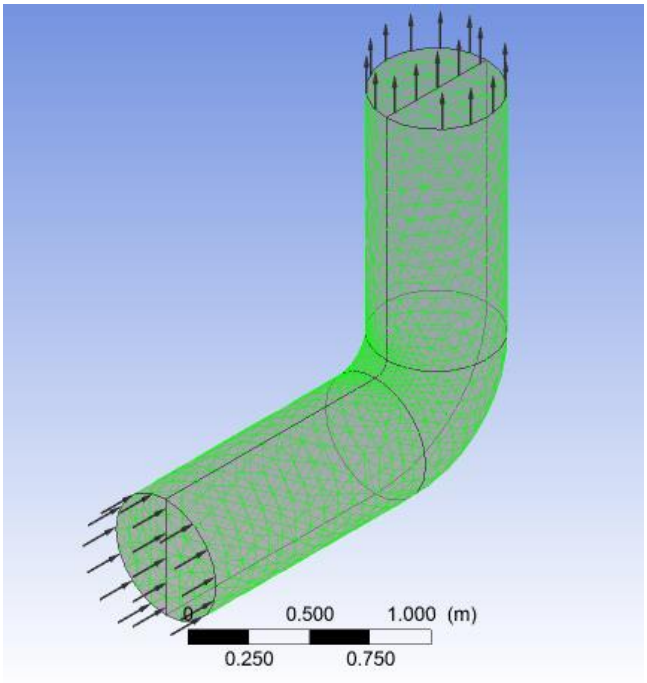

Figure III.3: Geometry, meshing and boundaries conditions of elbow model.

In order to analyze the effect of the cracked elbow on the safety of piping system at critical zones, the radius bending was taken into our consideration as it plays an important role in the security and assessment for pipeline failure where the critical zones are affected by the interaction fluid/ structure including elbow geometry. Figures (III.4 - III.6) show the distribution of pressure, velocity and Von-Mises stress along the pipe elbows, respectively.

The Effect of elbow radius was investigated in order to obtain the radius value at which the stress is stabilized. The change in the elbow radius leads to change the behavior flow including

the maximum stress and therefore to security and defect assessment of pipeline as shown in figure III.7.

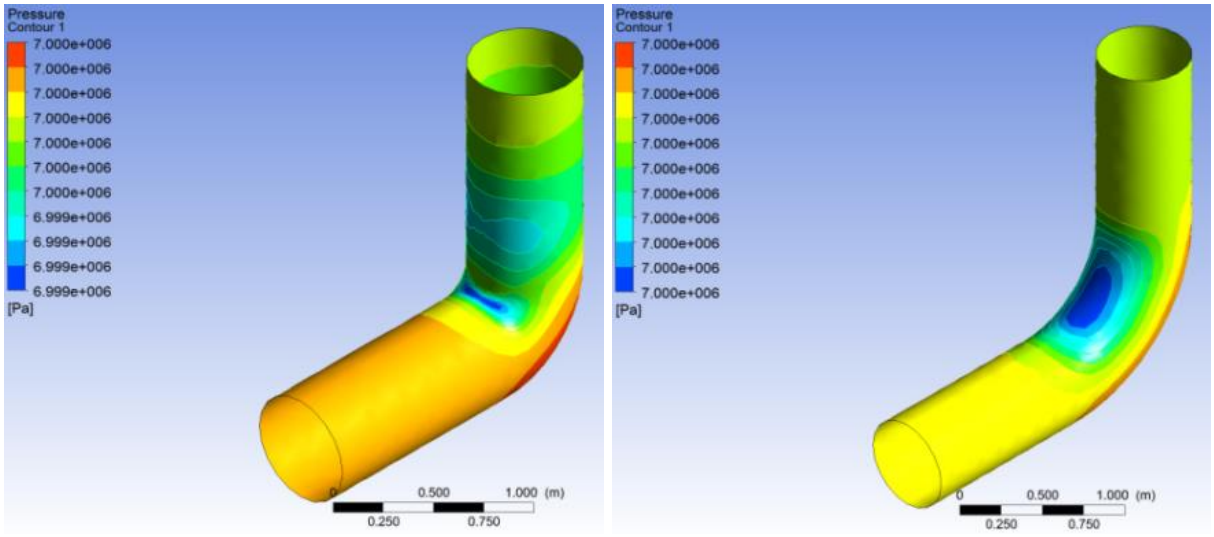

(a) (b)

Figure III.4: Pressure distribution along the elbow for (a) ρ = 50 mm and (b) ρ = 500 mm.

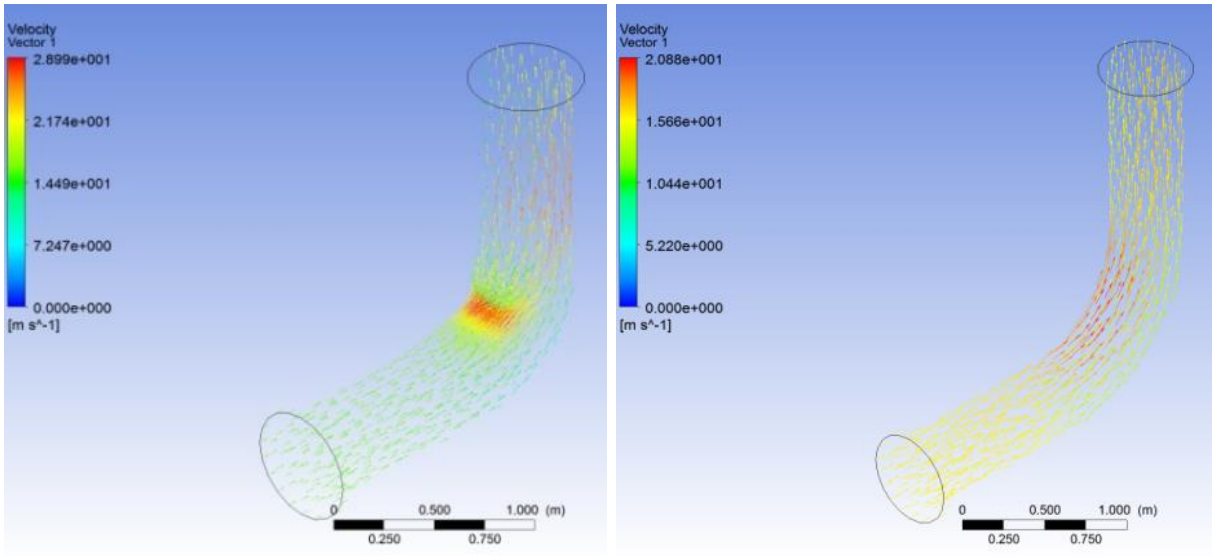

(a) (b)

Figure III.5: Velocity distribution along elbow for (a) ρ = 50 mm, (b) ρ = 500 mm.

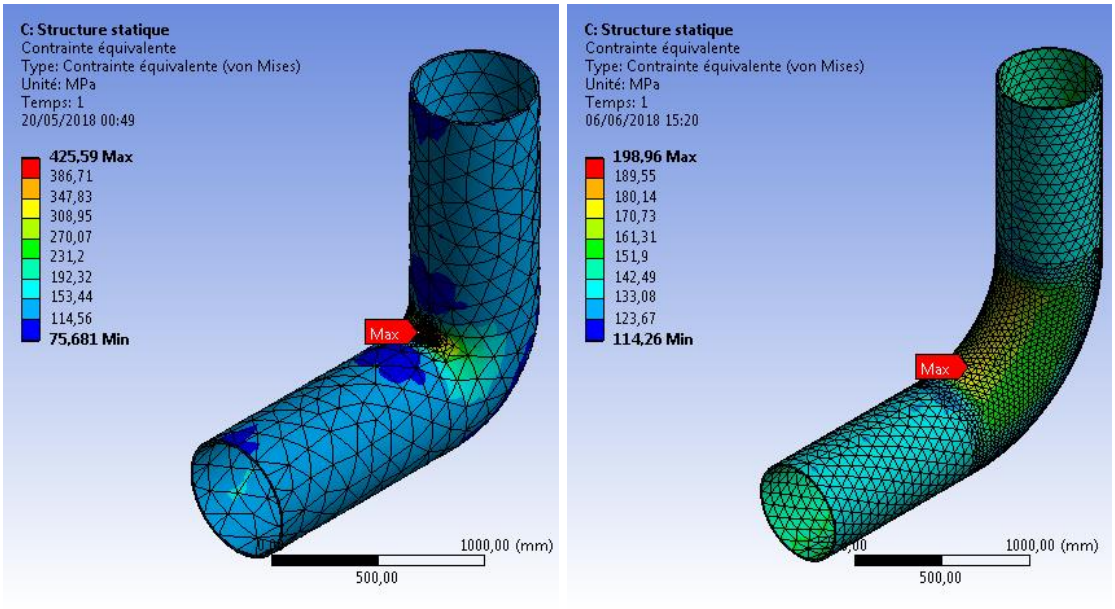

(a) (b)

Figure III.6: Von-Mises stress distribution along pipe elbow for (a) ρ = 50 mm, and (b) ρ = 500 mm.

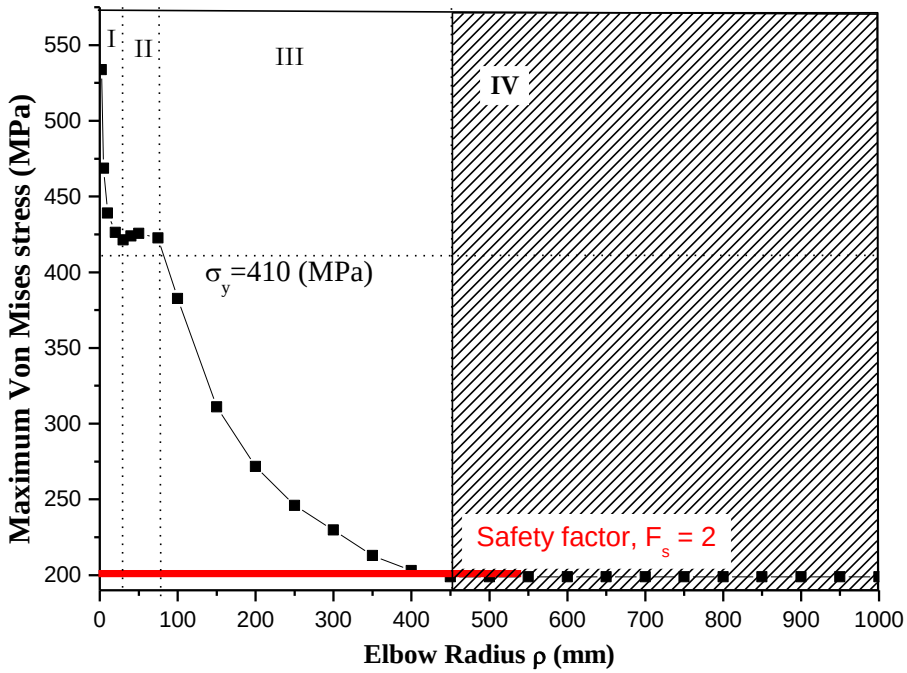

Figure III.7: Effect of elbow radius on maximum Von Mises Stress.

Table III.1: Evaluation of the effect of elbow radius on maximum Von Mises Stress.

Radius	$\rho < 25$	$25 < \rho < 85$	$85 < \rho < 450$	$\rho > 450$
Admissibility	no ($\sigma_{\theta\theta} > \sigma_y$)	no ($\sigma_{\theta\theta} \sim \sigma_y$)	No ($F_s < 2$)	Yes ($F_s > 2$)
Stress evolution	Decrease	Stabilization	Decrease	Stabilization

The effect of elbow radius was also examined according to the maximal values of Von-Mises stress as it shown in figure III.7. Von Mises stress evolution can be divided into four zones as indicated in Table III.1. The admissible elbow radius refers to the value of Yield strength of API X52 pipeline steel which is equal to 410 MPa and the traditional safety factor taken as $F_s = 2$. Any bending radius leading to a maximum stress greater than 410 MPa divided by the safety factor is not acceptable for industrial service. As a real case (Figure III.1a), a value of 500 mm of elbow radius was taken in our investigation. For this case: the stress amplification due to the presence of elbow is $k_t = 1.2$.

III.2.2 Critical position along elbow

The numerical software provides the approximate solutions under the operating condition and a good way to increase the pipeline efficiency and to prevent the occurrence of corrosion. The presence of high pressure in elbow is one of serious problems which can be the main reason to occur the corrosion phenomenon and hence, it leads to explosion the piping systems. Critical zone presented as a red zone in figure III.6 that is resulting from the internal natural gas pressure. Figure III.8 presents the corresponding distribution of different stresses (Von-Mises, normal stress and principal stress).

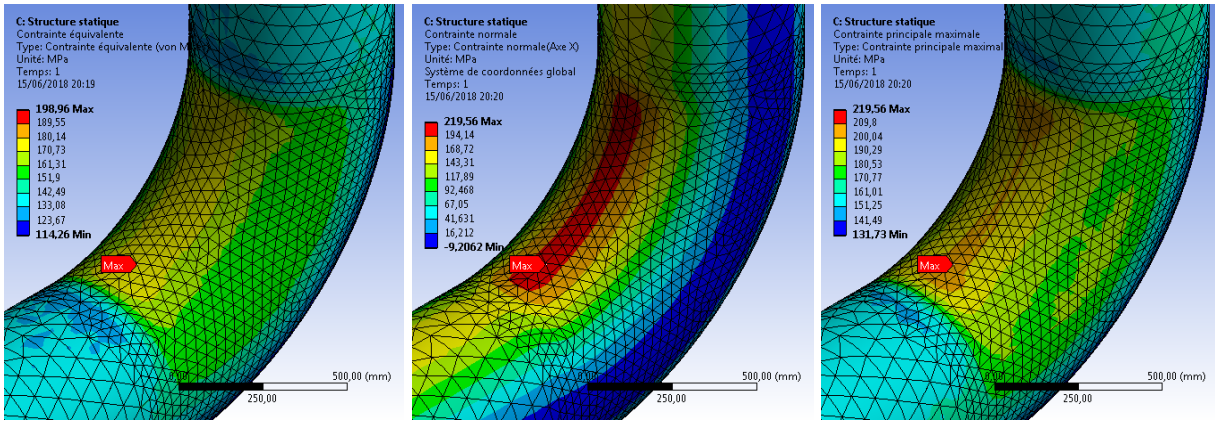

(a) (b) (c)

Figure III.8: Stresses distribution in elbow (a) Von-Mises stress, (b) Normal stress σ_{xx} and (c) Principal stress $\sigma_{\theta\theta}$.

Figure III.8 indicates that the maximum value of Von-Mises stress is 198.96 MPa. Normal stress σ_{xx} and principal stress $\sigma_{\theta\theta}$ have the same value equal to 219.56 MPa. The maximum stress criterion apply to the three different stresses gives a maximum stress localization in the

same node with an angle α = 72°. In the next part, a semi-elliptical crack is introduced with in different angular position along the intrados of elbow (α = 5° to α = 85°);α is defined in figure III.9.

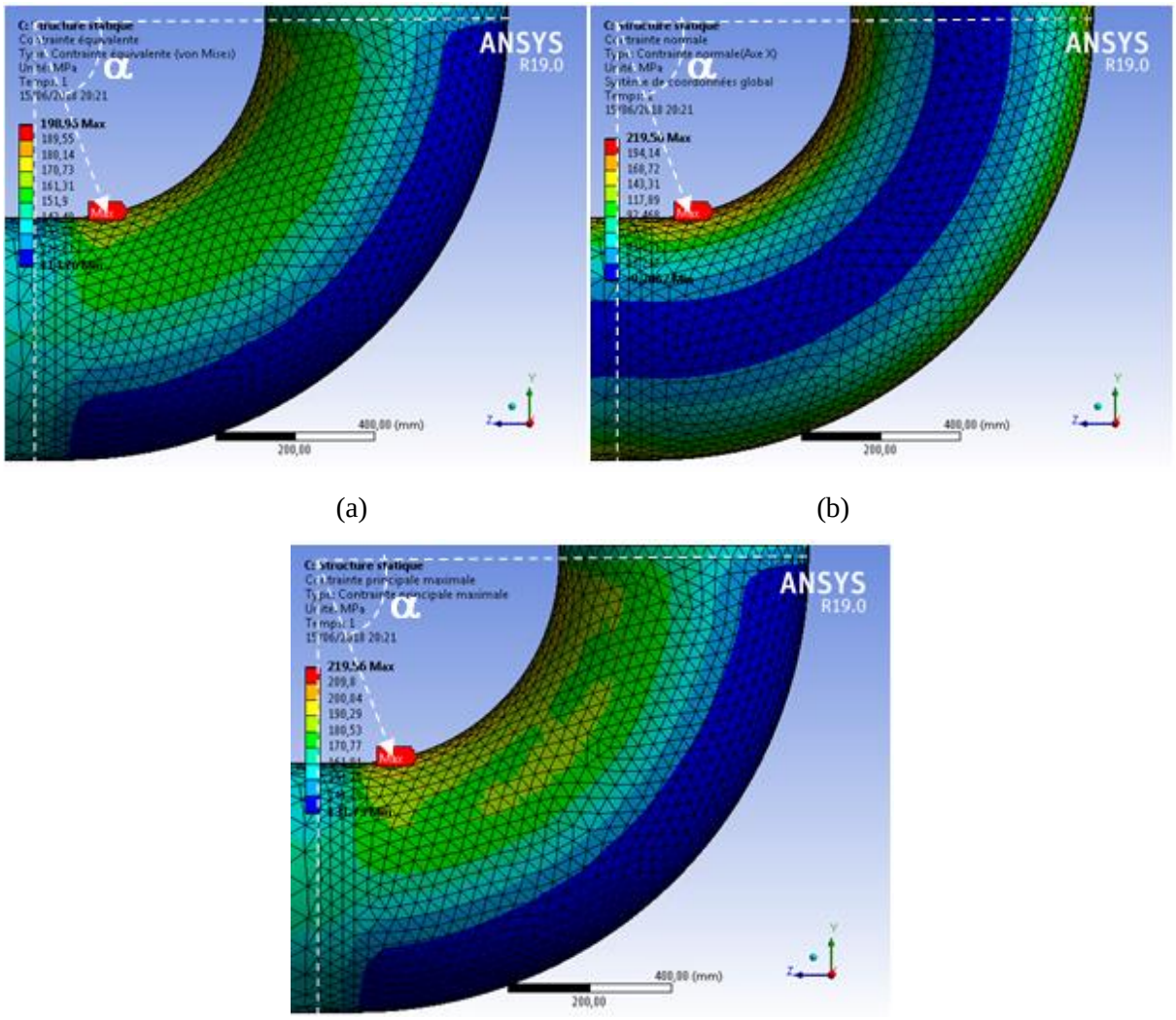

(a) (b)

(c)

Figure III.9: Maximum stresses distribution versus crack angle α in elbow (a) Von-Mises stress, (b) Normal stress σ_{xx} and (c) Principal stress $\sigma_{\theta\theta}$.

Depending on the depth ratio d/t = 0.5 and d/c = 0.5 which are considered as principal parameters of the semi-elliptical crack in our study in order to predict the behavior of elbow under the severe conditions. In addition, the stress intensity factor in mode I versus the crack tip angle ϕ is used to shows the behavior along the elbow for defining the critical zones. There are many reasons to generate the crack along the elbow, the industrial defect and join welded are still the original

of small crack where the maximum stresses are concentrated at weak zones.

Figure III.10 shows the stress intensity factor distributions in a semi-elliptical surface crack for different angular positions ϕ along the elbow intrados surface (α). Maximum mode I stress intensity factor $K_{I,Max}$ is localized at $\alpha = 75°$ and is given by the following formulae :

$$K_{IMax} = \sigma_{max} \times F \times \sqrt{2\pi d} \qquad \textbf{(III.1)}$$

σ_{max} is the maximum applied stress, d is the crack depth and F is the geometric function which depends of crack length, aspect ratio, as well as the type of applied load.

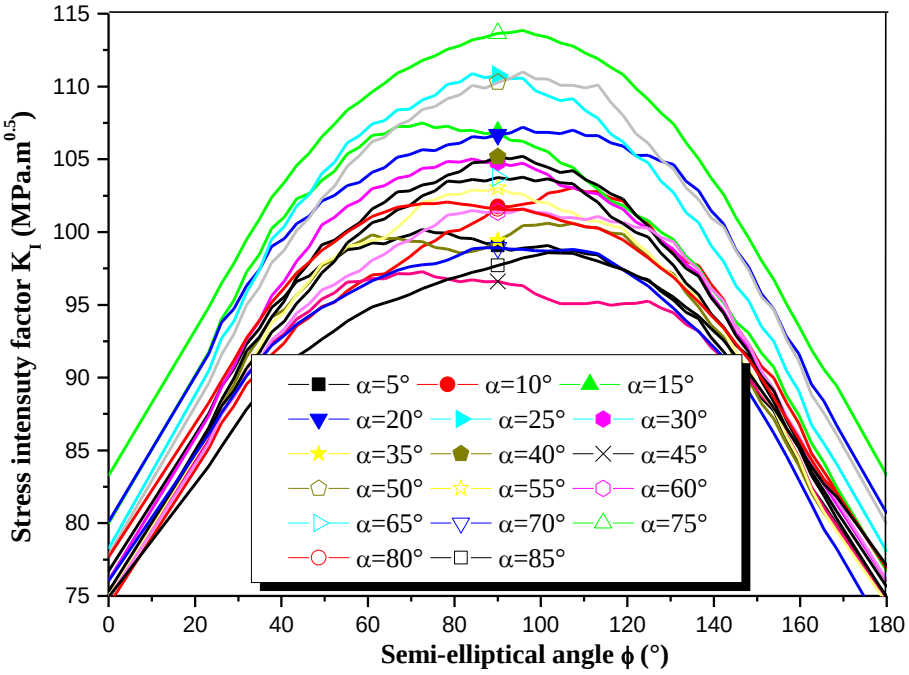

Figure III.10: Mode I stress intensity factor of semi-elliptical surface crack in elbow versus angular crack ϕ and for different angle position α (d/t =0.5, d/c =0.5, P =7 MPa).

III.2.3 Effect of angle crack orientation on SIFs

In fracture mechanics, the crack phenomenon is considered as the dangerous issue in the hydrocarbon industries which may lead to pipeline failure. Appearing the crack in elbow under the high pressure leads to create the small cracks along the elbow with different orientations. For this reason, the mixed mode of stress intensity factors (K_I, K_{II}, K_{III}) is accurately used to predict the crack behavior taking into consideration the pressure and the bend angle. In this work, crack is not naturally oriented perpendicular to normal stress therefore mixed mode of

loading (K_I, K_{II}, K_{III}) is applied. In addition, elbow curvatures induce mixed mode of loading however crack orientation is $\alpha = 0°$. The shape geometry and stress distributions at semi-elliptical external surface cracks in the critical position of intrados pipe elbow are illustrated in figure III.11 for three crack orientations (a) $\theta = 0°$, (b) $\theta = 45°$ and (c) $\theta = 90°$. According to the numerical calculation (Figure III.10), the crack is created in the critical zone at 75° of elbow steel which is subjected to the internal pressure (P = 7 MPa) resulting from natural gas that may affects the internal surface wall of pipe bend.

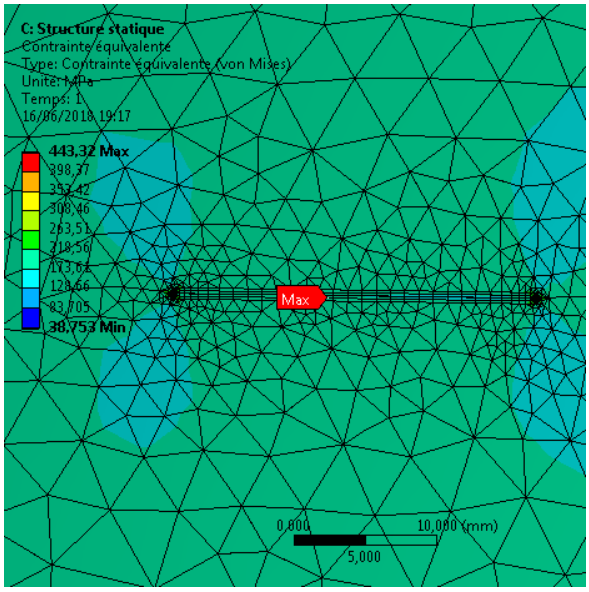

(a)

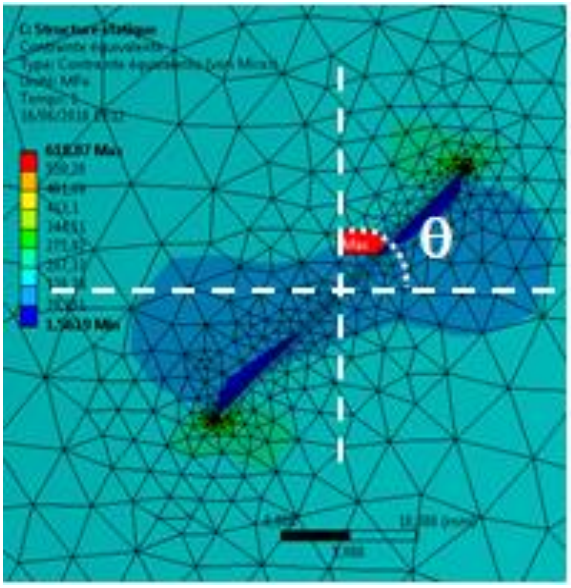

(b)

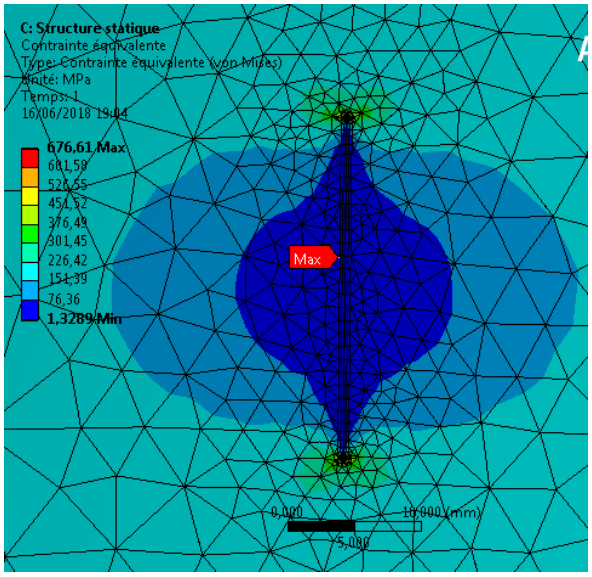

(c)

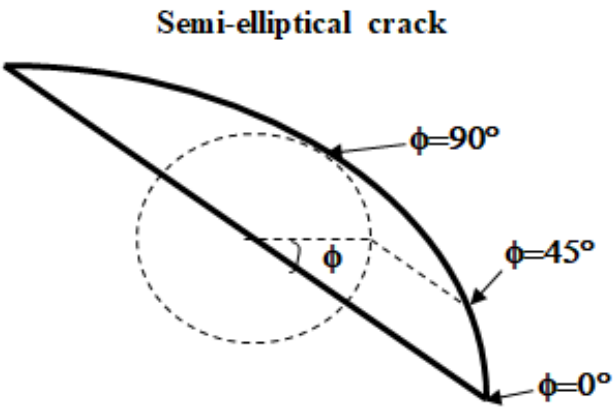

(d)

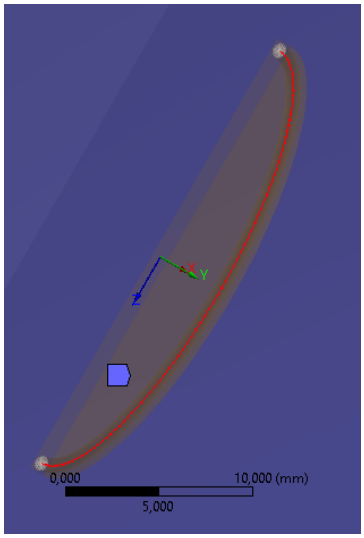

(e)

Figure III.11: Stress distribution at semi-elliptical crack tip for 3 crack orientations. (a) $\theta = 0°$, (b) $\theta = 45°$ and (c) $\theta = 90°$, (d) definition of angular position ϕ, and (e) shape of semi elliptical crack.

Next, the stress intensity factors are considered for a critical crack orientation ($\alpha = 75°$). The next figures present the stress intensity factors (K_I, K_{II}, K_{III}) distribution of semi elliptical crack tip for different crack angular positions (ϕ).

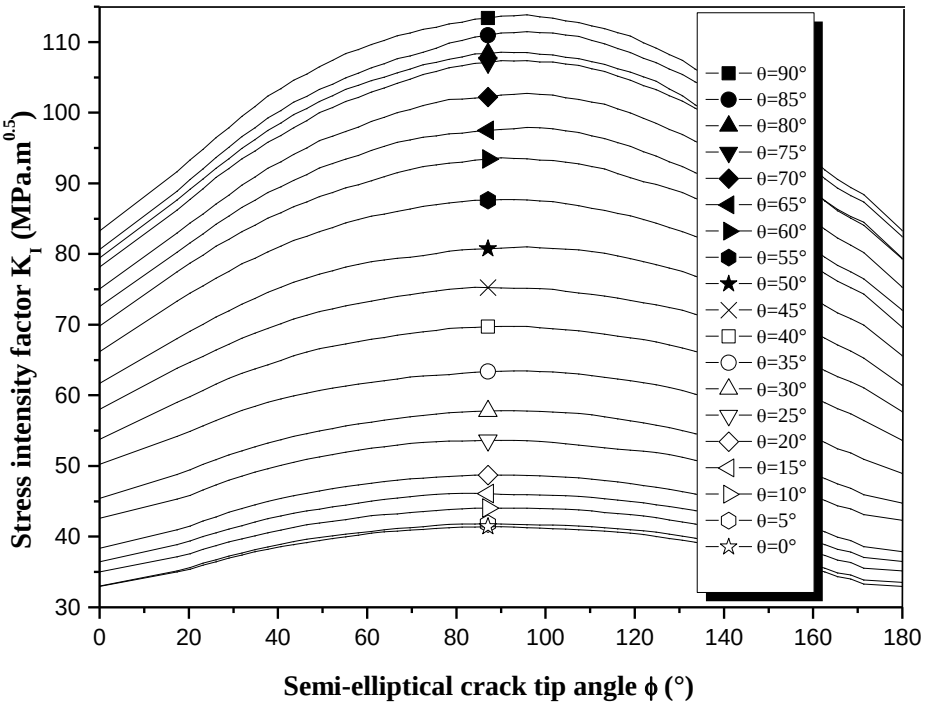

(a)

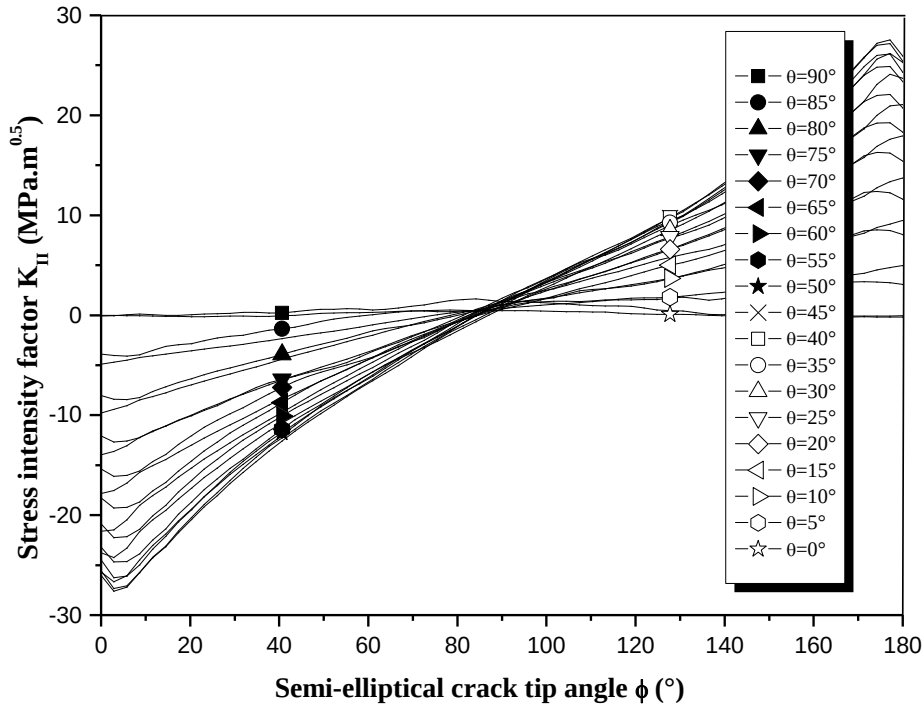

(b)

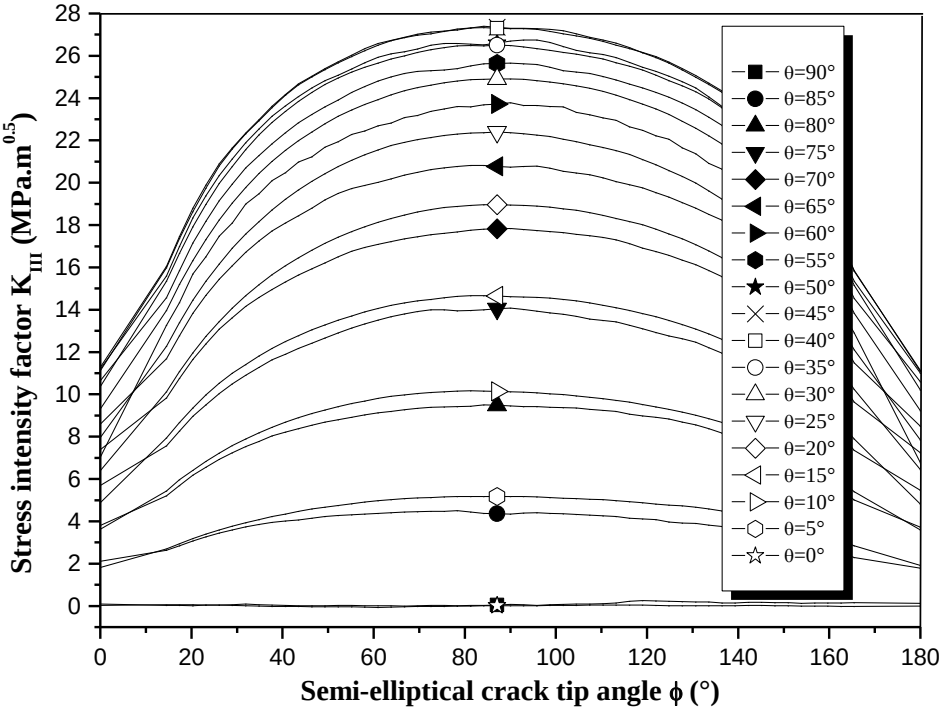

(c)

Figure III.12: Stress intensity factor with different orientations of crack-tip angle (a) mode I, (b) mode II, and (c) mode III.

III.2.4 Effect of crack depth ratio on SIF

Depending on the obtained results, the stress intensity factors including (K_I, K_{II}, K_{III}) allows to study the crack behavior along the elbow, in despite on the opening mode (I) is the most important mode than the modes II and III. Due to the complex geometry of elbow, the mode II is induced by longitudinal stress where mode III is influenced by the elbow curvatures taking into account the geometry, thickness and the bend of elbow. The SIF of mode I becomes the maximum value at $\phi = 90°$ which can be called as the critical angle.

However, the K_{II} value is very small and K_{III} value is less than K_I. Due to the presence of three modes (K_I, K_{II} and K_{III}), failure equation is based on the equivalent stress intensity factor which was presented in the precedent chapter (equation II.17).

$$K_{eq}^2 = K_I^2 + K_{II}^2 + (1+\nu)K_{III}^2 \qquad \textbf{(III.2)}$$

where ν is the Poisson's ratio. K_{eq} for crack orientation angle $\theta = 90°$ is higher than K_I, this parameter is able to show all values of three modes (K_I, K_{II} and K_{III}) as shown in simulated results. Figure III.13 presents the equivalent stress intensity factor with the orientation θ of semi-elliptical crack in different angular position ϕ. It shows that orientation of 90° has more efficiency for elbow pipeline. The influence of relative depth ratios (d/t) changing from 0.1 to 0.8 on stress intensity factors (K_I, K_{II}, K_{III}) is shown in figure III.14 for $d/t = 0.5$.

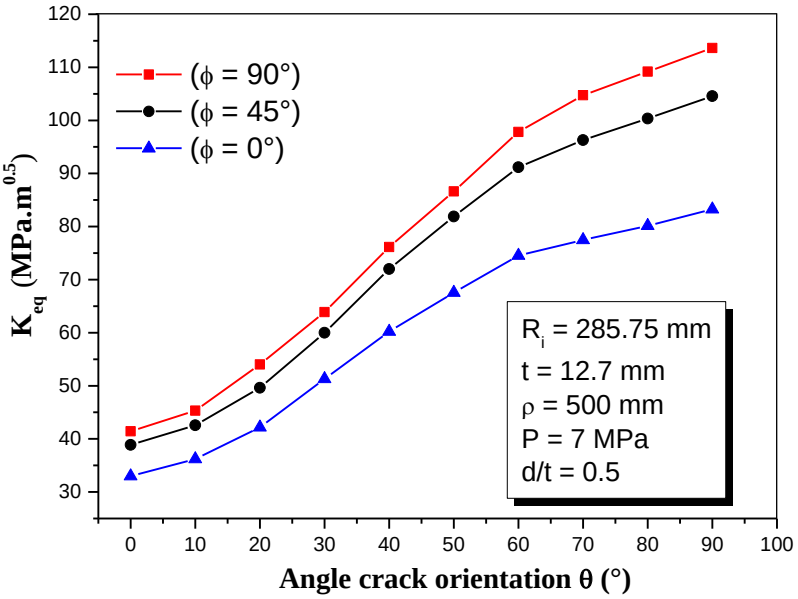

Figure III.13: Equivalent stress intensity factor versus relative crack orientation for different angular position.

Due to the concentration of crack's energy in the critical zones in the elbow, stress intensity factors in mode K_I and K_{eq} increase with relative crack depth ratios (d/t) as seen in figures III.13 and III.14.

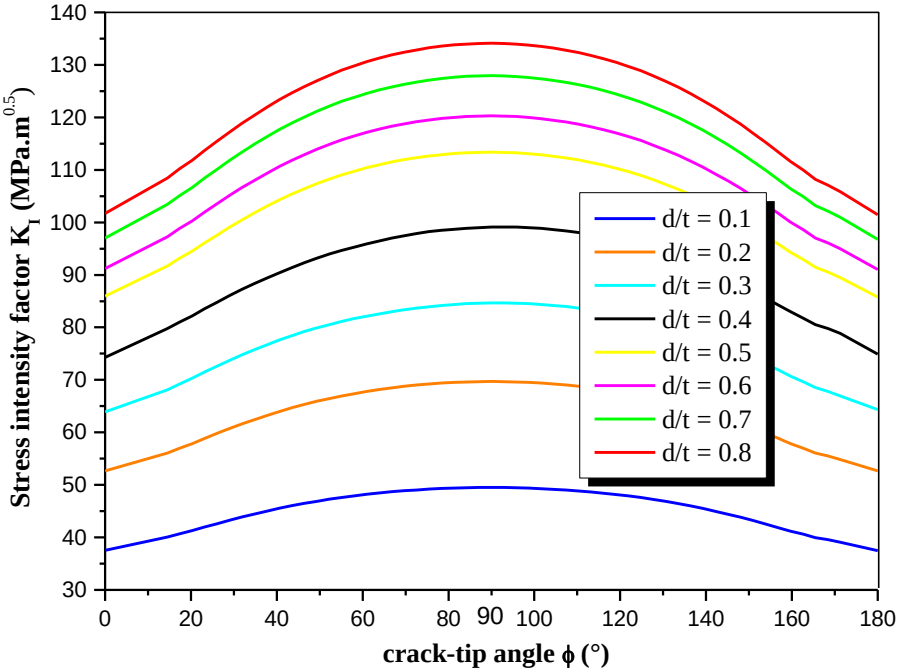

Figure III.14: Stress intensity factor in mode K_I versus angular position for different relative crack depth ratios (d/t).

Based on the operating conditions including the internal pressure and elbow curvature, the maximum equivalent of stress intensity factor K_{eq} was obtained at θ = 90° while K_{II} is approximately negligible. Semi-elliptical crack with different relative depths was examined at a critical position (α = 75°) and a critical crack angle (θ = 90°). Depending on the numerical data, the failure criterion for mixed mode is used to explain the phenomenon of crack:

$$\left(\frac{K_{I\phi}}{K_{IC}}\right)^2+\left(\frac{K_{II\phi}}{K_{IIC}}\right)^2+\left(\frac{K_{III\phi}}{K_{IIIC}}\right)^2=C \qquad \textbf{(III.3)}$$

Failure condition is given by C=1, $K_{I\phi}$, $K_{II\phi}$ and $K_{III\phi}$ are applied in elbow at critical zone for mode I, II and III K_{IC}, K_{IIC} and K_{IIIC} are the fracture toughness of three modes equal to 116.6, 116.6 and 67.27 MPa $\sqrt{}$ m respectively for API X52 pipe steel [2-4]. In steel;

$$K_{IC} = K_{IIC} \qquad \textbf{(III.4)}$$

and where the equation of calculation K_{IIIC} is given as follow:

$$K_{IIIC} = \frac{\tau_C}{\sigma_C} K_{IIC} \qquad \textbf{(III.5)}$$

where τ_c and σ_c are critical shear and normal stresses.

Figure III.15 gives an evolution of fracture condition *C* for different crack orientations under the same internal pressure and for a relative crack depth *d/t* =0.5.

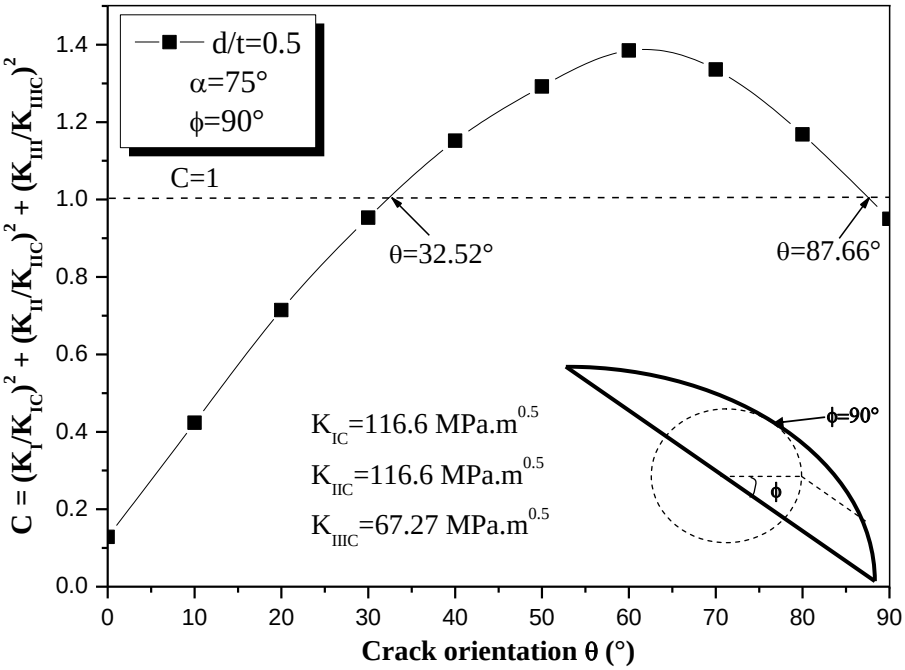

Figure III.15: Evaluation of fracture condition equation with crack orientation *C = f(θ)*.

Fracture condition is fulfilled for crack orientation in the value range of θ from 32.52° to87.66° for semi-elliptical crack front position ($\phi = 90°$).

III.2.5 Particular Failure Assessment Diagram (FAD) use for Elbow crack defect

The failure Assessment Diagram is one of the most techniques which used to study the behavior of elbow integrity and predict the failure time. It allows to determine the critical crack depth at a critical position and a critical angle with the aid of stress intensity factors and fracture toughness. In the case that the stress intensity factors were not enough to show the critical zones along the propagation of the cracks in the elbow, the FAD becomes a necessary step to predict the crack zones depending on three zones: the security zone, the safety zone, and the failure zone.

Figure III.16 represents the FAD curve for elbow and straight pipe for different value of relative depth crack ratio (*d/t*) in the range 0.1 - 0.8. The value of fracture toughness in the present study is based on the references [5, 6] where the constraint is represented by T stress [7] which calculated using the stress difference method [8, 9] through Material Failure Master Curve (MFMC).

Hence this technique expresses on the fracture toughness with the effective critical constrain $T_{ef,}$. For pipe steel, MFMC has been determined by equation III.6 where it obeys a linear relationship.

$$K_{IC} = aT_{ef,C} + K_{IC,0} \qquad \textbf{(III.6)}$$

where a is equal to -0.069√m and $K_{IC,0}$ is the reference fracture toughness for $T_{ef,c}$ = 0 and $K_{IC,0}$ = 77.28 MPa√m. For a straight pipe, a value of K_{IC} = 116.6MPa√m was obtained and corresponds to a low constraint under the internal pressure. For elbow, the value of fracture toughness was reduced to $K_{IC,0}$ = 95 MPa√m due to a higher constraint. Evolutions of assessment points for different relative crack depth ratios are reported in FAD for straight pipe and elbow with same pressure, diameter and thickness in figure III.16.

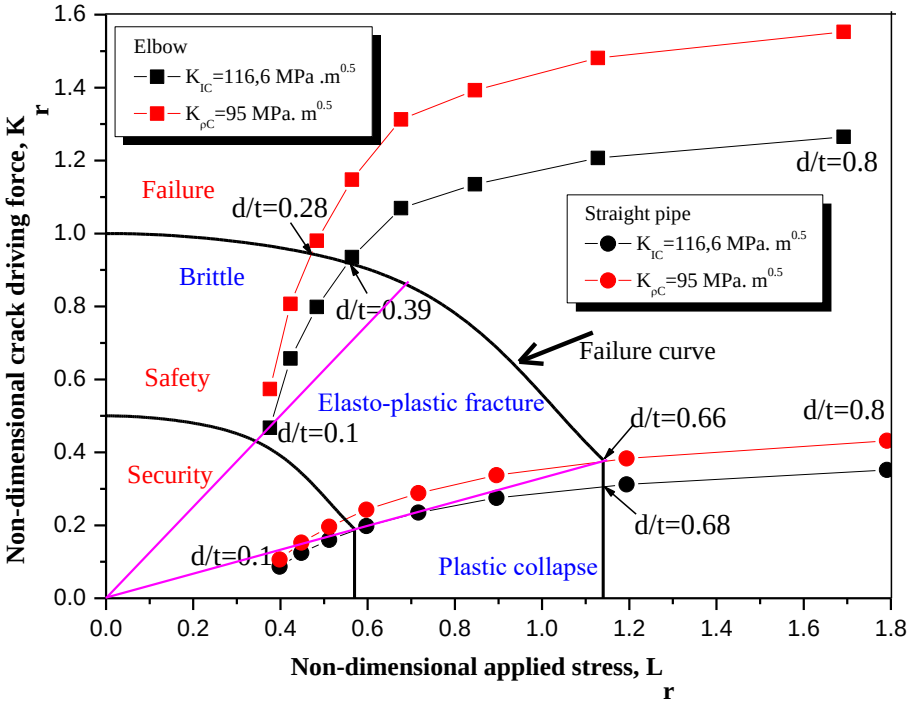

Figure III.16: Failure Assessment Diagram for straight pipe and elbow Evolution of assessment points with relative crack depth (*d/t*=0.1 - 0.8) and ($K_{\rho C}$ = 95 MPa.m$^{0.5}$ and K_{IC} = 116.6 MPa.m$^{0.5}$).

It is noted that due to stress amplification and higher constraint, the assessment points for the same defect size are located with higher ordinates. Critical defect sizes are defined when evolution curves cross the failure curve. For elbow, the relative critical defect depth is (d/t = 0.28), which is higher for a straight pipe (d/t = 0.66). Assessment points for elbow and below failure are located in the brittle zone of the FAD. This is proving the use of a linear behavior for computing SIF. This assumption is not valid for a straight pipe but it is given here for comparison.

III.3 ASSESSMENT OF CORRODED PIPE ELBOW

This section focuses on the simulation of 90° elbow with the parallelepiped rounded borders shaped corrosion defects with different relative defect depth ratios at the critical intrados locations which is performed using the FEA technique on the one hand. On the other hand, the numerical results are compared with the results which obtained by industrial models to modify the limit pressure equations of industrial models (ASME B31G, modified ASME B31G, and DNV RP-F101), presented in chapter II. The modification includes the use of the Goodall formula [10] (equation (III.7)) for the hoop stress σ_θ in the pipe elbow during the calculation of the limit pressure P_L according to three industrial models originally developed for the straight pipe.

$$\sigma_\theta = \frac{Pr}{t} \times \frac{1 - r/2R}{1 - r/R} \qquad \textbf{(III.7)}$$

The present results allow studying the behaviour of elbow defects, where the obtained results with discussions are divided into three subsections. First, in subsection III.3.1, the hoop stress at the intrados location of the pipe elbow without defect was examined and calculated using the equations suggested in the literature for the straight pipe (Chapter II) and Goodall formula for the pipe elbow (equation (III.7)). In addition, the obtained results are compared with the results for the distribution of hoop stress on the intrados (ϕ = 0°) sections of the pipe elbow obtained by numerical FEA. In the next subsection III.3.2, the results of the limit pressure calculation for different corrosion defect depth ratios using three modified industrial models (ASME B31G, modified ASME B31G, and DNV RP-F101), and the Goodall formula [11] for calculation of the hoop stress (σ_θ) in the pipe elbow, is presented and compared with numerical FEA results. Furthermore, the NFAD for the straight pipe and elbow with corrosion defects for the safety factor calculation is presented and further analyzed in the final subsection III.3.3.

III.3.1 Hoop stress at intrados section of the pipe elbow

An elbow is subjected to the internal service pressure P_s = 7 MPa. The FEM results are shown in figure III.17. Figure III.17a shows the 90° pipe elbow geometry and figure III.17b shows the mesh constructed with a 16-node quadrilateral element. Figure III.17c illustrates the hoop stress distribution along the pipe elbow. Figure III.18a presents the distribution of hoop stresses at different angles along the pipe elbow, as illustrated in figure III.18b.

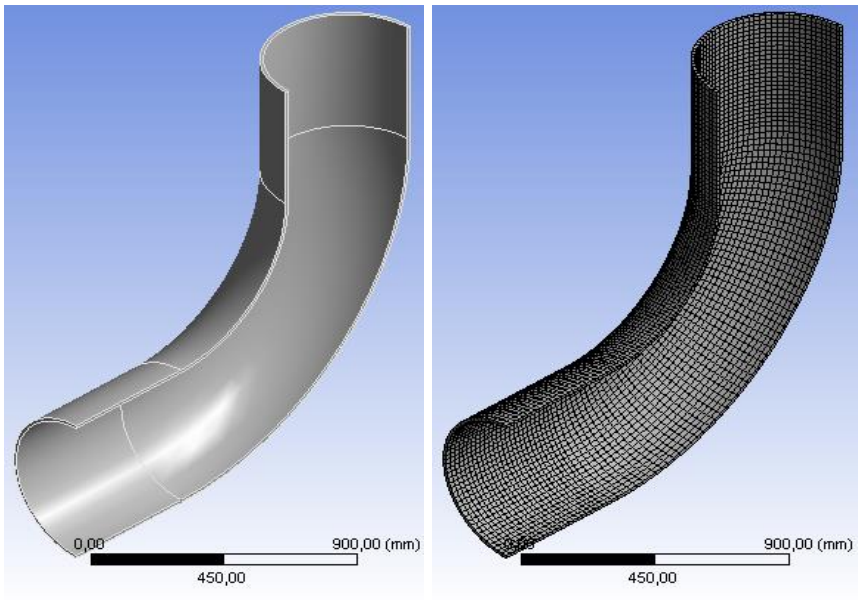

(a) (b)

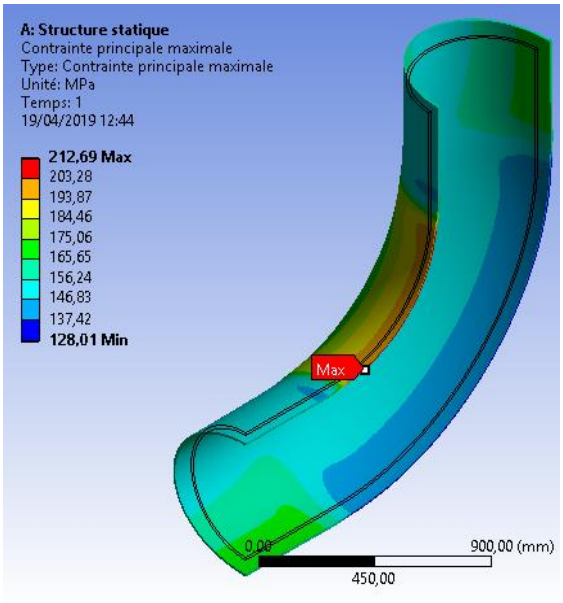

(c)

Figure III.17: Pipe elbow without corrosion defects subjected to the internal service pressure P_s= 7 MPa, (a) geometry, (b) meshing, and (c) hoop stress distribution.

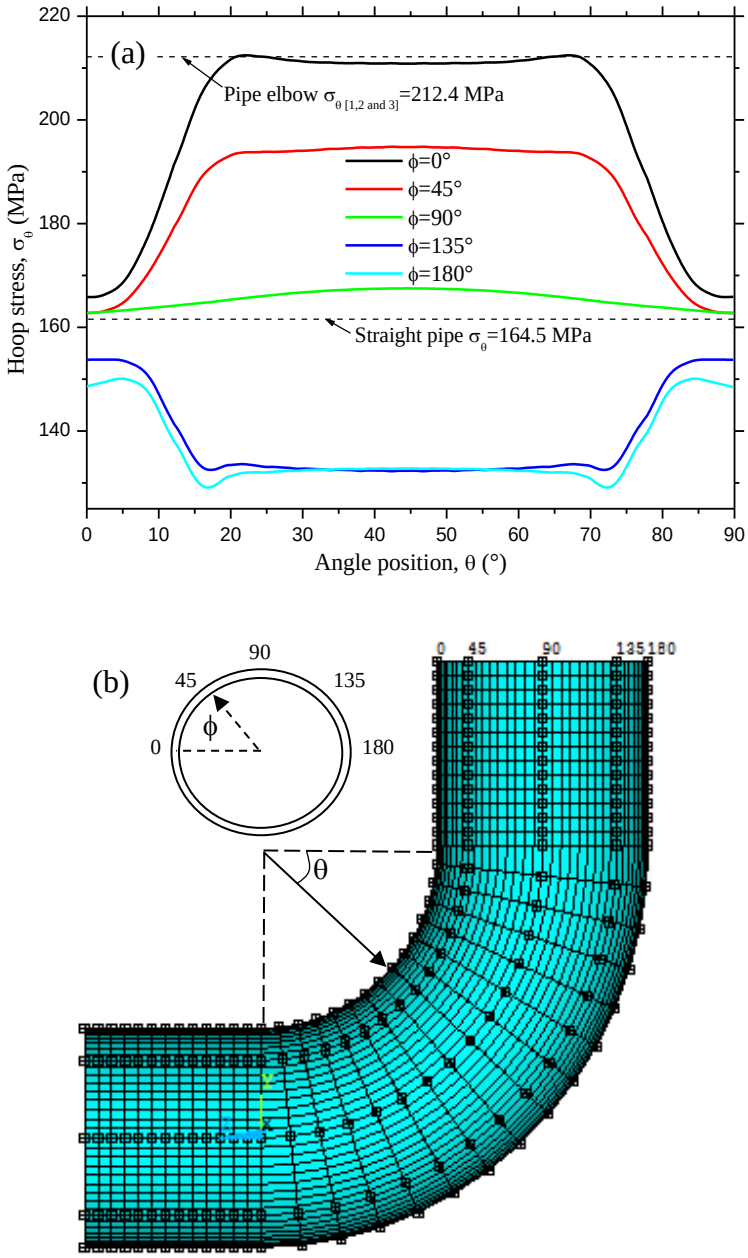

Figure III.18: Pipe elbow without corrosion defects: (a) distribution of the hoop stress; (b) different paths angles along the pipe elbow.

Due to the operating conditions, the mechanical characteristics change during the flow in pipeline, where the maximal value of hoop stress is concentrated at the intrados side of elbow, as shown in figures III.17 and III.18. Depending on the analyses of elbow crack phenomenon, figures III.18a and III.18b show the distribution of hoop stress along the intrados ($\phi = 0°$), extrados ($\phi = 180°$) and crown ($\phi = 90°$) sides of the elbow. Moreover, the obtained results prove

that the critical zones focus on the intrados section of the elbow according to the obtained high hoop stress value that equals σ_θ = 212.4 MPa. In addition, the hoop stress value decreases at the crown side of the elbow, where it is near to the value for the straight pipe (σ_θ = 164.5 MPa) as shown in figure III.19.

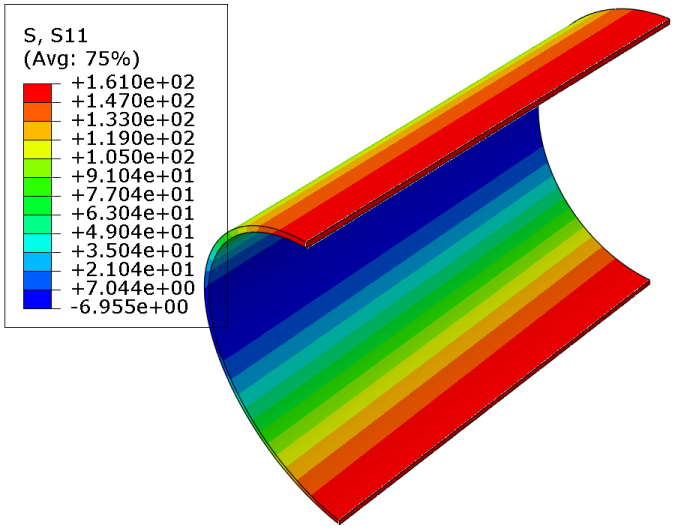

Figure III.19: Distribution of the hoop stress in the straight pipe (Internal pressure P = 7 MPa, internal radius R_i = 285.75 mm, wall thickness t = 12.7 mm, and the length L = 1000 mm).

Table III.2: Hoop stress σ_θ at the intrados section of the pipe elbow without corrosion defects.

Method of calculation	Hoop stress, σ_θ (MPa)	Error (%) = $(\sigma_{\theta\,(FEA)} - \sigma_{\theta\,(Eq.II.6\ and\ Eq.\ III.7)}) / \sigma_{\theta\,(FEA)}$ x 100%
Numerical FEA model (Figure III.17)	$\sigma_{\theta\,(FEA)}$= 212.69	-
Goodall formula [10] (equation (III.7))	$\sigma_{\theta\,(Eq.III.7)}$= 201.39	5.32
Straight pipe formula (equation (II.6))	$\sigma_{\theta\,(Eq.II.6)}$= 157.50	25.94

Table III.2 shows the maximal hoop stress values obtained by the numerical FEA model together with values obtained using the Goodall formula (equation (III.7)), and the formula for the straight pipe (equation (II.6)). It is clear that the hoop stress value obtained using the Goodall formula - equation (III.7) (σ_θ = 201.39 MPa) is close to the value obtained by the numerical

FEA model, figure III.17 (σ_θ = 212.69 MPa), with the small error of 5.32 %, Table III.2. The error is calculated using the following formula: Error (%) = ($\sigma_{\theta\,(FEA)}$-$\sigma_{\theta\,(Eq.II.6,\ III.7)}$)/$\sigma_{\theta\,(FEA)}$ x 100%, where $\sigma_{\theta\,(FEA)}$, and $\sigma_{\theta\,(Eq.II.6,\ III.7)}$ are the hoop stress values obtained by FEM model, equation (II.6), and equation (III.7), respectively. On the other hand, the much higher error (25.94%) is obtained using the straight pipe formula (equation (II.6)) for calculation of the hoop stress (σ_θ= 157.50 MPa), Table III.2. Such a large discrepancy between hoop stress values at the intrados section of the pipe elbow, obtained by both FEA and the Goodall formula, and the value obtained using the formula for the straight pipes indicate on the high criticality of this section of pipe elbows. A good agreement between the hoop stress value obtained using the Goodall formula [10] for calculation of the hoop stress (σ_θ) in a pipe elbow, and the value obtained by numerical FEA model (see Table III.2, error = 5.32%), provides a solid background for checking the limit pressure calculations results using three modified industrial models. Also, the obtained numerical FEA value for the hoop stress ($\sigma_{\theta\,(FEA)}$ = 212.69 MPa) as well as the error in comparison with the Goodall formula [10] results (5.32%) are in close agreement with the maximum error of 6.58% reported by Duan and Shen [12]. Once again, the hoop stress value obtained by the Goodall formula is somewhat higher than that obtained by the numerical FEA. The comparison of results obtained using modified industrial models and the FEA results is the topic of the next subsection III.3.2.

III.3.2. The limit pressure calculation using modified industrial models and FEA results

In this part, the corroded pipe elbow assessment is studied to prevent their burst and the results of the limit pressure calculation using modified industrial models are compared with the FEA results. Previous research indicates that there is a serious need to determine a perfect formula to calculate a limit pressure at the intrados section of the pipe elbow [11-17]. Therefore, the limit pressure of the corroded pipe elbow is analyzed using FEA, as shown in figures III.21 and III.22. The parallelepiped rounded borders shape corrosion defect is simulated at the intrados section of the pipe elbow. The pipe elbow with a length (L = 174 mm), width (W = 208 mm), and with different geometrical corrosion defect depth to wall thickness ratio (d/t = 0.1 - 0.8, see Figure III.20) is investigated, figure III.21. The defects with different d/t depth ratios were modeled at the intrados section of the 90° pipe elbow, figures III.21a and III.21b. The hoop stress distribution for d/t = 0.5 is shown in figure III.21c.

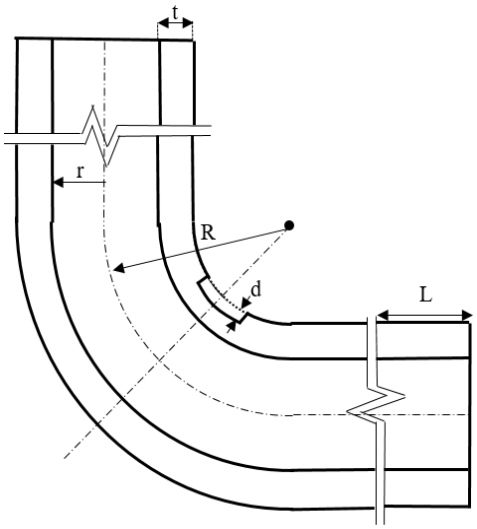

Figure III.20: The position of rectangular parallelepiped-shaped in the center intrados location.

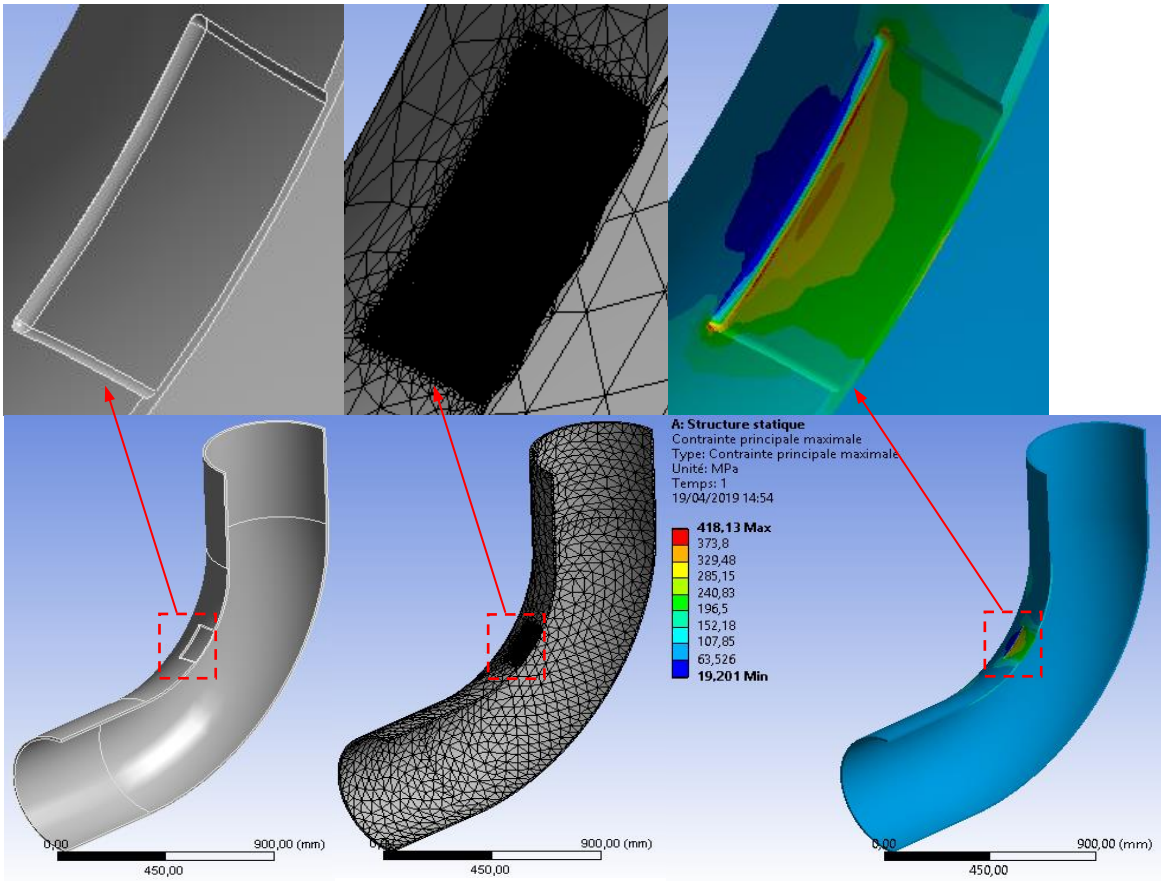

(a) (b) (c)

Figure III.21: (a) the geometry of rectangular corrosion defect, (b) meshing, and (c) hoop stress distribution (d/t= 0.5).

In conducted FEA, for each defect depth (d/t= 0.1 - 0.8, see Figure III.20), the applied pressure

is increased with an increment of 1 MPa, from 1 MPa to the maximal 16 MPa. The hoop stress that is equal to the yield or ultimate strength can be considered as a limit pressure, as indicated in figure III.22a. The effects of defect depth ratios (d/t= 0.1 - 0.8) on the hoop stress were analyzed at different internal pressures. Below the yield strength value (σ_y= 410 MPa), a typical linear increase of the hoop stress can be observed, figure III.22a. Due to the entering into the plastic regime, above σ_y while approaching the ultimate strength value (σ_{ult}= 520 MPa), nonlinearity in the hoop stress increase was observed, figure III.22a. Figure III.22b illustrates the numerical FEA obtained limit pressures based on the yield σ_y and ultimate strength σ_{ult} values for API 5L X52 steel with different defect depth ratios (d/t= 0.1 - 0.8, see Figure III.20) at the intrados section of the pipe elbow.

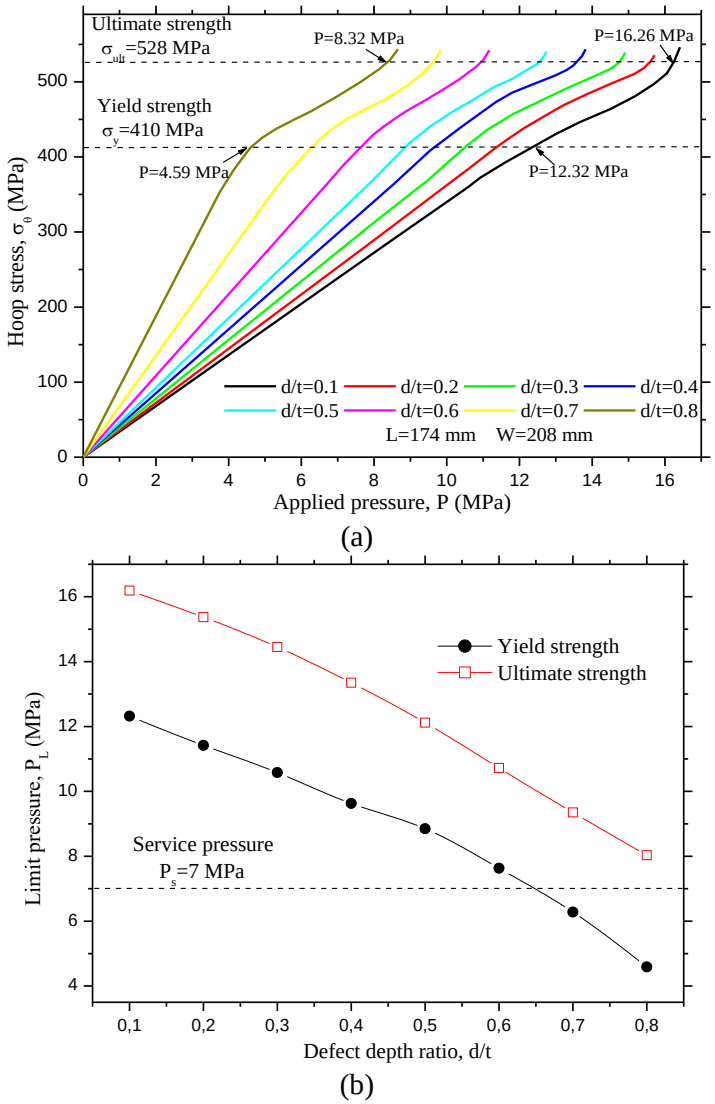

Figure III.22: (a) hoop stress versus internal pressure; (b) limit pressure P_L according to the yield and ultimate strength.

As previously discussed, the limit pressure determines the pipe burst. It depends on two main mechanical properties (i) yield strength σ_y and (ii) ultimate strength σ_{ult}. As indicated in figures III.22a and III.22b, the limit pressure for the pipe elbow made of API 5L X52 steel with defect depth ratio d/t= 0.1 is almost 16 MPa based on the ultimate strength, and 12 MPa based on the yield strength. While the limit pressure for defected pipe elbow with defect depth ratio d/t= 0.8 is much lower, approximately 8 MPa based on the ultimate strength and only 4.5 MPa based on the yield strength. The reduction of the internal service pressure P_s = 7 MPa (Figure III.22b) in the pipe elbow is necessary when a critical defect depth reached d/t = 0.65, based on the yield strength σ_y = 410 MPa for API 5L X52 steel. In this study of pipe elbows, the presented numerical FEA results (Figure III.22b) indicate that the use of yield strength as a limit value for the limit pressure determination does not represent a conservative solution as it was in the case of straight pipe made of the same steel [18,19]. Nevertheless, during comparison of the suitability for application of the ultimate strength or yield strength as a limit value for the limit pressure determination and the conservatism estimation, it is necessary to take into account other important factors. These factors are (i) the pipeline component: straight pipe or a pipe elbow, (ii) the type of the defect: cracks (the stress intensity factor - SIF) or corrosion defects without the crack, (iii) geometrical characteristics of the corrosion defect (the degree of stress intensification), and (iv) the defect depth ratio d/t [18- 26].

The comparison between the numerical FEA results for the limit pressure, and results obtained using three modified industrial models (ASME B31G, modified ASME B31G, and DNV RP-F101) for different corrosion defect depth ratios are presented in figure III.23. The decrease of the limit pressure in API 5L X52 made steel pipeline is compared for the straight pipe case, using three standard industrial models, and for the pipe elbow case, using both modified industrial models together with the Goodall formula for calculation of the hoop stress in the pipe elbow and FEA results. The numerical FEA results for the limit pressure based on both yield strength and ultimate strength are presented in figure III.23. The parallelepiped rounded borders shape corrosion defects with different corrosion defect depth ratios (d/t= 0.1 - 0.8) are located at the straight pipe, and at the intrados section of the pipe elbow (Figure III.21), respectively. As expected, the limit pressure values in the straight pipe, obtained using all three industrial models, are significantly higher than for the pipe elbow. This indicates that the application of unmodified - original industrial models developed for the straight pipe in the case of the pipe

elbow is not advisable and justified because of the significant overestimation of the allowable limit pressure.

Contrary, the results for the modified industrial standards that take into account the pipe elbow geometry by using the Goodall formula for calculation of the hoop stress in the pipe elbow are found to be in close agreement with the numerical FEA results. When the ultimate strength is used to determine the limit pressure in the numerical FEA ($P_L\ \sigma_{ult(FEA)}$), a much better agreement with results for all three modified standards are confirmed, Table III.3. The maximal error within the range 10.56% (d/t = 0.1) - 17.93% (d/t = 0.8), (error (%) = ($P_{L\ (B31G)}$ - $P_L\ \sigma_{ult(FEA)}$) / $P_L\ \sigma_{ult(FEA)}$ x 100%) is obtained using ASME B31G industrial model for all defect depth ratios, Table III.3. For defect depth ratios d/t below 0.5, the ASME B31G industrial model calculation results are conservative (error: 1.40% (d/t = 0.5) up to 10.56% (d/t = 0.1)), and the gap between the FEA and ASME B31G results is diminishing while approaching the defect depth ratio of 0.5. At defect depth ratios higher than d/t = 0.5, the ASME B31G results for the limit pressure are higher than those obtained by the FEA (error: 4.39% (d/t = 0.6) - 17.93% (d/t = 0.8)), and the gap (error) becomes higher with further defect depth ratio increase up to d/t= 0.8, Table III.3. The similar conservative trend when using ASME B31G industrial model was also observed by Lee et al. [15] and Amandi et al. [27]. The results for the limit pressure ($P_{L\ (Mod.\ B31G)}$ and $P_{L\ (DNV)}$) obtained using other two modified industrial standards (modified ASME B31G, and DNV RP-F101) are less conservative, higher than those obtained by the FEA, and in better agreements with the numerical FEA results based on the ultimate strength ($P_L\ \sigma_{ult(FEA)}$), see Figure III.23 and Table III.3. The curvature of the FEA results and for both ASME B31G and DNV RP-F101 industrial models follow a similar trend.

The results for both modified industrial models are slightly less conservative than FEA results and similarly for all defect depth ratios. The similar trend of the burst pressure values of the damaged pipe elbows obtained using ASME B31G and DNV RP-F101 industrial models was also observed by Lee et al. [15], albeit their study indicates that both models have shown more conservatism than the FEA. The results obtained in this study using the modified ASME B31G standard ($P_{L\ (Mod.\ B31G)}$) are closest to the numerical FEA results ($P_L\ \sigma_{ult(FEA)}$) for all defect depth ratios, Figure III.23. The error is relatively small for all depth ratios and within the range 2.49 - 10.27%, Table III.3. On the other hand, the numerical FEA results for the limit pressure in the

pipe elbow using the yield strength ($P_L\ \sigma_{y(FEA)}$) for different defect depth ratios are consistently much more conservative, figure III.23. These numerical model results obtained using the Goodall formula for calculation of the hoop stress in the pipe elbow are in good agreement with results reported by Duan and Shen [12] for the case when the maximum strain is located in the inner wall at the intrados of the pipe elbow.

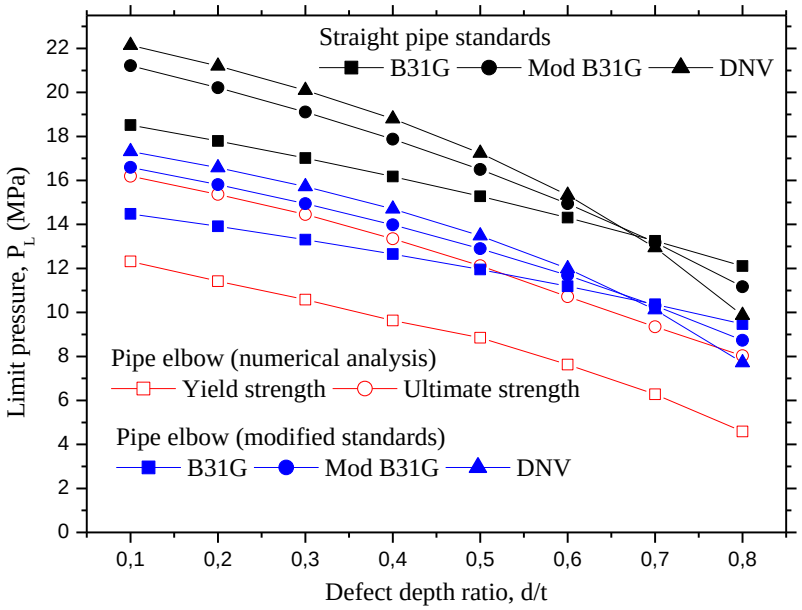

Figure III.23: Comparison between the limit pressure values in the straight pipe and the pipe elbow (at the intrados section) for different depth ratios (d/t = 0.1 - 0.8).

Table III.3: The difference in the limit pressure P_L values for the pipe elbow based on the ultimate strength ($P_L\ \sigma_{ult(FEA)}$) obtained by FEA, and by modified industrial standards (B31G, modified B31G, and DNV RP-F101) using the Goodall formula for calculation of the hoop stress in the pipe elbow.

Defect depth ratio, d/t	P_L (MPa), see Figure III.23, and Error (%) = ($P_{L\ (B31G,\ Mod.\ B31G,\ and\ DNV)}$ - $P_L\ \sigma_{ult(FEA)}$) / $P_L\ \sigma_{ult(FEA)}$ x 100%						
	$P_L\ \sigma_{ult(FEA)}$ (MPa)	$P_{L\ (B31G)}$ (MPa)	Error (%)	$P_{L\ (Mod.\ B31G)}$ (MPa)	Error (%)	$P_{L\ (DNV)}$ (MPa)	Error (%)
0.1	16.19	14.48	10.56	16.59	2.49	17.32	6.95
0.2	15.37	13.91	9.48	15.81	2.86	16.58	7.87
0.3	14.45	13.31	7.91	14.94	3.41	15.72	8.79
0.4	13.35	12.65	5.21	13.98	4.72	14.70	10.14
0.5	12.12	11.95	1.40	12.90	6.45	13.48	11.25
0.6	10.72	11.19	4.39	11.69	9.03	11.99	11.85
0.7	9.35	10.37	10.87	10.31	10.27	10.12	8.26
0.8	8.03	9.47	17.93	8.73	8.77	7.72	3.89

III.3.3 Notch Failure Assessment Diagram (NFAD)

In this final subsection, the notch failure assessment diagram (NFAD) for the straight pipe and pipe bends with corrosion defects is presented and analyzed. The assessment point in NFAD is defined with two non-dimensional parameters - coordinates (L_r, K_r), where L_r is applied stress (load), and K_r is a driving force.

Figure III.24 shows the NFAD for the straight pipe and pipe elbow with different parallelepiped rounded borders shaped corrosion defect depth ratios (d/t= 0.1 - 0.8) at the intrados section. Evolutions of the function point coordinates, which define the assessment point on the NFAD, indicate that the pipe elbow is a more endangered component of the pipeline. For all corrosion defect depth ratios, the assessment points for the pipe elbow have a higher value of both coordinates (L_r, K_r) then for the straight pipe due to the stress amplification and higher constrain in pipe elbows. Particularly, the non-dimensional applied crack driving force K_r coordinates for all corrosion defect depth ratios are higher for the pipe elbows. The difference between the K_r coordinate for the pipe elbow and straight pipe increases significantly with an increase of the corrosion defect depth ratio d/t from 0.1 to 0.8. Therefore, only at the lowest corrosion defect depth ratio (d/t= 0.1), the pipe elbow assessment point is in the elasto-plastic failure domain of the NFAD. A further significant rise of the K_r coordinates at somewhat higher d/t ratios ($0.1 < d/t \leq 0.38$), provokes conditions for the pipe elbow assessment points to be shifted into the brittle zone of the NFAD, but still within the safety zone. The loading path increases in a more non-linearly way with the rise of crack depth ratio d/t ($0.38 < d/t \leq 0.8$) at the intrados section of the pipe elbow. Also, for the corrosion depth ratios higher than the critical (d/t> 0.38), all assessment points are located in the failure zone of the NFAD, figure III.24. The obtained critical parallelepiped rounded borders shaped relative corrosion defect depth ratio (d/t= 0.38) for the pipe elbow is somewhat higher than the critical semi-elliptical relative crack depth ratio (d/t= 0.28) in the pipe elbow obtained in figure III.16.

The loading path increases in a more linear way for the straight pipe with different corrosion defect depth ratio. More linear behavior is mainly the consequence of the lower increments of the corresponding K_r coordinates for the straight pipe with the increase of d/t. The obtained critical parallelepiped rounded borders shaped relative corrosion defect depth ratio (d/t= 0.69) for the straight pipe is significantly higher than for the pipe elbow (d/t= 0.38). Moreover, all

assessment points for the straight pipe with corrosion defect depth ratios below the critical ($0.1 < d/t \leq 0.69$) are located in the least dangerous plastic collapse fracture domain of the NFAD, as shown in figure III.24. The obtained critical parallelepiped rounded borders shaped relative corrosion defect depth ratio (d/t= 0.69) for the straight pipe, figure III.24, is slightly higher than for the critical semi-elliptical relative crack depth ratio (d/t= 0.66) in the straight pipe obtained in figure III.16. Also, for the crack depth ratios lower than the critical ($0.1 < d/t \leq 0.66$), investigated in figure III.16, all assessment points were located in the more dangerous elasto-plastic fracture domain of the NFAD. Contrary, in this section of the parallelepiped rounded borders shaped corrosion defects in the straight pipe, for all defect depth ratios lower than the critical ($0.1 < d/t \leq 0.69$), the assessment points are located in the less dangerous plastic collapse fracture domain of the NFAD, as shown in figure III.24.

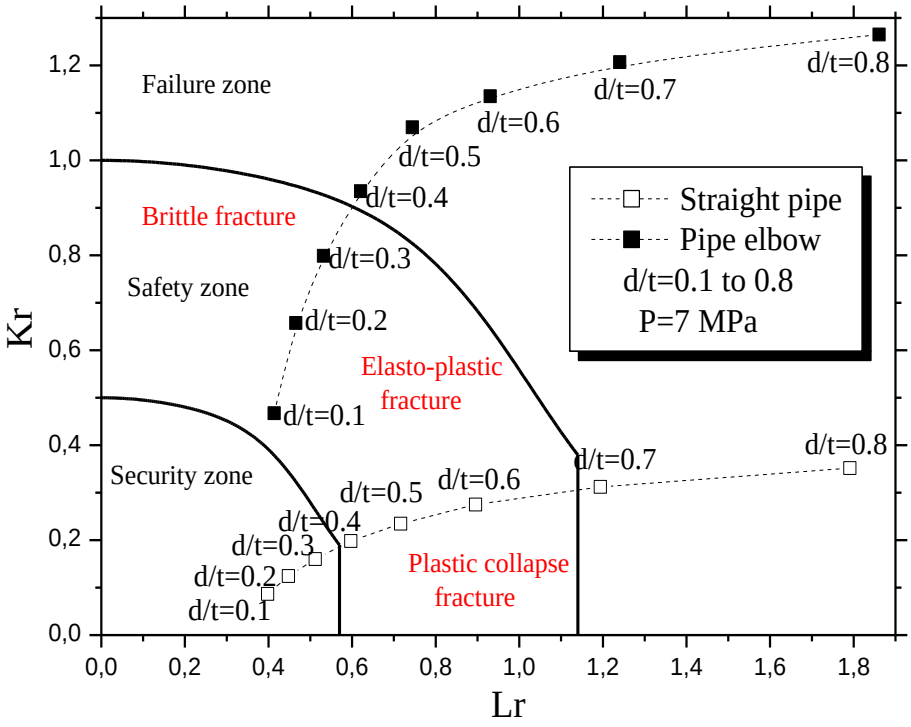

Figure III.24: Notch failure assessment diagram (NFAD) for the straight pipe and pipe elbow with different parallelepiped rounded borders shaped corrosion defect depth ratios (d/t= 0.1 - 0.8) at the intrados section.

It can be concluded that due to more pronounced stress intensification provoked by the semi-elliptical cracks with different relative depth rations, the structural integrity and reliability of both straight pipe and pipe elbow is more threatened that in the case of a parallelepiped rounded

borders shaped corrosion defects. The results presented in this section indicate further that the more severe stress conditions in pipe elbows with corrosion defect at the intrados section in comparison to the straight pipe lead to the shift of assessment points into the brittle zone of the modified NFAD. According to industrial models, previously analyzed in the subsection III.3.2, the straight pipe can resist the defect depths which reach 80-85% of pipe wall thickness [15, 28-29]. The results presented in this section and the NFAD for the straight pipe indicate that such a criterion is overly optimistic and hence not universally applicable. The presented results are proving the applicability and practical benefits of the modified NFAD. The NFAD is useful for the reliability assessment of corroded pipes and particularly critical pipe elbows taking into account the different shapes and depth of defects and the significant stress intensification in pipe elbows.

Refernces

[1] https://www.ansys.com/products;

[2] Hadj Meliani, M., Pluvinage, G. and Capelle, J., 2009. Gouge assessment for pipes and associated transferability problem. *In Defect and Diffusion Forum, Trans Tech Publications Ltd*, 294, pp. 15-25, https://doi.org/10.4028/www.scientific.net/DDF.294.15;

[3] Hadj Meliani, M., Matvienko, Y.G. and Pluvinage, G., 2011. Corrosion defect assessment on pipes using limit analysis and notch fracture mechanics. *Engineering Failure Analysis*, 18(1), pp.271-283, https://doi.org/10.1016/j.engfailanal.2010.09.006;

[4] Pluvinage, G., Capelle, J. and Hadj Meliani, M., 2019. Pipe networks transporting hydrogen pure or blended with natural gas, design and maintenance. *Engineering Failure Analysis*, 106, p.104164, https://doi.org/10.1016/j.engfailanal.2019.104164;

[5] Bouledroua, O., Hadj Meliani, M. and Pluvinage, G., 2017. Assessment of pipe defects using a constraint-modified failure assessment diagram. *Journal of Failure Analysis and Prevention*, 17(1), pp.144-153, https://doi.org/10.1007/s11668-016-0221-z;

[6] Amara, M., Bouledroua, O., Hadj Meliani, M., Muthanna, B.G.N., Tahar Abbes, M. and Pluvinage, G., 2018. Assessment of pipe for CO_2 transportation using a constraint modified CTOD failure assessment diagram. *Structural Integrity and Life*, 18(2), pp.149-153, http://divk.inovacionicentar.rs/ivk/ivk18/149-IVK2-2018-MA-OB-MHM-BGNM-MTA-GP.pdf ;

[7] Bouledroua, O., Hadj Meliani, M. and Pluvinage, G., 2016. A review of T-stress calculation methods in fracture mechanics computation. *Nature & Technology*, (15), pp. 20-30, https://www.univ-chlef.dz/revueNatec/issue-15/Article_A/A_O.%20Bouledroua.pdf;

[8] Elazzizi, A., Hadj Meliani, M., Khelil, A., Pluvinage, G. and Matvienko, Y.G., 2015. The master failure curve of pipe steels and crack paths in connection with hydrogen embrittlement. *International Journal of Hydrogen Energy*, 40(5), pp.2295-2302, https://doi.org/10.1016/j.ijhydene.2014.12.040;

[9] Hadj Meliani, M., Azari, Z., Al-Qadhi, M., Merah, N. and Pluvinage, G., 2015. A two-parameter approach to assessing notch fracture behaviour in clay/epoxy nanocomposites. *Composites Part B: Engineering*, 80, pp.126-133, https://doi.org/10.1016/j.compositesb.2015.05.034;

[10] Goodall, I.W., 1978. Lower bound limit analysis of curved tubes loaded by combined internal pressure and in-plane bending moment. Research Division *Report RD/B N*, 4360, p.14;

[11] Yang, S., Li, C.Q. and Yang, W., 2016. Analytical model of elastic fracture toughness for steel pipes with internal cracks. *Engineering Fracture Mechanics*, 153, pp.50-60, https://doi.org/10.1016/j.engfracmech.2015.11.014 ;

[12] Duan, Z.X. and Shen, S.M., 2006. Analysis and experiments on the plastic limit pressure of elbows. *International Journal of Pressure Vessels and Piping*, 83(10), pp.707-713, https://doi.org/10.1016/j.ijpvp.2006.08.003 ;

[13] Xie, Y.J., Zhang, H., Liu, S., Yang, P. and Luo, X., 2013. A Study on Stress Corrosion Crack of Thick-Walled Elbow in Manifold for Acid Fracturing. *Journal of Pressure Vessel Technology*, 135(2), p.021207, https://doi.org/10.1115/1.4023420 ;

[14] Li, Z., Yinpei, W., Jin, C. and Cengdian, L., 2001. Evaluation of local thinned pressurized elbows. *International Journal of Pressure Vessels and Piping*, 78(10), pp.697-703, https://doi.org/10.1016/S0308-0161(01)00125-9 ;

[15] Lee, G.H., Pouraria, H., Seo, J.K. and Paik, J.K., 2015. Burst strength behaviour of an aging subsea gas pipeline elbow in different external and internal corrosion-damaged positions. *International Journal of Naval Architecture and Ocean Engineering*, 7(3), pp.435-451, https://doi.org/10.1515/ijnaoe-2015-0031 ;

[16] Tee, K.F. and Wordu, A.H., 2020. Burst strength analysis of pressurized steel pipelines with corrosion and gouge defects. *Engineering Failure Analysis*, 108, p.104347, https://doi.org/10.1016/j.engfailanal.2019.104347 ;

[17] Pluvinage, G., 1998. Fatigue and fracture emanating from notch; the use of the notch stress intensity factor. *Nuclear Engineering and Design*, 185(2-3), pp.173-184, https://doi.org/10.1016/S0029-5493(98)00183-6 ;

[18] Amara, M., Bouledroua, O., Hadj Meliani, M., Azari, Z., Abbess, M.T., Pluvinage, G. and Bozic, Z., 2019. Effect of corrosion damage on a pipeline burst pressure and repairing methods. *Archive of Applied Mechanics*, 89(5), pp.939-951, https://doi.org/10.1007/s00419-019-01518-z ;

[19] Adib, H. and Pluvinage, G., 2003. Theoretical and numerical aspects of the volumetric approach for fatigue life prediction in notched components. *International Journal of Fatigue*, 25(1), pp.67-76, https://doi.org/10.1016/S0142-1123(02)00040-3 ;

[20] Popov, B.N., Lee, J.W., and Djukic, M.B., 2018. Hydrogen permeation and hydrogen-induced cracking. In Myer Kutz, editor. *Handbook of Environmental Degradation of Materials, Third Edition. William Andrew Publishing*, pp.133-162, https://doi.org/10.1016/B978-0-323-52472-8.00007-1 ;

[21] Kusmono and Khasani, 2017. Analysis of a failed pipe elbow in geothermal production facility. *Case Studies in Engineering Failure Analysis*, 9, pp. 71-77, https://doi.org/10.1016/j.csefa.2017.08.001 ;

[22] Zelmati, D., Ghelloudj, O. and Amirat, A., 2017. Reliability estimation of pressurized API 5L X70 pipeline steel under longitudinal elliptical corrosion defect. *The International Journal of Advanced Manufacturing Technology*, 90(9-12), pp.2777-2783, https://doi.org/10.1007/s00170-016-9580-6 ;

[23] Zelmati, D., Ghelloudj, O. and Amirat, A., 2017. Correlation between defect depth and defect length through a reliability index when evaluating of the remaining life of steel pipeline under corrosion and crack defects. *Engineering Failure Analysis*, 79, pp.171-185, https://doi.org/10.1016/j.engfailanal.2017.04.025 ;

[24] Bouledroua, O., Zelmati, D. and Hassani, M., 2019. Inspections, statistical and reliability assessment study of corroded pipeline. *Engineering failure analysis*, 100, pp.1-10, https://doi.org/10.1016/j.engfailanal.2019.02.012 ;

[25] Ainsworth, R.A., Gintalas, M., Sahu, M.K., Chattopadhyay, J. and Dutta, B.K., 2015. Failure Assessment Diagram Assessments of Large-Scale Cracked Straight Pipes and Elbows. *Transactions, SMiRT-23 Manchester, United Kingdom* - August 10-14, 2015, http://www.lib.ncsu.edu/resolver/1840.20/33859 ;

[26] Meriem-Benziane, M., Abdul-Wahab, S.A., Zahloul, H., Babaziane, B., Hadj-Meliani, M. and Pluvinage, G., 2015. Finite element analysis of the integrity of an API X65 pipeline with a longitudinal crack repaired with single-and double-bonded composites. *Composites Part B: Engineering*, 77, pp.431-439, https://doi.org/10.1016/j.compositesb.2015.03.008 ;

[27] Amandi, K.U., Diemuodeke, E.O. and Briggs, T.A., 2019. Model for remaining strength estimation of a corroded pipeline with interacting defects for oil and gas operations. *Cogent Engineering*, 6(1), pp.1663682, https://doi.org/10.1080/23311916.2019.1663682;

[28] Escoe, A.K., 2006. Piping and Pipelines Assessment Guide. *Gulf Professional Publishing, Burlington, MA*, https://doi.org/10.1016/B978-0-7506-7880-3.X5000-4 ;

[29] Miller, A.G., 1988. Review of limit loads of structures containing defects. *International Journal of Pressure Vessels and Piping*, 32(1-4), pp.197-327, https://doi.org/10.1016/0308-0161(88)90073-7.

CHAPTER IV:

EROSION-CORROSION IN THE CRITICAL POSITIONS OF PIPE ELBOWS : CASE STUDY

IV.1 INTRODUCTION

The natural energy is still an important source for humanity including the crude oil, natural gas and water. Furthermore, they face a great challenge to explore, exploit and transport them with safety conditions. Due to the shortage of fresh water and its demand increasing in the desert areas, the world turned into the seawater desalination technique and treatment. The appearing of corrosion along piping systems such as the elbows and desalination equipment becomes as a dangerous phenomenon due to the aggressive components in the seawater and chemical solutions. Moreover, the use of piping network including pipelines and elbows consider the best method to transport the aggressive fluids such as Carbon dioxide (CO_2), Hydrogen, Methanol, H_2S, HCl, H_2SO_4, ammonia (NH_3) by safest way over great distance. Depending on the good mechanical and physical properties and lower cost despite the corrosion resistance of relatively low, pipelines are made generally by the carbon steels [1-2].

The water transport networks defects including the corrosion phenomenon are a major challenge facing many desalination plants due to the dangerous factors which occur during the flow of fluid. One of the main damage problems is the corrosion due to the aggressive fluids taking into account their chemical components and reactions. In addition, erosion is one of the serious reasons which lead to the corrosion issue. Most flow liquids through piping system lade some solid particles which can make a damage in the critical zone of internal wall of elbow.

In the current case study, the production of CO_2 is one of the processes in the desalination plant. It needs a solution of Monoethanolamine (MEA) mixed with distilled water (11% of MEA pure to one litre of distilled water) to absorb CO_2 from flue gas (The gas residue is exhausted from the top of the absorber). The aim of this chapter is to inspect two corroded pipe elbows which transport the solution of MEA with highly contains of CO_2. Generally, sodium carbonate (Na_2CO_3) is added to this process in order to control final pH correction range as to prevent or reduce the corrosion issue [6]. As primary observations, it was noted that there are some elements that have the biggest affect. These elements are referred to the type of welding material, respect the time using of Sodium carbonate (Na_2CO_3) and the nature of solution liquid. Depending on the inspection methods such as; scanning electron microscope (SEM), X-ray diffraction (XRD) and X-ray fluorescence (XRF) test, the obtained results illustrate the main reasons of erosion in the critical positions of pipe elbows.

IV.2 PROCESS STRUCTURE OF CO_2 PRODUCTION

Firstly, it is going to introduce in brief the station and CO_2 production section in order to understand the importance of this work. The desalination plant is located on the Mediterranean coast of Algeria about seven kilometers west of the Ténès city in Chlef. Its capacity of production of drinking water is almost 200,000 m^3/ day. It started its service operation in February 2015 under Abengoa Spanish multinational company management which will be the responsible of its operation and maintenance for a period of 25 years [7, 8].

In addition, the plant features a system to produce CO_2 from flue gases. The production of CO_2 liquid is one of the principal processes in the large refineries and power plants. This process must be passed by three main steps; (i) absorption, (ii) compression, and (iii) transportation. First step needs for chemical absorbent in order to capture CO_2 from the flue gas as shown in figure IV.1. The flue gas will be passed first in an absorber which containing the amine solution to capture CO_2 gas. Secondly, the CO_2 will be transformed to the liquid phase Last step, CO_2-rich amine will be transported into stripper using piping system. CO_2 will be separated from amine solution using stripper heat process.

This process can be concluded by two reactions; (i) Absorber reactions, and (ii) Regenerator reactions. Their expressions can be written by the following reactions respectively [9]:

$$CO_2 + H_2O + RN \rightarrow HCO_3^- + RNH^+ \quad \textbf{(IV.1)}$$

$$HCO_3^- + RNH^+ + heat \rightarrow CO_2 + H_2O + RN \quad \textbf{(IV.2)}$$

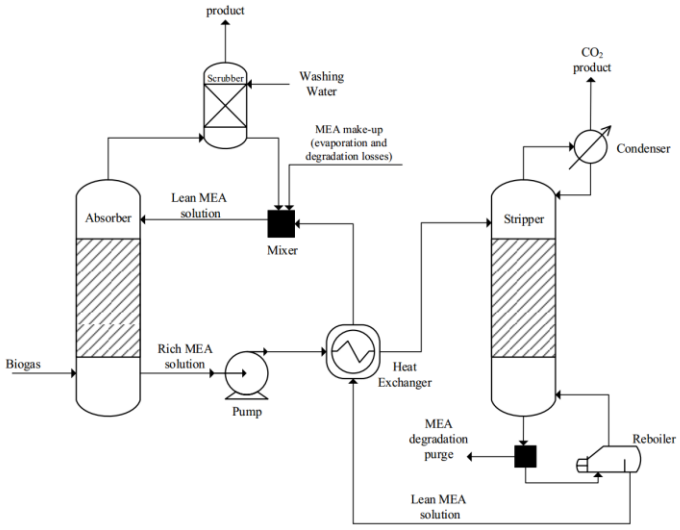

Figure IV.1: General description of CO_2 production using MEA solution [10].

IV.3 EROSION-CORROSION IN THE PIPE ELBOWS

Many studies [11-20] proved that the CO_2 in gaseous state has no corrosive effect on steel of transport network in despite of the presence of oxygen molecules. On the other hand, it has a great effect to appear the corrosion phenomenon after dissolution in water with the presence of chemical solvents especially MEA which helps to activate the chemical reactions. This process leads to the dissociation of acidic ions to CO_2.

In this case study, two pipe elbows of carbon steel which transport a MEA with highly contains of CO_2 were exposed to the erosion-corrosion phenomenon in the critical zones as shown in figure IV.4. In order to investigate the failure causes, samples from critical positions of carbon steel are inspected using SEM, XRD and XRF analyses. These corroded elbow samples were taken from the desalination plant. The positions of these corroded elbows are depicted in figure IV.2 and identified as part I and II. Figure IV.2 shows a schematic presentation for the solution process and the location of the failed elbows. The liquid solution passes through the pipe in a vertical direction as shown in the figure IV.2a. There are two elbows shown in figure IV.2; the valve of the first elbow (Part I) is opened completely for 90° while the valve of the second elbow (Part II) is opened partially with 35°.

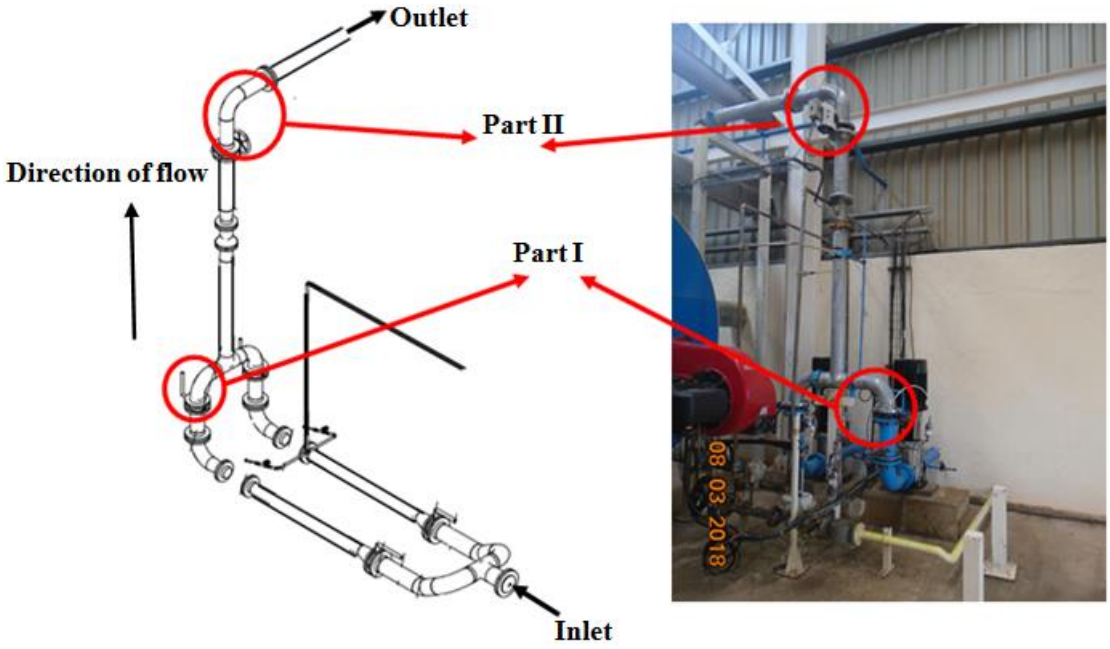

(a) (b)

Figure IV.2: (a) A schematic view of the carbon steel elbows at the corroded location and (b) a photo-digital image of the real installed elbows.

IV.3.1 External surface

Based on the steps of the desalination plant, the flow fluid is performed under the complex operation conditions, where the valve of elbow is opening to allow the distribution of the flow between the two internal zones. In addition, the interactions which occur between the wall of elbow and solution suspensions (solid-liquid) helpful to activate the corrosion taking into account the including complex corrosive conditions.

In fact, the welding supposed to be used as a solution method for corrosion. Unfortunately, the type of welding encountered in the elbow has also an impact on creating the corrosion problem. In this case, the appearance of corrosion problem is one of the negative signs which lead to damage, where it was started in zone 3 (Part II) at the critical welding position between flange and elbow. Successive welding treatments (five times) did not help in solving this problem as corrosion occurred again on the same location. This complicated issue spurred us to investigate in detail this corrosion phenomenon. Figure IV.3 shows an external view of the corroded positions in three regions of the elbow pipe (indicated by arrows). During the service operation, the internal inlet pressure is in the range 3.5 to 4 bar whereas the outlet pressure reaches only up to1 bar (Figure IV.2). The flowing temperature reaches about 85 °C. The corroded area in the two positions (3 and 9 O'clock) of the first elbow (Part I) is clearly shown in figure IV.3 (a and b) and the damaged area for the second elbow (Part II) can be seen in figure IV.3c and is indicated by arrow 3 (6 O'clock).

(a) (b) (c)

Figure IV.3: General view of the external surface of failed pipe elbows, (a) 3 O'clock of part I (b) 9 O'clock part I, and (c) 6 O'clock of part II.

IV.3.2 Visual Observation

Depending on the operating conditions of desalination plant system, the pipeline should be inspected in the locations having the highest interaction with effluents especially in the critical zones that surround the valves. In fact, the elbow bend has a great effect on the safety of systems where the elbow is an important part which can be used to change the directions of fluid flow or to link the transport networks according the need of companies. In addition, the degree of elbow bend may create a great stress along on the internal wall where it can appear in the critical zones, taking into account the pressure let-down valves.

In this section, samples from the heavily corroded elbow of the two parts I and II (shown in figure IV.3) were used to find out the reasons for the erosion-corrosion occurrence. The corrosion position of samples was experimentally analyzed which occurred close to the welding zone on the two elbows as shown in figure IV.3. Figures (IV.4 and IV.5) show the visual observations of the corroded sites in the internal surface along the elbow in varying degrees. Due to the seriousness of corrosion problem which takes many forms such as pits and grooves where the crack of corrosion propagates in the same direction of fluid flow.

It can be observed that the thicknesses of the elbow pipe and flange (part I) are degraded as shown in figures (IV.4 and IV.5) and Tables (IV.1 and IV.2). The eroding of wall thickness is related to the attack of the flowing fluid taking into consideration the opening of valves which also contributed greatly the activation of the suspension interactions (fluid-solid). Such type of problems leads to hypothesize that the leaks are resulted from the attack of the flowing fluid that is rich with CO_2. Depending on these notes, the experimental results are able to show the problem causes, thus, the accuracy solutions and some recommendations will be suggested to avoid the corrosion in future.

(a) (b)

Figure IV.4: General view of the internal surface of failed pipe elbows, (a) elbow I, and (b) elbow II.

(a) (b)

Figure IV.5: Degradation of wall thickness (a) elbow pipe (part I), and (b) flange steel.

Table IV.1: Degradation of pipe elbow thickness (part I).

Thickness	t_0	t_1	t_2	t_3	t_4	t_5	t_6	t_7
Value (mm)	3	3	2.3	2.55	2.8	2.6	3.1	3.45

Table IV.2: The change of wall thickness of flange.

Thickness	t_{b1}	t_{b2}	t_{b3}	t_{b4}	t_{b4}	t_{b5}	t_{b6}
Value (mm)	26.95	26.90	19	22.85	22.75	25.75	26.85

IV.3.3 Chemical composition and mechanical characterization

Knowing the mechanical behavior of the piping system is necessary to predict and avoid corrosion problems. The chemical composition of the corroded elbow was studied via microstructural and mechanical properties investigations including the tensile and hardness measurement tests. In this part, the chemical composition of the standard material DIN 17175 (ST 35.8) [21] is shown in Table IV.3. Table IV.4 shows the mechanical properties of the steel elbow and its dimensions.

Table IV.3: Chemical composition of DIN 17175 pipe steel (%) [21].

Grade	C	Si	Mn	P	S
ST 35.8	0.17 max	0.10-0.35	0.40-0.80	0.040% max	0.040% max

Table IV.4: Mechanical properties of DIN 17175 (ST 35.8) pipe steel standard [21].

Tensile strength (MPa)	**Yield strength (MPa)**	**Elongation (% min)**	**Pipe outside diameter (mm)**	**Elbow bending (°)**
360 to 480	235	25	140	90
Wall thickness (mm)	**Pressure inlet (bar)**	**Pressure outlet (bar)**	**The conductivity of Solution (ms/cm)**	**pH of Solution**
4	4	1	3.76	9.96

IV.4 ANALYSIS OF CORRODED CRITICAL ZONES

Most companies of transport suffer from corrosion and erosion phenomena in the elbows which become a huge challenge for engineers due to the change of structural and mechanical properties of materials. Understanding the behavior of the corroded elbow is greatly associated with the fluid-solid interaction inside the pipe. In this study, samples for different zones of corroded elbow were used to analyze its corrosion behavior. A series of experiments were performed along the corroded elbow to detect the major causes of the corrosion-erosion phenomenon. In this section, the obtained results are analyzed to reveal the corrosion reasons and its propagation along the elbow.

The inspection was carried out on three specimens taken from three different surfaces of elbow (part II) as shown in figure IV.6. The three cut specimens according to the friction of fluid flow in the internal surface of elbow were analyzed. Figure IV.6 shows also a photo-digital image that illustrates the effect of corrosion on the internal surface of the elbow. It is clear that the surface layer in which the liquid passes is corroded and surrounded by a rough layer as indicated by arrows named “A”, “B” and “D”. Zone “A” is a proper surface which does not have signs of corrosion, while “B” is the area of where the fluid passes from and has a uniform corrosion but without defects. Finally, part “D” is the corroded zone where the flowing fluid attacks the indicated location in the image.

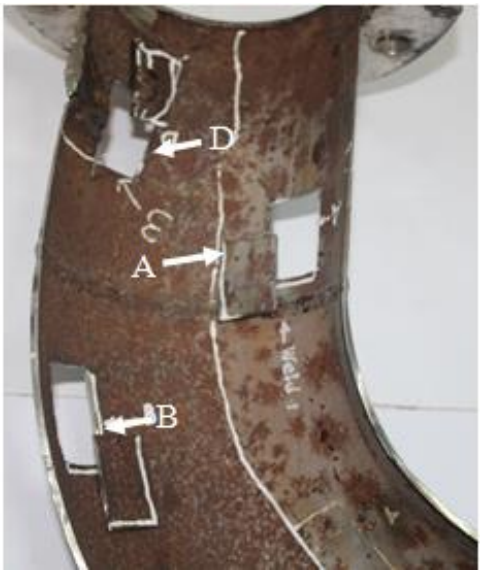

Figure IV.6: Internal surface view of the analyzed specimens.

IV.4.1 Optical microscope

In order to illustrate the effect of corrosion on transport network, microscopic analyses were performed using a Carl Zeiss Axio Imager A1m microscope, coupled with a CANON camera model Power shot A640. This optical microscope allows us to show the visualization of the specimens' surface color, and their shape and distribution. Figures (IV.7 - IV.9) provide a better imaging for the surface of specimens shown in figure IV.6.

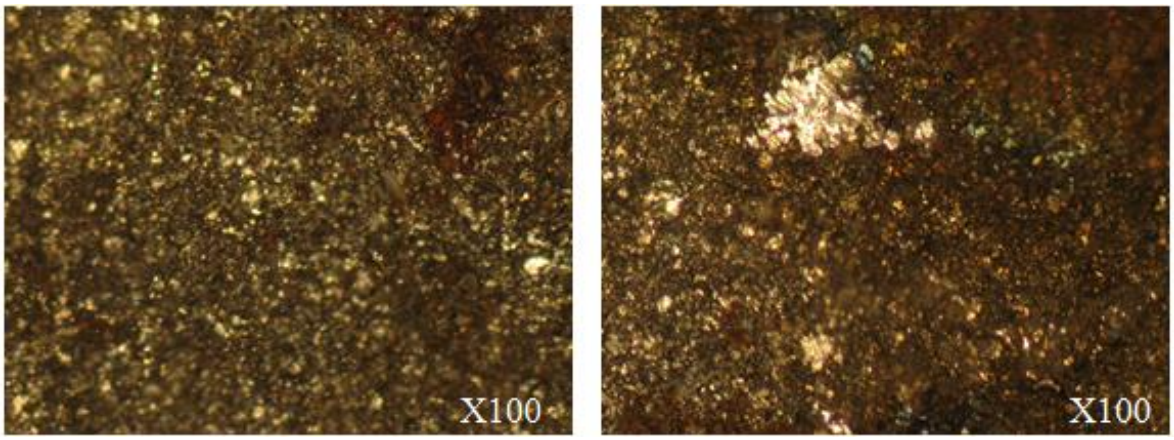

Figure IV.7: Optical microscopy at zone "A".

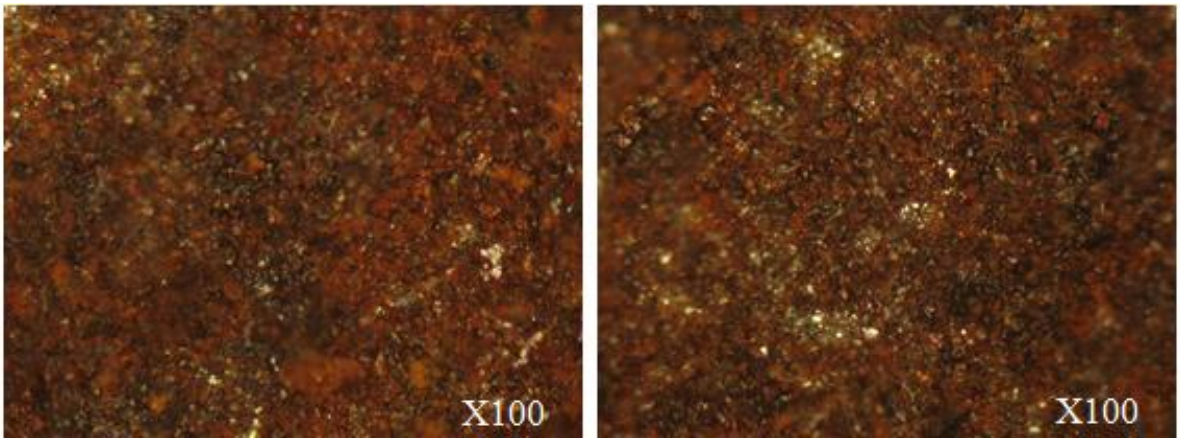

Figure IV.8: Optical microscopy at zone "B".

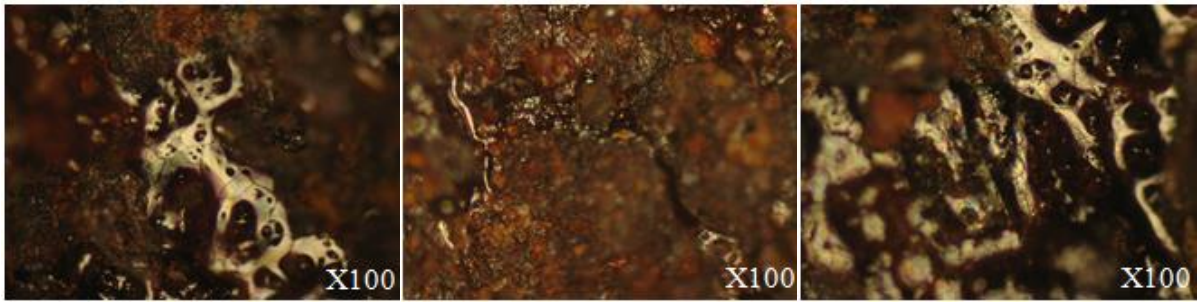

Figure IV.9: Optical microscopy at zone "D".

IV.4.2 Scanning Electron Microscopy (SEM)

The analyses of corroded elbow by optical microscope and SEM results indicate clearly the behavior of the elbow under the operating conditions. The combined results of the two techniques can give an idea on the nature of the pipe's effluent that is less corrosive to the pipe's material. The surface morphology and elemental compositions of different positions of corroded elbow specimens were studied by scanning electron microscopy (SEM) measurements.

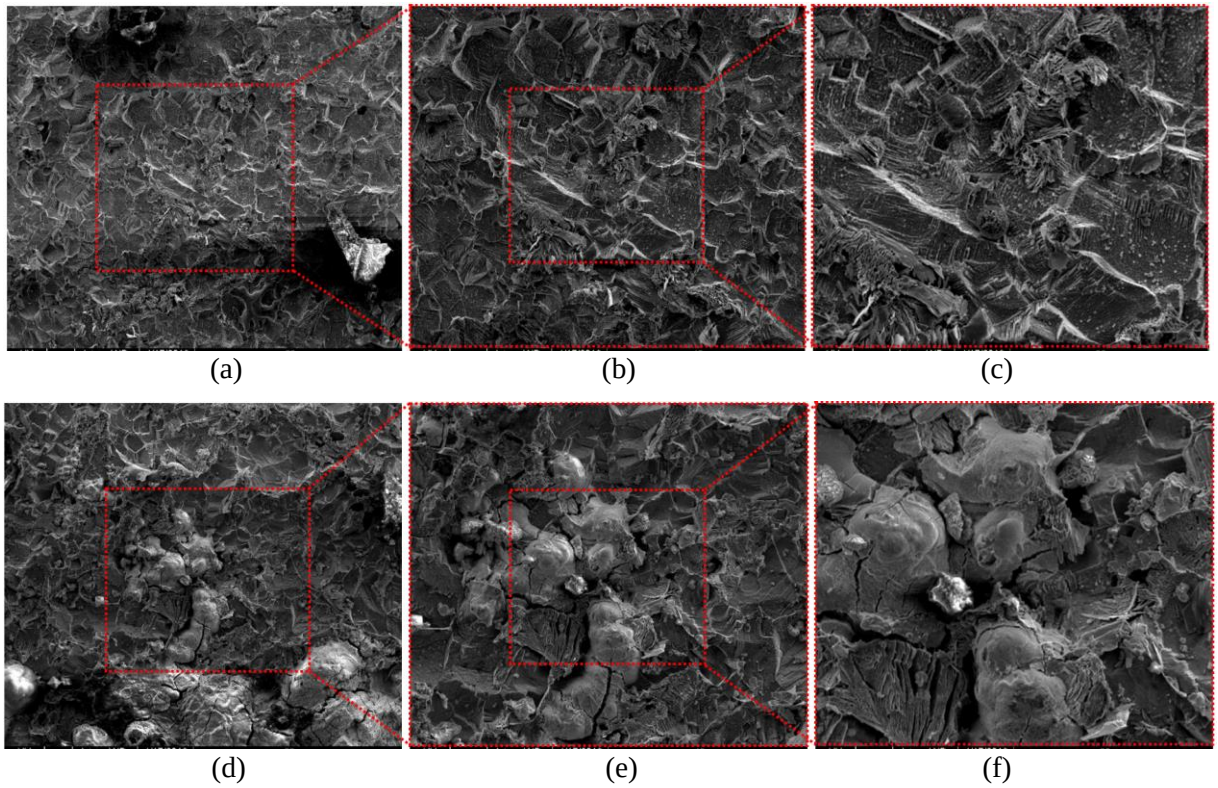

Figure IV.10: Top-surface SEM image of Region A for two positions with different sizes (a) position I with 50 μm, (b) position I with 40 μm, (c) position I with 20 μm, (d) position II with 50 μm, (e) position II with 40 μm, and (f) position II with 20 μm.

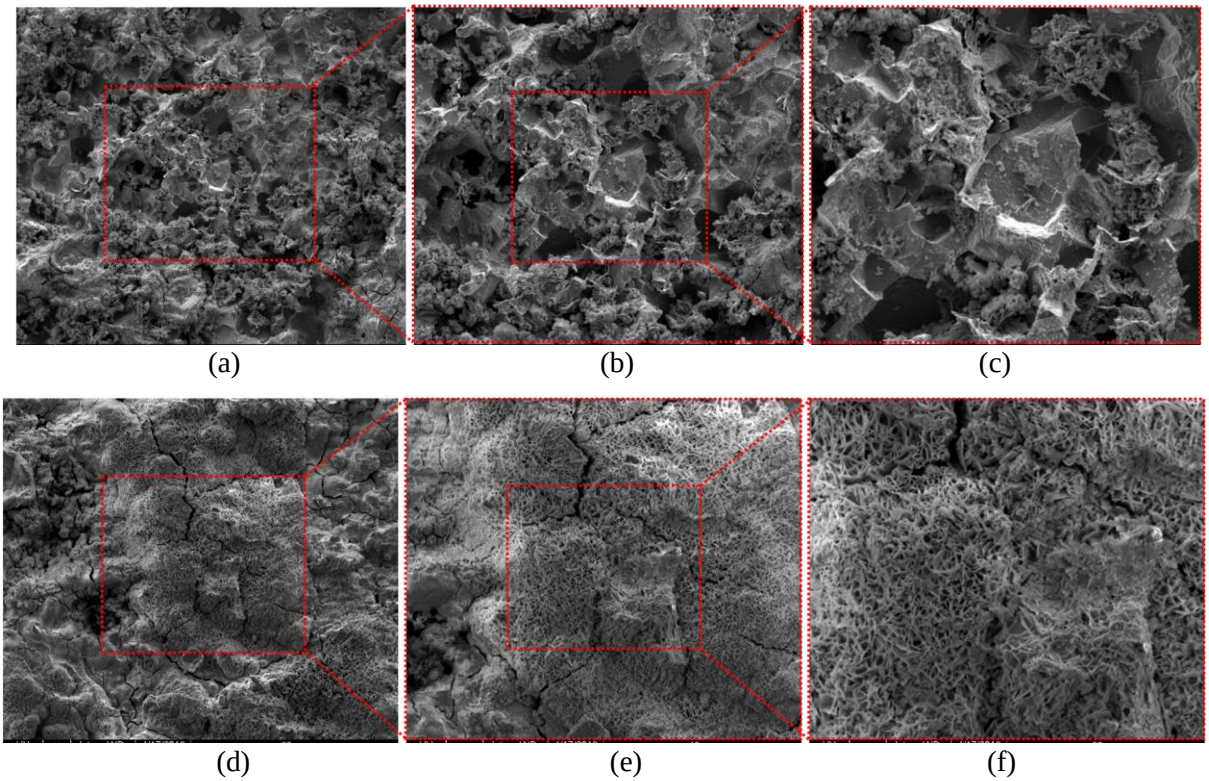

Figure IV.11: Top-surface SEM image of region B for two positions (a) position I with 50 µm, (b) position I with 40 µm, (c) position I with 20 µm, (d) position II with 50 µm, (e) position II with 40 µm, and (f) position II with 20 µm.

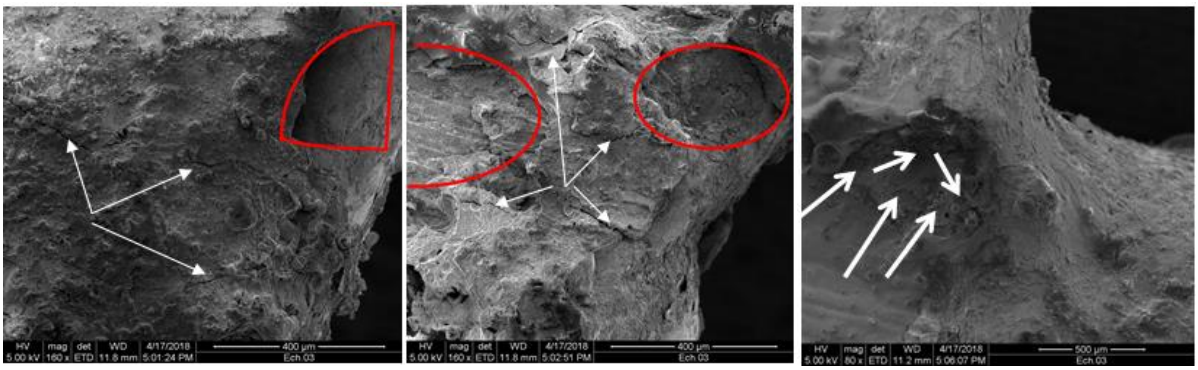

Figure IV.12: Top-surface SEM image of Region D.

From the images, it is clear that the surface of the elbow has degraded to different extents. Figures (IV.7 and IV.10) show the images of the non-corroded zone "A", while figures (IV.8 and IV.11) depicted the status of the surface of the second region "B" which might have a high degree of fluid-solid interaction that is responsible for the friction and corrosion phenomena (brown color) on the internal surface of steel. The dark brown color also visible in zone "D"

(Figures IV.9 and IV.10) and indicates the presence of cracks and serious corrosion-erosion problems on this part of the elbow. This zone has also a groove and pinhole due to the attack of CO_2-rich flowing fluid. In addition, the presence of small solid particles in the fluid is mainly responsible on the erosion problem in the elbow which will be further addressed in the following section.

IV.3.3 X-ray fluorescence (XRF) test

Micro X-ray fluorescence (XRF) instrument is one of the best non-destructive techniques which allow to analyze the qualitative and quantitative elemental composition of solids [22]. The peak energy component of the XRF spectrum identifies the chemical elements present in the specimen, while the height indicates the percentage of the element in the material. The XRF investigation of the specimens was performed using a XGT 5000 model instrument and under operating conditions consisted of 30 kV voltage and a current of 0.02 to 1.00 mA and incrementing by 0.02 mA.

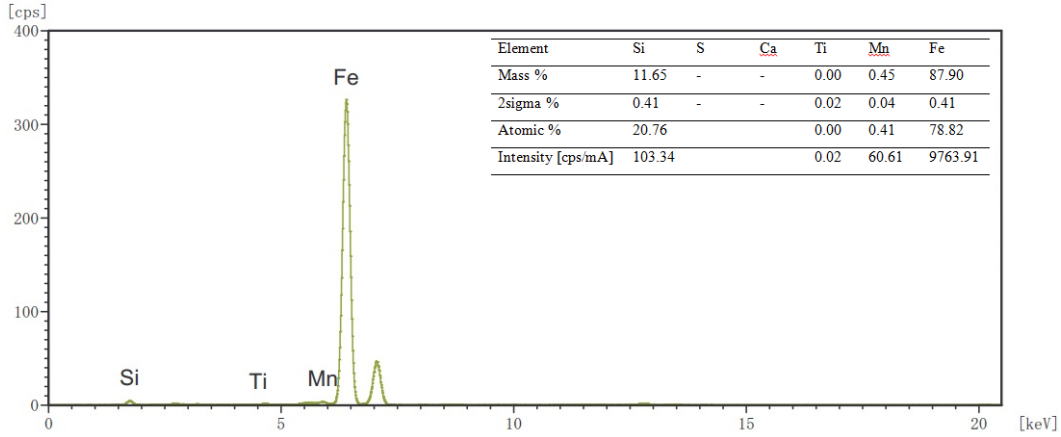

Element	Si	S	Ca	Ti	Mn	Fe
Mass %	11.65	-	-	0.00	0.45	87.90
2sigma %	0.41	-	-	0.02	0.04	0.41
Atomic %	20.76			0.00	0.41	78.82
Intensity [cps/mA]	103.34			0.02	60.61	9763.91

Figure IV.13: XRF spectrum of Region "A".

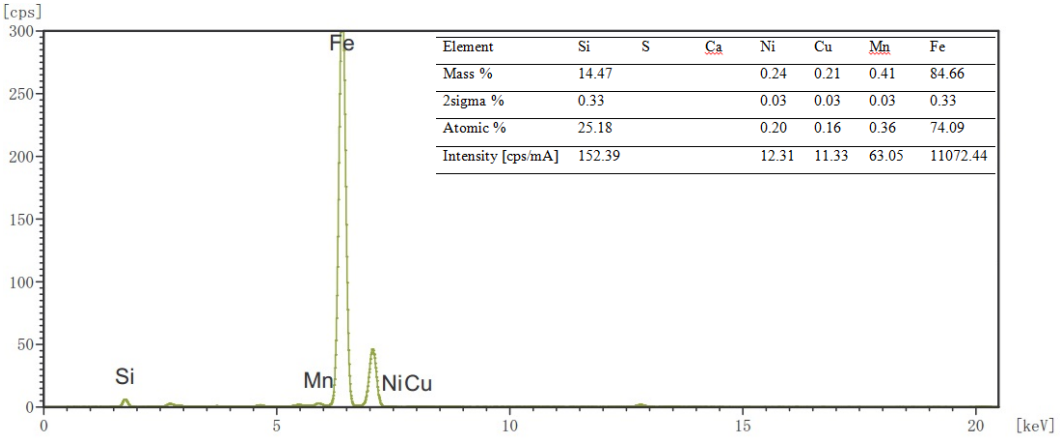

Element	Si	S	Ca	Ni	Cu	Mn	Fe
Mass %	14.47			0.24	0.21	0.41	84.66
2sigma %	0.33			0.03	0.03	0.03	0.33
Atomic %	25.18			0.20	0.16	0.36	74.09
Intensity [cps/mA]	152.39			12.31	11.33	63.05	11072.44

Figure IV.14: XRF spectrum of Region "B".

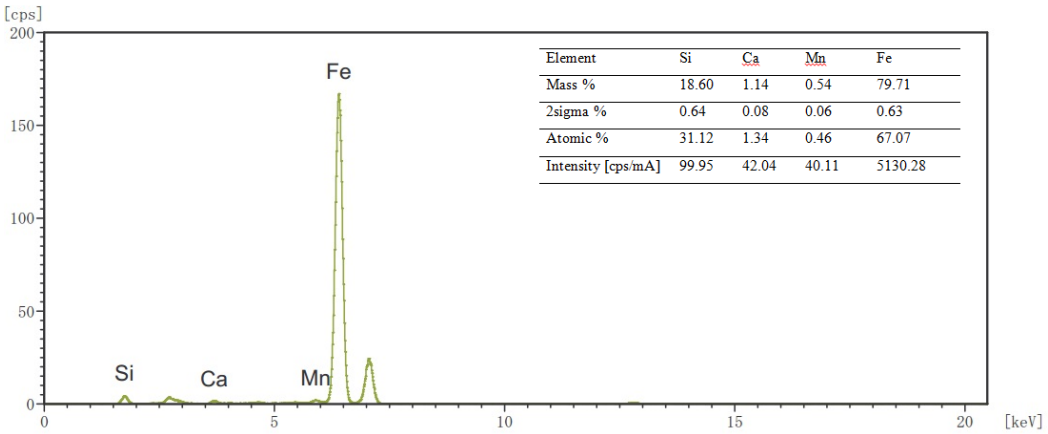

Figure IV.15: XRF spectrum of Region "D".

The obtained results were illustrated from all specimens derived from the corroded inner layer which is directly in contact with the steel carbon surface by XRF spectra as shown in figures (IV.13 - IV.15). From these spectra, a peak corresponding to Fe element can be observed. A peak for Ti is only observed in the spectrum of region "A" but in a small concentration (Figure IV.13). Furthermore, the spectra of all zones indicate clearly of the elbow material compounds that were significantly influenced by the geometry of elbow and valves as well as the operating conditions and the degree of fluid-solid interaction.

All specimens of corroded elbows were analyzed using the XRF which confirmed the presence of Si and Mn with small concentration. Depending on the suitable conditions which activate the complex chemical reactions where these elements were caused mainly the erosion-corrosion problem of the elbow pipe, hence, this phenomenon leads to the damage in piping systems. As observed in the XRF spectrum of the corroded layer in zone "D" (Figure IV.15), the presence of many elements such as Si, Ca, S, Ti, Mn and Fe in this corroded zone is an indication to the presence of sand particles in the fluid effluent.

IV.3.4 X-ray diffraction (XRD)

The XRD analysis becomes also an important instrument to study the behavior of corroded elbow specimens. It is used to discover the crystalline structures of the elbow's materials. Due to the increase of dangerous incidents in the desalination plants, XRD analysis considers as a necessary technique to detect the components of the corroded critical zones of metallic structures. The samples of corroded elbow were grinded into a finely ground powder in a cup

(mortar grinder). Based on the reflected X-rays, the deformation of the sample was detected by the sweep detector samples' intensity. Using APD 2000 XRD diffractometer model equipped with GD model Goniometer for the meter, the corroded elbow specimens were characterized by recording the intensity of the diffraction lines as a function of the deflection angle *2θ*. In addition, Bragg's law is used to locate the directions of diffractions. The obtained results were analyzed using WinDust32 software. θ is the half-deflection angle (half of the angle between the incident beam and the direction of the detector) while "λ" is the wave length of X-rays.

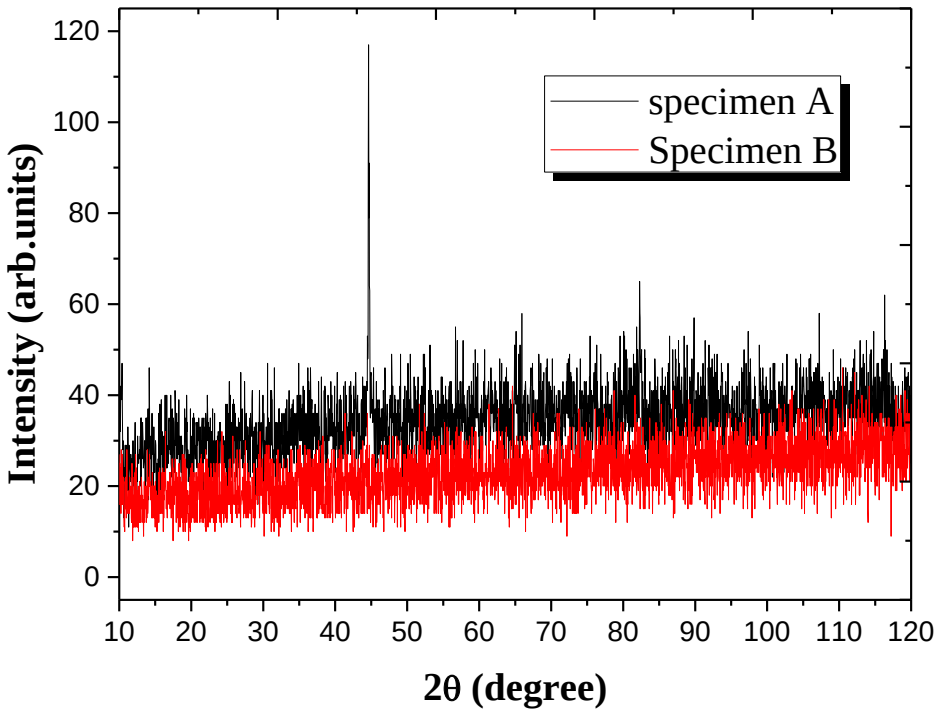

Figure IV.16: XRD test for specimens "A" and "B".

Several experimental were carried out to highlight the mechanical properties and chemical compositions of critical zones including the structure of the corroded layer of elbow. Figure IV.16 shows the obtained XRD diffractograms of the corroded zones "A" and "B". It is clearly observed that the crystal peaks of the hydrated phases in specimen "A" indicated that the corroded layers have contained complex compounds such as hematite. The disappearance of these peaks can be also noted in the spectra of specimen "B". Moreover, a change in the structural composition of the corroded layer is manifested by the appearance of oxides containing iron such as hematite Fe_2O_3.

IV.4 DISCUSSION

The inspection of transported liquid and corroded specimens using the mechanical tests and chemical analyses lead to discover the main causes of corrosion phenomenon. Furthermore, the use of microscopic is an important step to understand the failure of transport network. The microscopic images above proved the existence of the complex chemical reactions resulted from the interaction between the flowing fluid and the internal wall of elbow. This phenomenon led to the observed corrosion in the elbow under the special operating conditions taking into consideration the geometry of elbows, kind of valve, and transported fluid.

Based on the operating conditions, the MEA solution is transported through the piping network with adding precise concentrations of chemical additives to overcome the instability of this mixture. However, the unrespect of precise concentrations use under service conditions is still one of the major reasons which leads to activate the undesirable chemical reactions which degrade the wall thickness of the material.

As a result of the complex situation at the interaction zone, it appears that the leak was caused by a localized hole. In spite of the several times repairing by welding, the fluid attack by valve opening and the erosion-corrosion damage was repeated continue to appear again in the same zones surrounding the welding areas. This phenomenon was almost happened in the pipe elbow due to the different of welding properties to pipeline. Due to the direct fluid-solid interaction caused by valve angle opening and its quick flow, the elbow steel exhibited both general thinning and localized grooves caused by silicon particles taking into account the distinct morphology of elbow. The formation of a dark brown color coating layer on the surface of the elbow is direct proof on the evolution of corrosion process on the internal surface of pipeline. It was noticed that there is a reduction in the thicknesses along the elbow especially in the interaction zone. The layer of dark brown color at a valve angle of 35° is main proof on forming the oxidation process (corrosion phenomenon) on the internal surface of pipeline. According to the analysis, it is noted that the occurred defects on the pipe were caused by an inappropriate welding process which has also accelerated the corrosion process. This is matched with some of previous cases [23-25] that the corrosion in carbon steel can be occurred by poor welding.

The results indicated that the mechanical properties of elbow were significantly influenced by the solution contents and additives materials. Among the advantages of corrosion is to form a

ferrous layer on the internal wall when exposed to aggressive chemical reactions which protects the steel from additional corrosion especially under the aggressive operating conditions and the presence of silicon particles in the flowing fluid. However, it might lead also to a serious corrosion issue if the layer was unable to form. Thus, carbon steel is a very fit to be used in piping systems carrying aggressive solutions.

The reason for taking these tests into account was to identify the reasons and prohibit the elbow corrosion. This analysis was necessary in order to find the fit solutions to protect the piping systems. Improving the kind of valves and pipe quality can be considered as the appropriate solutions to reduce the friction and interaction fluid-solid along the elbow. They also can increase the efficiency of geometry and diminish the erosion phenomenon. The iron film is relatively fragile and can be eroded away or prevented it to be fully formed by turbulence or fluid flow attack. If this occurs, the underlying metal rapidly corrodes until a new film is formed and becomes stable. The general corrosion attack appears on the pipe elbow was most likely the result of corrosion caused by flowing fluid attack and turbulence. However, turbulence effects at elbows, flanges, and other disruptions can destroy the protectiveness of the corrosion product film and lead to the accelerated corrosion [26-28].

References

[1] Tawancy, H.M., Al-Hadhrami, L.M. and Al-Yousef, F.K., 2013. Analysis of corroded elbow section of carbon steel piping system of an oil–gas separator vessel. *Case Studies in Engineering Failure Analysis*, 1(1), pp.6-14, https://doi.org/10.1016/j.csefa.2012.11.001;

[2] Ilman, M.N., 2014. Analysis of internal corrosion in subsea oil pipeline. *Case Studies in Engineering Failure Analysis*, 2(1), pp.1-8, https://doi.org/10.1016/j.csefa.2013.12.003;

[3] Bagdasarian, A., Feather, J., Hull, B., Stephenson, R. and Strong, R., 2010. Crude unit corrosion and corrosion control. *General electric technical paper no. 1105*;

[4] Simanzhenkov, V. and Idem, R., 2003. Crude oil chemistry. *Crc Press*, https://doi.org/10.1201/9780203014042;

[5] Larché, N. and Dézerville, P., 2011. Review of material selection and corrosion in seawater reverse osmosis desalination plants. *Desalination and Water Treatment*, 31(1-3), pp.121-133, https://doi.org/10.5004/dwt.2011.2362;

[6] Al-Mutaz, I.S. and Al-Ghunaimi, M.A., 2001, October. pH control in water treatment plant by the addition of carbon dioxide. *In The Ida World Congress on desalination and water reuse, Bahrain*, pp.1-12, http://citeseerx.ist.psu.edu/viewdoc/download?doi=10.1.1.613.8964&rep=rep1&type=pdf;

[7] Algerian ministry of energy and mines, https://www.energy.gov.dz/ ;

[8] Manuel d'exploitation de la station de dessalement de l'eau de mer de Ténès ;

[9] Ooi, Z.L., Tan, P.Y., Tan, L.S. and Yeap, S.P., 2020. Amine-based solvent for CO_2 absorption and its impact on carbon steel corrosion: A perspective review. *Chinese Journal of Chemical Engineering*, 28(5), pp.1357-1367, https://doi.org/10.1016/j.cjche.2020.02.029;

[10] Dimitriou, I., García-Gutiérrez, P., Elder, R.H., Cuéllar-Franca, R.M., Azapagic, A. and Allen, R.W., 2015. Carbon dioxide utilisation for production of transport fuels: process and economic analysis. *Energy & Environmental Science*, 8(6), pp.1775-1789, https://doi.org/10.1039/C4EE04117H;

[11] Kittel, J., Idem, R., Gelowitz, D., Tontiwachwuthikul, P., Parrain, G. and Bonneau, A., 2009. Corrosion in MEA units for CO_2 capture: pilot plant studies. *Energy Procedia*, 1(1), pp.791-797, https://doi.org/10.1016/j.egypro.2009.01.105;

[12] Duan, D., Choi, Y.S., Nešic, S., Vitse, F., Bedell, S.A. and Worley, C., 2010, March. Effect of oxygen and heat stable salts on the corrosion of carbon steel in MDEA-based CO_2 capture process. *In CORROSION 2010. OnePetro*, https://doi.org/10.5006/1.3524834;

[13] Songolzadeh, M., Soleimani, M., Takht Ravanchi, M. and Songolzadeh, R., 2014. Carbon dioxide separation from flue gases: a technological review emphasizing reduction in greenhouse gas emissions. *The Scientific World Journal*, https://doi.org/10.1155/2014/828131;

[14] Fytianos, G., Grimstvedt, A., Knuutila, H. and Svendsen, H.F., 2014. Effect of MEA's degradation products on corrosion at CO_2 capture plants. *Energy procedia*, 63, pp.1869-1875, https://doi.org/10.1016/j.egypro.2014.11.195;

[15 Harston, J.D. and Ropital, F., 2007. Amine unit corrosion in refineries. *CRC Press, A volume in European Federation of Corrosion (EFC) Series*;

[16] Kanimozhi, K.R., Papavinasam, S., Shyamala, R. and Li, J., 2014. Effect of monoethanolamine (MEA) on the corrosion rates of carbon steels and stainless steels in CO_2 saturated NaCl solutions. *Paper presented at the CORROSION 2014, San Antonio, Texas, USA*, NACE-2014-4241;

[17] Dutcher, B., Fan, M. and Russell, A.G., 2015. Amine-based CO_2 capture technology development from the beginning of 2013-A Review. *ACS applied materials & interfaces*, 7(4), pp.2137-2148, https://doi.org/10.1021/am507465f;

[18] Zheng, L., Matin, N.S., Landon, J., Thomas, G.A. and Liu, K., 2016. CO_2 loading-dependent corrosion of carbon steel and formation of corrosion products in anoxic 30 wt.% monoethanolamine-based solutions. *Corrosion Science*, 102, pp.44-54, https://doi.org/10.1016/j.corsci.2015.09.015;

[19] Zhang, L., Xie, J.L. and Fu, D., 2018, December. Corrosion behavior of carbon steel in the CO_2 absorption process using MEA activated K_2CO_3 aqueous solutions. *In IOP Conference Series: Earth and Environmental Science*, 199(4), pp. 042041, IOP Publishing;

[20] Owen, J., Godfrey, J., Ma, W., de Boer, G., Al-Khateeb, M., Thompson, H., Neville, A., Ramsey, C. and Barker, R., 2020. An experimental and numerical investigation of CO_2 corrosion in a rapid expansion pipe geometry. *Corrosion Science*, 165, p.108362, https://doi.org/10.1016/j.corsci.2019.108362;

[21] DIN17175/EN10216 standard specification, http://www.sunnysteel.com/din-17175.php;

[22] Fitzgerald, S., 2008. Non-destructive micro-analysis of art and archaeological objects using micro-XRF. *Archeometriai Műhely*, 3, pp.75-80, http://www.epa.hu/00800/00846/00014/pdf/AM-08-03-SF.pdf;

[23] Qiao, Q., Cheng, G., Li, Y., Wu, W., Hu, H. and Huang, H., 2017. Corrosion failure analyses of an elbow and an elbow-to-pipe weld in a natural gas gathering pipeline. *Engineering Failure Analysis*, 82, pp.599-616, https://doi.org/10.1016/j.engfailanal.2017.04.016;

[24] Sudhakar, R., Kumar, G.V., Vignesh, S. and Vivek, S., 2017. Review on Erosion and Corrosion Studies on Steel Weldments. *International Research Journal of Engineering and Technology (IRJET)*, 4(10), pp.798-806, https://www.irjet.net/archives/V4/i10/IRJET-V4I10139.pdf;

[25] El-Sayed, M.H., 2014. Grooving corrosion of seam welded oil pipelines. *Case Studies in Engineering Failure Analysis*, 2(2), pp.84-90, https://doi.org/10.1016/j.csefa.2014.05.002;

[26] Kusmono and Khasani, 2017. Analysis of a Failed Pipe Elbow in Geothermal Production Facility. *Case Studies in Engineering Failure Analysis*, 9, pp.71-77, https://doi.org/10.1016/j.csefa.2017.08.001;

[27] Wu, W., Qiao, Q., Cheng, G., Pei, T., Li, Y., Yin, H. and Liu, D., 2018, July. Erosion-Corrosion of a Carbon Steel Elbow in a Natural Gas Gathering Pipeline. *In Pressure Vessels and Piping Conference, American Society of Mechanical Engineers*, Vol. 51593, p.V01BT01A025, https://doi.org/10.1115/PVP2018-84262;

[28] Zeng, L., Shuang, S., Guo, X.P. and Zhang, G.A., 2016. Erosion-corrosion of stainless steel at different locations of a 90 elbow. *Corrosion Science*, 111, pp.72-83, https://doi.org/10.1016/j.corsci.2016.05.004.

CONCLUSIONS AND RECOMMENDATIONS

1. CONCLUSIONS

The pipe elbow is a main part in the pipeline components which is considered as the weakest in piping system due to the change of its direction. It contains the welded zone, different bends and high concentration of stress at the critical zones because of the curvature. The results of analyses proved that the high internal pressure and the poorly defined geometry allow to the damage and decrease the safety of transport network. The experimental method and numerical techniques were used to study the effect of several aspects on the performance of piping systems including the elbow under operating conditions.

Firstly, the numerical investigations were applied for API X52 elbow steel with two different ways; (i) semi-elliptical cracks, and (ii) rectangular notch, in the critical position of the intrados section of elbow. The main conclusions of this numerical analysis can be drawn as follow:

- There is a good agreement between the hoop stress value obtained using the Goodall formula for calculation of the hoop stress at the intrados section of a pipe elbow without corrosion defects and the value obtained by the FEA with the small error of 5.32 %.
- The presence of elbow in piping system leads to activate a locally stresses.
- The stress amplification factor K_t was found to be 1.2.
- The maximum stress was located at a curvature angle $\alpha = 72°$.
- Severe stress conditions of a defect in elbow locate its assessment point in the brittle part of the FAD.
- For elbow, the relative critical defect depth is ($d/t = 0.28$), which is higher for a straight pipe ($d/t = 0.66$).

Regarding the results of the limit pressure calculation and the hoop stress values in the pipe elbow with different rectangular parallelepiped-shaped corrosion defect, the following conclusions can be drawn.

- The much higher error (25.94 %) is obtained using the straight pipe formula for the calculation of the hoop stress in the pipe elbow.

- The results of the limit pressure calculations using the modified codes that take into account the pipe elbow geometry by using the Goodall formula for calculation of the hoop stress in the pipe elbow are in close agreement with the numerical FEA results.
- Both conservative trend and overestimation in the limit pressure values obtained using ASME B31G code with the highest errors (from 10.56 up to 17.93 %) of all three used models in comparison with the numerical FEA results for analyzed defect depth ratios (d/t = 0.1 - 0.8) are observed.
- The results for the limit pressure obtained using the other two modified standards (modified ASME B31G, and DNV RP-F101) are less conservative and in much better agreement with the numerical FEA results based on the ultimate strength.
- The results for the limit pressure obtained using the modified ASME B31G standard are closest to the numerical FEA results for all defect depth ratios (error: 2.49 - 10.27 %).
- The numerical FEA results for the limit pressure in the pipe elbow using the yield strength for different defect depth ratios are consistently much more conservative and hence not applicable in this study.

It is worth noting that the corrosion phenomenon in API 5L X52 pipe elbows can be studied by Failure Assessment Diagram (FAD) to predict the lifetime of pipeline. The obtained results proved the practical benefits of the modified notch failure assessment diagram (NFAD) for the assessment of the structural integrity and reliability of straight pipes and pipe elbows with different corrosion defects. Based on the comprehensive reliability analysis using the NFAD for the straight pipe and pipe bends (API 5L X52) with different depth ratios (d/t= 0.1 - 0.8) of the rectangular parallelepiped-shaped corrosion defect with rounded corners at the intrados section the following conclusions can be drawn.

- For the calculation of a non-dimensional crack driving force K_r in the pipe elbow, a maximum equivalent notch stress intensity factor ($K_{\rho eq}$) should be computed and used since the elbow curvature provoked the complex mixed mode of loading. The obtained fracture toughness value for the pipe elbow is less than for the straight pipe due to a higher constraint.

- The assessment points for the pipe elbow have a higher value of both coordinates (L_r, K_r) for all corrosion defect depth ratios than for the straight pipe, due to the stress intensification and higher constrain in the pipe elbows.
- For the corrosion defect depth ratios higher than 0.2 (d/t > 0.2), the pipe elbow assessment points are located in the brittle zone of the NFAD, while the critical corrosion defect depth ratio (in the failure zone of the NFAD) is d/t = 0.38.
- The obtained critical corrosion defect depth ratio (d/t= 0.69) for the straight pipe is significantly higher than for the pipe elbow (d/t= 0.38). Also, all assessment points for corrosion defect depth ratios below the critical are located in the least dangerous plastic collapse fracture domain of the NFAD.

The inspection analyses were investigated on a real case of corroded elbow of carbon steel used in the desalination plant. The results of the failure phenomenon were carefully studied by analyzing the microstructure and the composition of the surface films on the surface of the corroded specimens using scanning electron microscope (SEM), X-ray diffraction (XRD) and X-ray fluorescence (XRF) techniques. The main conclusions of this investigation can be drawn as follow:

- Disrespect the specified time of Sodium carbonate (Na_2CO_3) usage can change the value of pH which may leads to corrosion.
- The bad process of welding can lead to the corrosion issue.
- The turbulence effects at elbows, flanges, and other disruptions can destroy the protectiveness of the corrosion product film and lead to the accelerated corrosion.
- The increase of silicone percentage in the corroded surface gives an information that the sand particles were responsible to the erosion-corrosion phenomenon.

2. RECOMMENDATIONS

This study confirms that the pipe elbow is a critical part of piping systems. Moreover, the stresses at the intrados section of the pipe elbow are higher than at extrados or crown sections. Due to these facts, unmodified codes developed for the straight pipes are not applicable for pipe

elbows. Further investigation of modified codes for the limit pressure calculation in the pipe elbow, taking into account the application of different contemporary formulas for the calculation of the hoop stress, is envisaged in our future research.

It is an important to reduce the internal pressure when the defect size is increasing to maintain the reliable operation of pipelines. It is always advisable to make a comparison between the deterministic and probabilistic approaches because of the confirmed trend of a decrease in the reliability index with an increase of the defect depth to wall thickness ratio.

Improving the kind of valves and pipe quality can be considered as the appropriate solutions to reduce the friction and interaction fluid-solid along the elbow. They also can increase the efficiency of geometry and diminish the erosion phenomenon. Finally, the followings can be recommended to prevent the repetition of erosion-corrosion problems inside the elbow:

- Checking frequently the quality of the used membranes to prevent the sand particles to enter the water treatment units.
- Looking after the design of the pumping system and its depth in sea water.
- Replacing the welding curing methodology of defected parts with the composite patching methodology.
- Controlling the pH of MEA solution.
- Adding green inhibitors to MEA solution for decreasing its corrosivity to the steel elbow.

LIST OF PUBLICATIONS AND COMMUNICATIONS

LIST OF PUBLICATIONS

[1] **Muthanna, B.G.N.**, Bouledroua, O., Meriem-Benziane, M., Setvati, M.R. and Djukic, M.B., 2021. Assessment of corroded API 5L X52 pipe elbow using a modified failure assessment diagram. *International Journal of Pressure Vessels and Piping*, p.104291, https://doi.org/10.1016/j.ijpvp.2020.104291;

[2] Meriem-Benziane, M., Bou-Saïd, B., **Muthanna, B.G.N.** and Boudissa, I., 2021. Numerical study of elbow corrosion in the presence of sodium chloride, calcium chloride, naphthenic acids, and sulfur in crude oil. *Journal of Petroleum Science and Engineering*, p.108124, https://doi.org/10.1016/j.petrol.2020.108124;

[3] Boura, M., Benzegaou, A., Mebarki, B., Hadj Meliani, M. and **Muthanna, B.G.N.**, 2021. A mechanical performance study and simulation of a hybrid electric vehicle powered by Ni-MH battery. *Structural Integrity and Life*, 21(2), pp. 146–152, http://divk.inovacionicentar.rs/ivk/ivk21/146-IVK2-2021-MB-AB-BM-MHM-BGNM.pdf ;

[4] Sadou, M., Hadj Meliani, M., Amara, M., **Muthanna, B.G.N.**, Merah, N. and Suleiman, R.K., 2020. Impact resistance of API 5L steel in aggressive environment with the presence of green inhibitors. *Structural Integrity and Life*, 20(1), pp. 57–62, http://divk.inovacionicentar.rs/ivk/ivk20/057-IVK1-2020-MS-MHM-MA-BGNM-NM-RKS.pdf;

[5] Mouna, A., Boukortt, H., Hadj Meliani, M., **Muthanna, B.G.N.**, Suleiman, R.K., Sorour, A.A., Pluvinage, G. and Azari, Z., 2020. Corrosion effect, constraint and path orientation estimated in cracked gas turbine blade. *Engineering Failure Analysis*, 110, p.104345, https://doi.org/10.1016/j.engfailanal.2019.104345;

[6] **Muthanna, B.G.N.**, Amara, M., Hadj Meliani, M., Mettai, B., Božić, Ž., Suleiman, R. and Sorour, A.A., 2019. Inspection of internal erosion-corrosion of elbow pipe in the desalination station. *Engineering Failure Analysis*, 102, pp.293-302, https://doi.org/10.1016/j.engfailanal.2019.04.062;

[7] **Muthanna, B.G.N.**, Bouledroua, O., Meriem-Benziane, M., Hadj-Meliani, M., Pluvinage, G. and Suleiman, R.K., 2019. Numerical study of semi-elliptical cracks in the critical position of pipe elbow. *Frattura ed Integrità Strutturale*, 13(49), pp.463-477, https://doi.org/10.3221/IGF-ESIS.49.44;

[8] Kelil, T., Amara, M., Hadj Meliani, M., **Muthanna, B.G.N.,** Božić, Ž., Suleiman, R., Sorour, A.A. and Pluvinage, G., 2019. Assessment of API X65 steel pipe puffiness by a strain based design (SBD) approach under bi-axial loading. *Engineering Failure Analysis*, 104, pp.578-588, https://doi.org/10.1016/j.engfailanal.2019.06.063;

[9] Boukortt, H., Amara, M., Meliani, M.H., Bouledroua, O., **Muthanna, B.G.N.**, Suleiman, R.K., Sorour, A.A. and Pluvinage, G., 2018. Hydrogen embrittlement effect on the structural integrity of API 5L X52 steel pipeline. *International Journal of Hydrogen Energy*, 43(42), pp.19615-19624, https://doi.org/10.1016/j.ijhydene.2018.08.149;

[10] Amara, M., Bouledroua, O., Hadj Meliani, M., **Muthanna, B.G.N.,** Tahar Abbes, M. and Pluvinage, G., 2018. Assessment of pipe for CO_2 transportation using a constraint modified CTOD failure assessment diagram. *Structural Integrity and Life*, 18(2), pp.149-153, http://divk.inovacionicentar.rs/ivk/ivk18/149-IVK2-2018-MA-OB-MHM-BGNM-MTA-GP.pdf;

[11] Amara, M., **Muthanna, B.G.N.,** Tahar Abbes, M. and Hadj Meliani, M., 2018. Effect of sand particles on the Erosion-corrosion for a different locations of carbon steel pipe elbow. *Procedia Structural Integrity*, 13, pp.2137-2142, https://doi.org/10.1016/j.prostr.2018.12.151;

[12] Soudani, M., Bouledroua, O., Hadj Meliani, M., El-Miloudi, K., **Muthanna, B.G.N.,** Khelil, A., Elhoud, A., Matvienko, Y.G. and Pluvinage, G., 2018. Corrosion inspection and recommendation on the internal wall degradation caused rupture of 6" gas line pipe. *Journal of Bio-and Tribo-Corrosion*, 4(2), p.28, https://doi.org/10.1007/s40735-018-0145-0.

LIST OF COMMUNICATIONS

[1] **Muthanna, B.G.N.,** Meriem-Benziane, M. and Hadj Meliani, M., 2019. Risk prediction and prevention of corroded pipe elbow using experimental and numerical integrity assessments. The First Doctoral Symposium on Technology: Process, Mechanical and Electrical Engineering (DST'01-2019) Chlef 13-14, November 2019, Algeria, https://www.univ-chlef.dz/ft/?p=1738;

[2] **Muthanna, B.G.N.,** Meriem-Benziane, M., Hadj Meliani, M. and Boualem, M., 2018. Experimental analysis of internal pipe elbow steel erosion-corrosion. The Fourth International Conference On Fracture Mechanics And Energy (FRACT'4), November 26-29, 2018, Chlef, Algeria, www.univ-chlef.dz/fract4;

[3] Meriem-Benziane, M., **Muthanna, B.G.N.,** Gadi, I. and Belhadj-Mokhtar, K., 2018. Evaluation of pipeline elbow steels deformation at critical zones. The Fourth International Conference On Fracture Mechanics And Energy (FRACT'4), November 26-29, 2018, Chlef, Algeria, www.univ-chlef.dz/fract4;

[4] **Muthanna, B.G.N.,** Meriem-Benziane, M., Hadj Meliani, M., Gadi, I. and Azzouz-Rached, W., 2018. Experimental investigation on pipe crack repaired by welding. The Fourth International Conference On Fracture Mechanics And Energy (FRACT'4), November 26-29, 2018, Chlef, Algeria, www.univ-chlef.dz/fract4;

[5] Soudani, M., **Muthanna**, **B.G.N.,** Boukortt, H., El-Miloudi, K. and Hadj Meliani, M., 2018. Effect of green inhibitors on the mechanical properties degradation for pipe steel in acid media. The Fourth International Conference On Fracture Mechanics And Energy (FRACT'4), November 26-29, 2018, Chlef, Algeria, www.univ-chlef.dz/fract4;

[6] Soudani, M., Mostefaoui, A., **Muthanna**, **B.G.N.,** El-Miloudi, K. and Hadj Meliani, M., 2018. Impact of green inhibitor compared with synthetic inhibitors for pipe corrosion in 1 M HCl. The Fourth International Conference On Fracture Mechanics And Energy (FRACT'4), November 26-29, 2018, Chlef, Algeria, www.univ-chlef.dz/fract4;

[7] Amara, M., Hadj Meliani, M., **Muthanna, B.G.N.** and Tahar Abbes, M., 2018. Particle Impact of sand on Internal surface of steel elbow. The Fourth International Conference On Fracture Mechanics And Energy (FRACT'4), November 26-29, 2018, Chlef, Algeria, www.univ-chlef.dz/fract4;

[8] Abdelwahab, M.S.A., Tahar Abbes, M. and **Muthanna, B.G.N.**, 2018. Study of the performance of the hydrodynamic bearing. The Fourth International Conference On Fracture Mechanics And Energy (FRACT'4), November 26-29, 2018, Chlef, Algeria, www.univ-chlef.dz/fract4;

[9] Hadj Meliani, M., **Muthanna**, **B.G.N.,** Božić, Ž. and Pluvinage, G., 2018. Assessment of a pipe puffiness by strain based design. 2nd International Conference on Structural Integrity and Durability – ICSID, Dubrovnik, Croatia, October 2 - 5, 2018, http://www.icsid2018.fsb.hr/preliminary.php;

[10] **Muthanna, B.G.N.,** Boualem, M., Meriem-Benziane, M., Hadj Meliani, M. and Božić, Ž., 2018. Internal corrosion-erosion of pipe elbow steel in the desalination plant: Case study. 2nd International Conference on Structural Integrity and Durability - ICSID, Dubrovnik, Croatia, October 2 - 5, 2018, http://www.icsid2018.fsb.hr/preliminary.php;

[11] Amara, M., **Muthanna, B.G.N.,** Tahar Abbes, M. and Hadj Meliani, M., 2018. Effect of sand particles on the erosion-corrosion for a different locations of carbon steel pipe elbow. 22nd European Conference on Fracture - ECF22 26-31. August, 2018, Serbia, http://www.ecf22.rs/.

[12] **Muthanna, B.G.N.,** Meriem-Benziane, M., Hadj Meliani, M. and Gadi, I., 2018. Effect of pressure for pipe elbow failure. The Third Students Symposium on Engineering Application of Mechanics (SSENAM'3), Mascara, Algeria, 02-03 Mai 2018;

[13] Mostefaoui, A., Soudani, M. El-Miloudi, K., **Muthanna**, **B.G.N.** and Hadj Meliani, M., 2018. Effect of green and synthetic inhibitors on the mechanical properties of API 5L X52 pipe steel. The Third Students Symposium on Engineering Application of Mechanics (SSENAM'3), Mascara, Algeria, 02-03 Mai 2018;

[14] Benali, A., Chaieb Eddra, M.A., **Muthanna**, **B.G.N.,** Soudani, M. and Hadj Meliani, M., 2018. Experimental study for the pipe elbow steel corrosion. The Third Students Symposium on Engineering Application of Mechanics (SSENAM'3), Mascara, Algeria, 02-03 Mai 2018;

[15] **Muthanna, B.G.N.,** Meriem-Benziane, M. and Gadi, I., 2018. Numerical study of semi-elliptical crack of API X70 pipeline. The Second Students Symposium on Engineering Application of Mechanics (SSENAM'2), Chlef, Algeria, 13-14 December 2017.